High-resolution Sequence Stratigraphy of the Southwestern Llanos Basin, Colombia: An integrated analysis

By

Yahir Augusto Valderrama Lopez

A thesis submitted in partial fulfillment of the requirements for the degree of

Master of Science
Department of Earth and Atmospheric Sciences
University of Alberta

Abstract

This research aims to enhance the understanding of the Upper Cretaceous sequence in the southwestern area of the Llanos Foreland Basin, Colombia. The core of this study revolves around the analysis of seven cored locations, which cover nearly the entire Cretaceous sequence. In addition to core data, gamma-ray logs, palynological data, micro-resistivity image logs, and formation pressure data were utilized. These diverse datasets were analyzed using an integrated approach that combines sedimentology, stratigraphy, palynology, and ichnology, ultimately leading to the development of a robust sequence stratigraphic framework.

The Upper Cretaceous wedge in the southwestern Llanos Basin is composed of three recognized formations: Une, Chipaque, and a portion of the Lower Guadalupe. The Upper Cretaceous sequence is differentially bounded by several subaerial unconformities primarily related to the evolution of the Cretaceous back-arc basin and to the compressional phases during the Cenozoic period. The relative chronostratigraphic framework (from palynology) indicates that the Cretaceous wedge sequence in the studied area corresponds to the Middle Cenomanian through the Middle Campanian.

The Une and Lower Guadalupe formations correspond to classic terrigenous coarse-grained reservoirs, while the Chipaque Formation is primarily a fine-grained source rock. However, at the base of the Chipaque Formation, there are some coarse-grained bodies embedded within a fine-grained matrix. In general, the rock record exhibits a wide variety of facies. The Une Formation is primarily composed of tabular and trough cross-bedded sandstone beds. In contrast,

the Chipaque Formation displays a more pronounced facies variability, characterized by heterolithic rocks, dark gray mudrocks, and sandstone beds with variable stratification. The Lower Guadalupe Formation shows similar sand-to-mud ratios as the Une Formation; however, the monotonous presence of tabular and trough cross-bedding is no longer observed, instead additional internal sedimentary structures are found.

Fluctuations in the ratio of continental to marine palynomorphs suggest variations in proximity to, and/or influence from, continental or marine environments within the three main formations. For the Une Formation, palynological data suggest a continental to continental marine-influenced setting. While the Chipaque Formation is interpreted as a marine to marginal marine setting, though some minor intervals can be seen as continental marine-influenced. For the Lower Guadalupe Fm., a continental marine-influenced to marginal marine setting is interpreted.

The integration of palynology, sedimentology, stratigraphy, basic ichnology, and sequence stratigraphy allows us to propose the following depositional settings for the studied units: an alluvial setting for the sparse deposits at the base of the sequence; a lower and upper delta plain for the Une Formation; a transgressive brackish water tidally-modulated setting for the lower section of the Chipaque Formation; a regressive proximal offshore/embayed area setting for the upper section of the Chipaque Formation; and a lower delta plain to upper delta front for the portion of Lower Guadalupe Formation.

Bioturbation within Chipaque Formation primarily occurred as an opportunistic behavior, characterized by diminutive forms and low diversity. The intensity of bioturbation increased

seaward (toward the west and northwest) and decreased landward (toward the east and southeast).

Paleocurrent measurements from Une, Chipaque, and Lower Guadalupe formations supported by core data, indicate that the main sediment transport directions were toward the west and northwest, this means that the depositional settings toward the east and southeast became increasingly continental-influenced or dominated, while those to the west and northwest were more marine or marine-influenced. Inherently, the paleocurrent data suggest that paleocoastlines were likely oriented (NE-SW, NNE-SSW) perpendicular to the sediment transport directions.

In terms of sequence stratigraphy, the basal lowstand systems tract represents the sedimentation's onset of the Upper Cretaceous, followed by a transgressive systems tract corresponding to the lower section of the Chipaque Formation, and a highstand systems tract associated with the upper section of the Chipaque Formation. The intra-Campanian subaerial unconformity, occurring landward of the proto Guaicaramo fault system, marks the presence of a falling-stage systems tract. Subsequently, after a period of sediment bypass and erosion, sedimentation resumes to the area with a lowstand systems tract represented by the Lower Guadalupe Formation. The proposed sequence stratigraphic framework from this effort, explains the geological processes before, during, and after the sedimentation of the three formations that comprise the Upper Cretaceous wedge, and also predicts reservoir spatial variations, including the occurrence of forced regressive deposits westward of the proto Guaicaramo fault system.

Preface

This is the original work of Yahir Valderrama under the supervision of professor Dr. Octavian Catuneanu.

In this thesis, Chapter One provides an overview of the regional- and local-scale geologic setting and establishes the general goals of this study. I was responsible for manuscript preparation. O. Catuneanu provided supervision. M.J. Duvall provided edits during the preparation of the chapter.

Chapter Two details the facies descriptions and classifications of the Cretaceous rock sequence along the southwestern Llanos Basin of Colombia. It uses the organic-walled microfossil content as the basis for the initial approximations for paleoenvironmental interpretation. Alongside facies analysis, a core data bioturbation index (BI) analysis was also conducted, providing additional insights into the paleoenvironmental interpretation. This chapter also integrates a paleocurrent directions analysis conducted for the three Upper Cretaceous units.

Chapter Two is structured as a short-form paper intended to be submitted for publication under the authorship of Valderrama, Y., and Catuneanu, O., in a geological journal. In addition, its findings are also intended to contribute to Chapter Three. I was responsible for data interpretation and manuscript preparation. O. Catuneanu provided editorial input and supervision, and R. Fisher provided edits during the preparation of the chapter.

Chapter Three is formatted as a short-form paper intended to be submitted for publication under the authorship of Valderrama, Y., and Catuneanu, O., in a geological journal. This chapter uses palynology data as a proxy tool to establish the chronostratigraphic framework and integrates the main findings of Chapter Two to support the interpretation of a regional sequence stratigraphic framework. I was responsible for data interpretation and manuscript preparation. O. Catuneanu provided editorial input and supervision, and R. Fisher provided edits during the preparation of the chapter.

Finally, Chapter Four provides a summary of the main conclusions of this thesis and discusses the future research directions of this study. I was responsible for manuscript preparation, and O. Catuneanu provided supervision.

Acknowledgements

First and foremost, I want to express my most sincere gratitude to Professor Dr. Octavian Catuneanu, who constantly shared his deep knowledge in a crystal-clear manner without any restrictions, as well as creating proper ‘accommodation spaces’ filled with strong foundations and challenges. Sincerely many thanks for your patience and support.

I’m also grateful to all the professors at the department, whose passion for their work is evident. Special thanks to Melissa, a wonderful person who is always willing to collaborate.

I extend my thanks to Ecopetrol S.A., for its support policies for studies abroad and for providing the data presented in this thesis.

I would also like to thank my parents (Raul and Socorro) for their love and unconditional support throughout all my life, and to my own family Maria, Emanuel, and Natalia.

I’m grateful to Canada, for embracing me as part of its community; especially during its long, beautiful, and painful winter season, something that I won’t ever forget.

Last but for sure not least, thanks to my Edmontonian friends, Angee, Gustavo, Juan, Alejandro (the Che), and especially Mike, my squash rival, for their companionship and support.

Table of Contents

List of Figures

List of Tables

List of abbreviations in the text

BI	Bioturbation Index
BSFR	Basal surface of force regression.
CC	Correlative conformity
Fm	Formation
FSST	Falling-stage systems tract
F#	Facies number 1, 2, … n.
ft	feet
Gp	Group
HCS	Hummocky cross stratification
HST	Highstand systems tract
ICP	Instituto Colombiano del Petróleo
LST	Lowstand systems tract
Ma	Million years ago
md	Measured depth.
MFS	Maximum flooding surface
MI	Marine index
MRS	Maximum regressive surface
My	Million years
P#	Photo number
SU	Subaerial unconformity
SWLB	Southwestern Llanos Basin
TST	Transgressive systems tract

Chapter 1. Introduction

1.1. Tectonic setting

The Northwestern region of South America was an active margin, subject to multiple episodes of plate tectonic activity before, during, and after the Cretaceous period (Aspden et al., 1987; Sarmiento-Rojas, 2001; Bayona et al., 2020). The tectonic history of the Cretaceous basin can be envisaged throughout two different stages: one for the Early Cretaceous, driven by rifting system (that began in the late Triassic to early Jurassic), and one for the Late Cretaceous, driven by a back-arc basin (Cooper et al., 1995; Horton et al., 2010; Figs. 1-1 and 1-2).

The rift system was characterized by grabens and their associated large bounding vertical faults such as Guaicaramo fault-system (Fig. 1-2), which, to some extent, controlled the creation of accommodation space. Subsequently, some of the vertical faults were inverted during the contractional phases of the Cenozoic (Sarmiento-Rojas, 2001; Villamil, 2003; Mora et al., 2009).

The uplift of the ancestral Central Cordillera and the back-arc basin resulted from an active subduction along the western margin of the South American plate during the Upper Cretaceous. (Villamil, 1999, 2003; Figs. 1-1 and 1-2). This subduction progressively transported large masses of oceanic crust, which were subsequently accreted to the margin along the Romeral fault system suture zone (Cooper et al., 1995; Villamil, 2003; Villagomez et al., 2011; Fig. 1-2). As a consequence of the ongoing subduction and accretion processes, the Cretaceous Sea retreated by the Late Cretaceous and/or Early Paleocene (Montes et al., 2019), resulting in a new basin configuration.

This new basin comprised a vast foreland basin extending from the ancient east side of the proto-Central Cordillera to significant portion of the eastern Amazon region (Hoorn et al., 2010); however, the subsequent uplift of the Eastern Cordillera brought about modifications to the internal configuration of the foreland basin. The uplift of the Eastern Cordillera, resulted in two new physiographic landmarks: a hinterland, situated between the two ranges (Central and

Eastern Cordillera) known as the Magdalena Valley and the current foreland basin, located to the east of the Eastern Cordillera, known as the Llanos Basin (Cooper et al., 1995; Moreno et al., 2011; Fig. 1-2).

From the Cretaceous period to the present, the area of the Cretaceous Basin has been through two sedimentary phases: an underfilled phase that took place during the Cretaceous, constituted mainly of shallow marine and marine rocks, and less frequently, by continental rocks; and an overfilled phase predominantly characterized by continental rocks, and some minor marine and shallow-marine rocks. The overfilled phase resulted from polyphase deformation of up to five deformation pulses that occurred from the late Cretaceous to the present (Bayona et al., 2008). These deformation pulses are associated to the 'pre-Andean' Orogeny (with its maximum expression during the Middle Eocene (Villamil, 1999)), and to the Andean Orogeny with its two tectonic pulses; one during the Middle Miocene and one during in the Pliocene-Pleistocene (Sarmiento-Rojas, 2001).

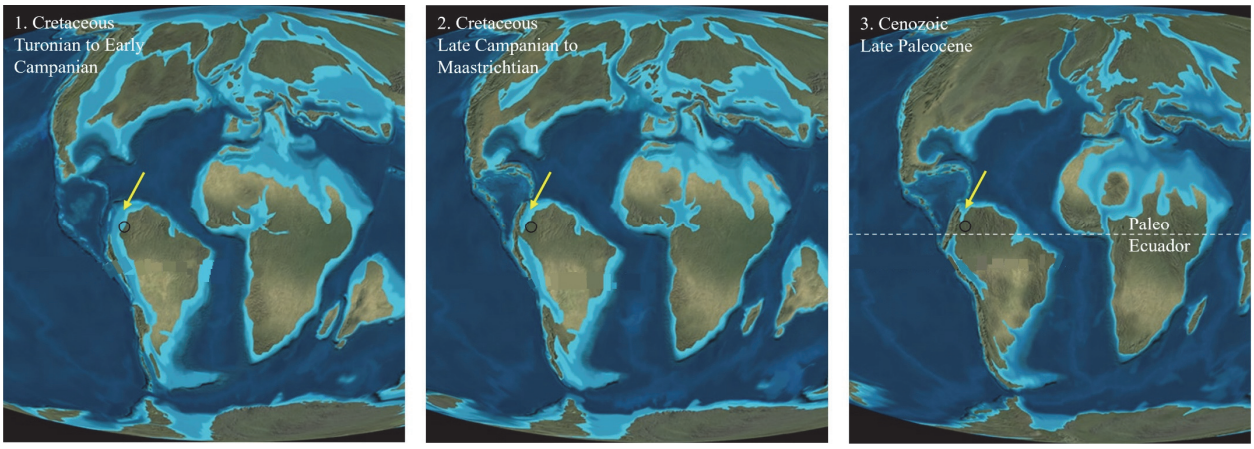

Figure 1-1. Approximate paleogeographic location of the study area from the Turonian up to Late Paleocene. The yellow arrow indicates the location of the ancient epicontinental sea that covered part of the northwestern side of South America. Over time, as a result of tectonic regime change, from rift to back-arc, to accretion of new terrains on the western border, the influence area of the epicontinental sea gradually reduced. The black circle denotes the approximate location of the study area, initially interpreted to be situated in a coastal to shallow marine environment during the Upper Cretaceous and, evolving to a continental setting during the Late Paleocene. (Modified from Blakey, 2008).

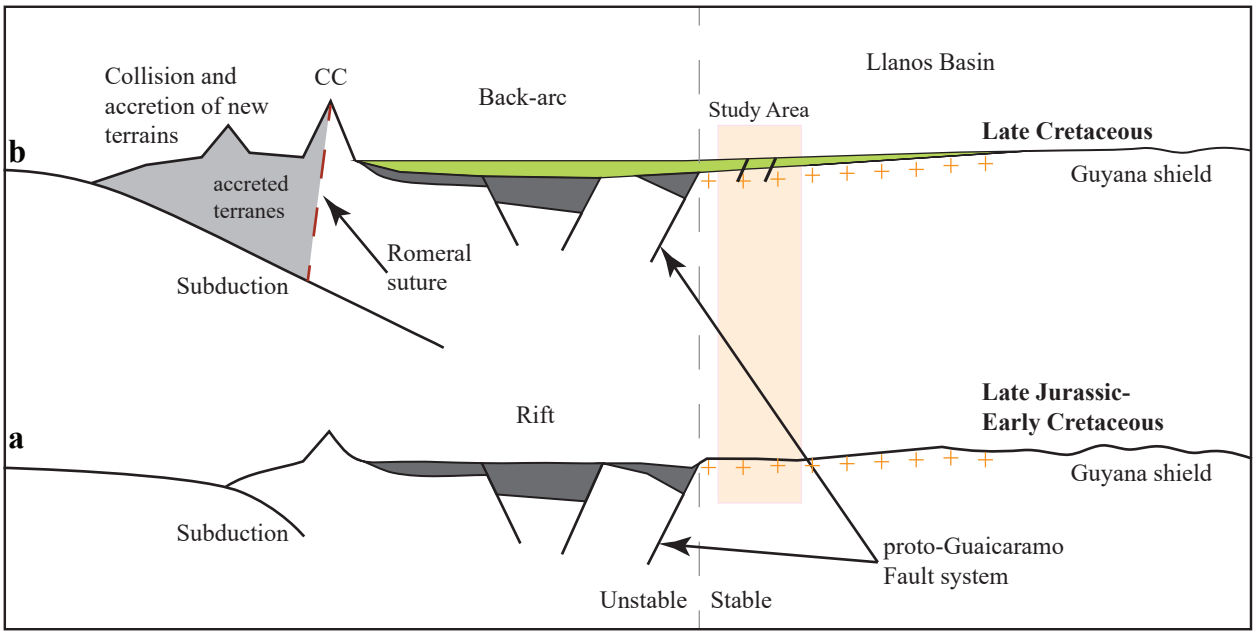

Figure 1-2. Schematic cross-sections showing the tectonic development of the Cretaceous Basin. For the study area, the Early Cretaceous (**a**) was a period of exposure and sediment by-pass, while during the Upper Cretaceous (**b**), sedimentation (but also erosion) occurred. The Guaicaramo fault system marks the boundary between tectonically unstable and stable terrains. Subduction processes intensified notably during the Late Cretaceous. Central Cordillera (CC). (Adapted from Horton et al., 2010).

Globally, the Cretaceous period was characterized by high temperatures, particularly during the Middle Turonian when the Cretaceous thermal maximum was reached (Poulsen et al., 2003). This climate anomaly has been attributed to the separation of Africa and South America, leading to a major reorganization of ocean circulation patterns (Poulsen et al., 2003). In addition, the Cretaceous was accompanied by volcanic activity in the form of new oceanic plateaus and associated submarine volcanism, possibly contributing to elevated levels of CO2 of atmospheric concentrations, the acidification of oceanic water, and oceanic anoxia (Kerr, 1998; Leckie et al., 2002; Kerr, 2005). A substantial portion of the Caribbean plate and some accreted terranes in Colombia are interpreted to have formed as a result of these eruptive events in the eastern Pacific during the Cenomanian-Turonian ages, which were subsequently transported by tectonic activity towards the East and Northeast (Kerr, 1998; Fig. 1-3). As a result of this tectonic evolution, the Late Cretaceous seaway in the northwestern corner of South America was closed from south to north (Cardona et al., 2019; Fig. 1-4).

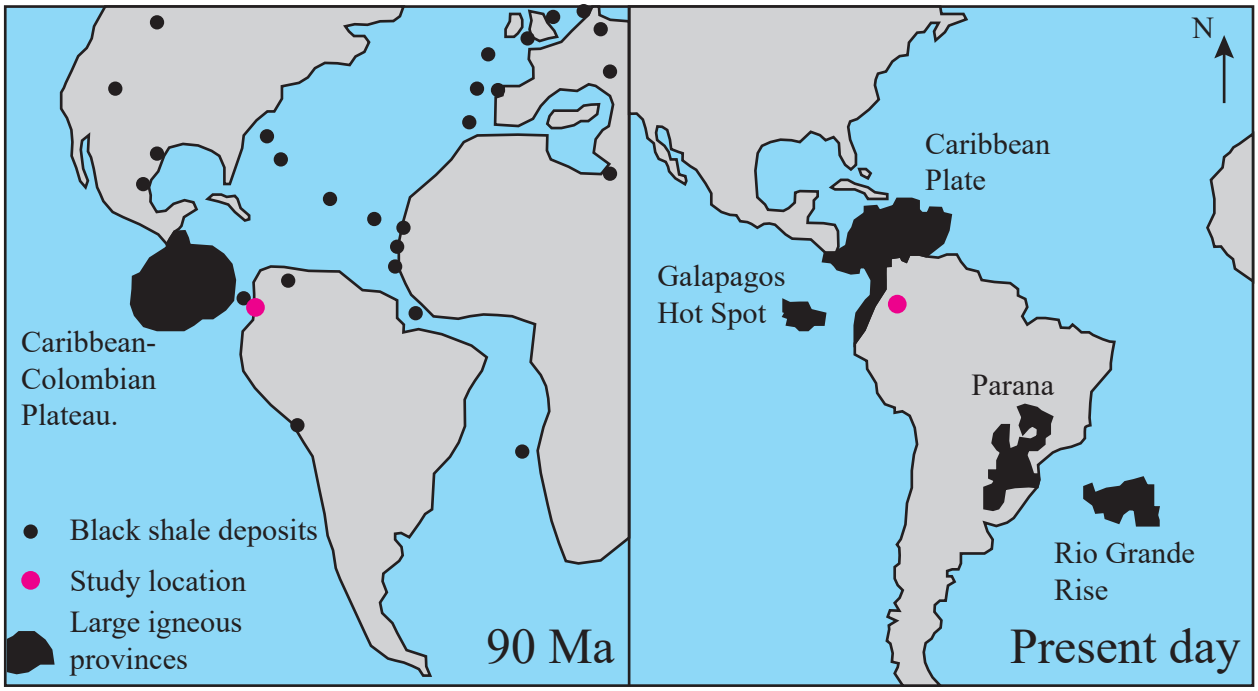

Figure 1-3. Eastern pacific large igneous provinces during the Turonian and their present-day locations. Part of the igneous material was transported and accreted to the northwestern margin of South American plate. (Modified from Kerr, 1998).

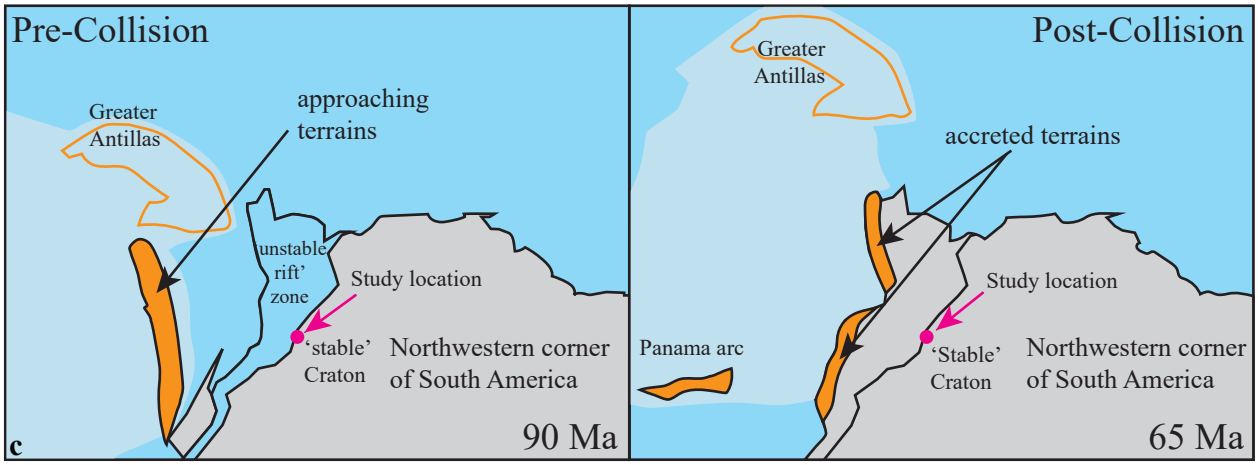

Figure 1-4. Palinspastic reconstruction of the northwestern corner of South America. The closure of the marine seaway occurred from south to north. (Modified from Montes et al., 2019).

1.2. Stratigraphy

Part of the Upper Jurassic sequence, the entire Cretaceous sequence, and part of the Lower Paleogene can be classified as a mega depositional sequence (Sarmiento-Rojas, 2001), with a maximum transgression close to the Early Turonian (Villamil, 2003), including smaller transgressive-regressive cycles (e.g., Guerrero et al., 2000; Sarmiento-Rojas, 2001). In some areas of the Cretaceous Basin, especially in the depo-centers, sedimentation was locally continuous from the uppermost Jurassic to the Cretaceous without any apparent discontinuity (Sarmiento-Rojas, 2001). However, most of the Cretaceous sequence rests unconformably on older rocks, and the sequence becomes thinner outside of the depo-center areas (Sarmiento-Rojas, 2001), such as the Llanos foreland Basin (Fig. 1-2).

The Cretaceous rock record (Fig. 1-5) toward the west of the study area begins with the Brechas de Buenavista Formation, succeeded by the mudstones of Macanal and Caqueza Formations; these Formations are overlain by the Villeta Group, which comprises the Fomeque, Une and Chipaque formations. Moving further east of Guaicaramo fault-system (Fig. 1-5), only the Une and Chipaque formations are present as part of the Villeta Group, for that reason the term Villeta Group is not commonly used eastward of this major fault system (Guerrero and Sarmiento, 1996).

Overlying the Villeta Group, is the Guadalupe Group, composed of three formations: the Lower, Middle and Upper Guadalupe (also known in the Eastern Cordillera as Dura, Plaeners, and Labor-Tierna formations, respectively). Similar to the Villeta Group, the Guadalupe Group is not completely present to the east of the Guaicaramo fault-system, as erosion in this area took place in several stages, resulting in incomplete parts of the Cretaceous record. Therefore, applying the same criteria of Guerrero and Sarmiento, (1996), the name Guadalupe as a Group is not applicable eastward of this fault system (Fig. 1-5).

Within the study area, solely the equivalent to the lower part of Guadalupe Group or Dura Formation is present, however, the term Dura Formation, is not used in the western area of the Llanos Basin, whereas the term Guadalupe is. Therefore, this document will employ the most

commonly used term (Lower Guadalupe) to refer to the youngest Cretaceous rocks present in the study area, which were deposited during the Middle Campanian.

The main units of interest of this study are the Une, Chipaque, and Lower Guadalupe formations. The Une and Lower Guadalupe formations represent conventional reservoirs, composed mainly of sand-dominated packages. The Chipaque Formation is typically a fine-grained source rock, although, within the study location, some embedded coarser-grained beds commonly occur within this unit. Basinward, the La Luna and Villeta formations, are equivalent source rocks to Chipaque Formation, (Villamil, 2003), with larger lateral distribution and less continental influence.

The three Cretaceous units partially appear east of Guaicaramo fault-system and pinch out eastward, due to erosion and/or non-deposition. Although the Cretaceous wedge is bounded by several regional unconformities, core data suggests the presence of additional intra-Cretaceous periods of erosion (Fig. 1-5).

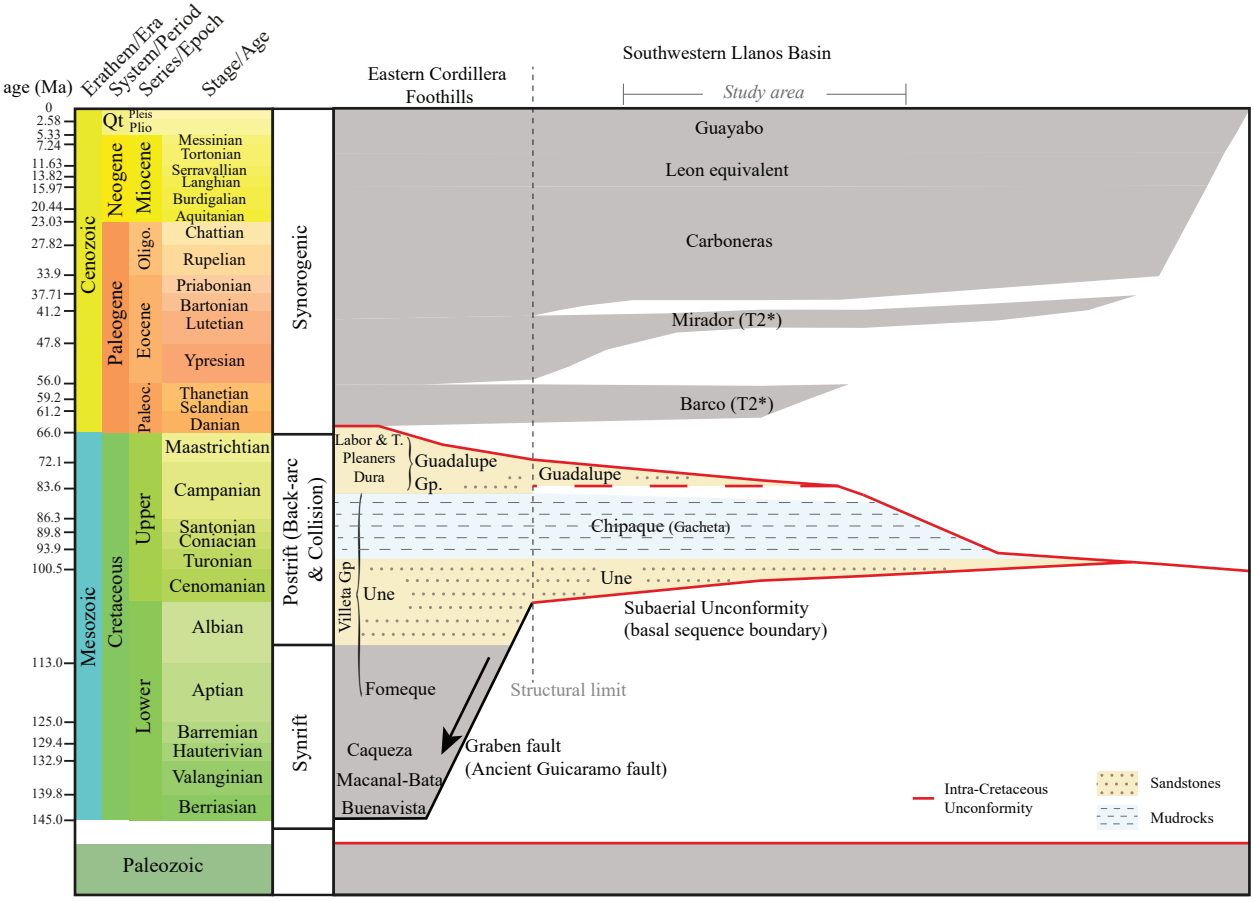

Figure 1-5. Schematic stratigraphic chart for the southwestern Llanos Basin. Rock ages for the study area based on relative palynological dates (ICP, 2012, 2013, 2014a, 2014b, 2015, 2021). The Intra-Campanian unconformity was added based on sedimentological analysis (see Chapter Two for further details). It is likely that the Guaicaramo fault system controlled the extension of the Intra-Campanian unconformity. (Stratigraphic chart modified from Guerrero and Sarmiento, 1996; Sarmiento-Rojas, 2011; Reyes-Harker et al., 2015; Sarmiento-Rojas, 2019; Valderrama and Catuneanu, 2024).

1.3. Study location

The study area is situated approximately 90 km southeast of Bogota city, specifically in the southwestern region of the present-day Llanos Foreland Basin. Geographically, it is bounded to the west and north by the foothills of the Eastern Cordillera; to the south, it is bordered by the Macarena mountains, and to east by the Guyana shield (Fig. 1-6).

The sedimentary succession exhibits a wedge-shaped geometry, with the thickest package concentrated under and near the foothills. The succession gradually thins eastward until it pinches out against the Guyana Craton (Figs. 1-5 and 1-6).

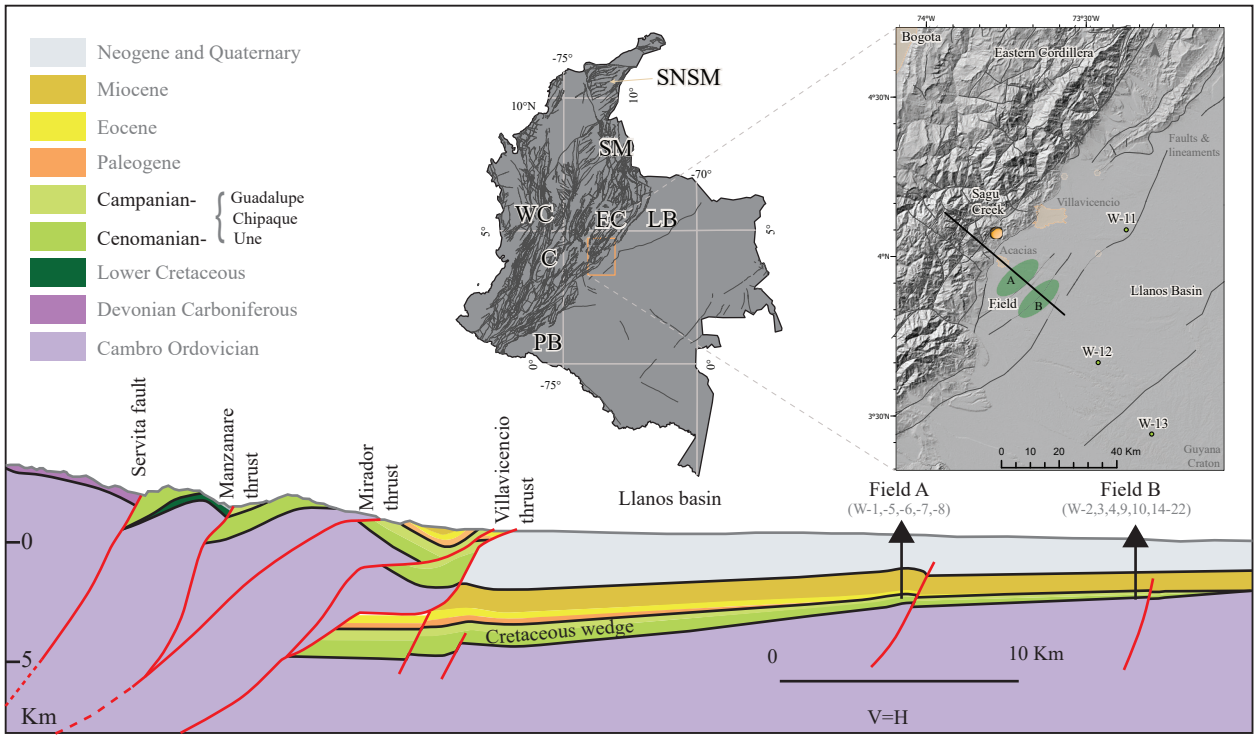

Figure 1-6. Cretaceous wedge geometry. Well-data inventory can be found in Table 1. (Modified from Parravano et al., 2015). Western Cordillera (WC); Central Cordillera (C); Eastern Cordillera (EC); Santander Massif (SM); Sierra Nevada de Santa Marta (SNSM); Llanos Basin (LB); Putumayo Basin (PB).

1.4. Problem statement

While previous studies have contributed with valuable insights into the evolution of the basin (e.g., Fajardo et al., 2000; Caballero et al., 2015; Gelvez et al., 2016; Caballero et al., 2020; Carvajal, 2021), a practical approach to reservoir geology in a sequence stratigraphic framework has not been fully applied, and a complete integration of tools such as palynology, ichnology, sedimentology, and stratigraphy is still pending.

Despite the progress in sequence stratigraphic knowledge, significant opportunities for improvement persist, particularly around the correct interpretation and placement of sequence stratigraphic surfaces (e.g., Caballero et al., 2015, Fig. 1-7; Carvajal, 2021, (pages 106, 163), Fig. 1-8), as these surfaces are the building blocks of the stratigraphic framework.

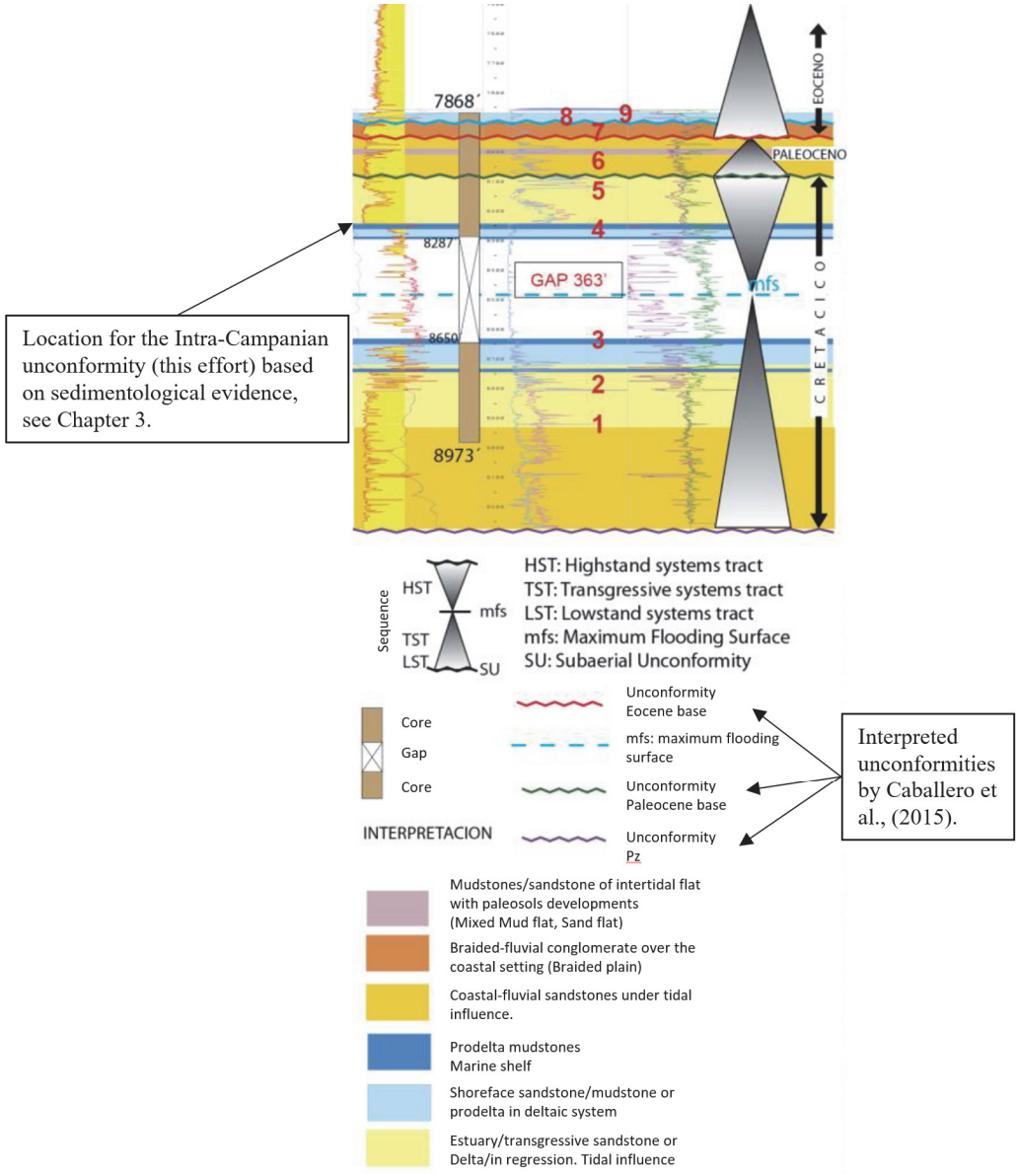

Figure 1-7. The three commonly recognized unconformities in the study area: Eocene, Paleocene and basal Cretaceous. Modified from Caballero et al., 2015, page 323. Core data suggest the presence of an additional Intra-Cretaceous unconformity in the area, further details in Chapter 2 and 3.

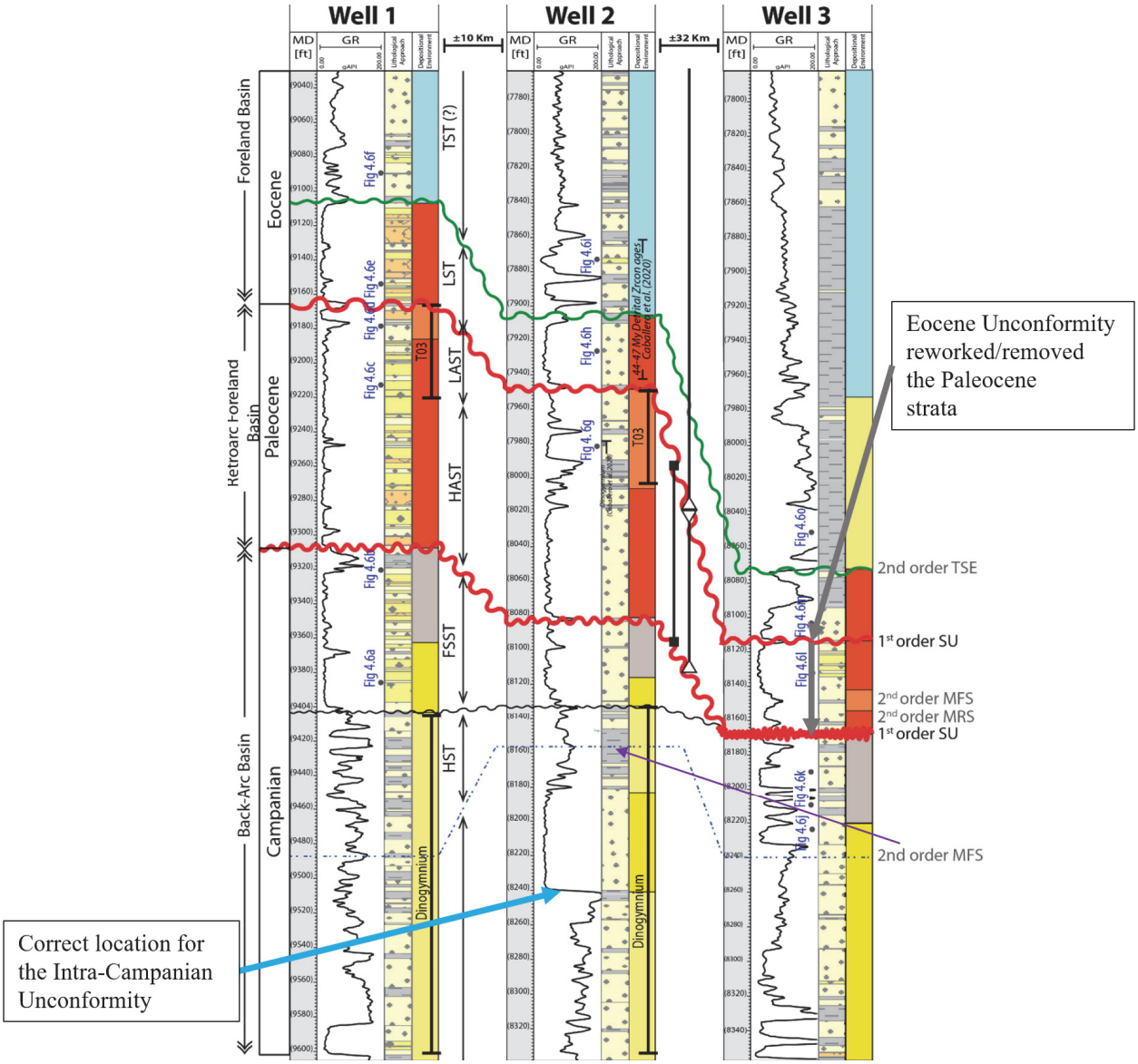

Figure 1-8. Recent sequence stratigraphic interpretation for the Campanian to Eocene. Modified from Carvajal, (2021, p. 163). Although Carvajal, (2021) documented the intra-Cretaceous unconformity, however, misplaced in its interpretation of Well 2; this omission automatically invalidates its second-order maximum flooding surface (MFS) interpretation, as this surface cannot cross an unconformity. Additionally, toward the southeast of the study area (location of its Well 3) Paleocene strata are eroded by the Eocene unconformity, placing Eocene rocks on top of Cretaceous rocks. The left blue arrow indicates the correct placement of the Intra-Campanian unconformity based on the sedimentological evidence of this effort (further details can be found in Chapter Two). Highstand systems tract (HST). High accommodation

systems tract (HAST). Low accommodation systems tract (LAST). Lowstand systems tract (LST). For future comparisons Well 2 of Carvajal, (2021) corresponds to W-7 in this study.

1.5. Study Objectives

The main objective of this study is to: build a robust sequence stratigraphic framework for the entire Upper Cretaceous sedimentary succession of the Southwestern area of Llanos Basin Colombia.

To achieve a complete sequence stratigraphic framework, we will address other missing elements of the area's sedimentary history such as: depositional environments, paleoshoreline trajectories, and how the sequence stratigraphic surfaces occur at reservoir scale.

This effort focuses on integrating diverse geological disciplines, including sedimentology, biostratigraphy, stratigraphy, and tectonics, to result in a robust depositional environment interpretation for the entire Upper Cretaceous sedimentary wedge in the southwestern area of Llanos Basin Colombia. This refined understanding of the Cretaceous sequence will ultimately inform a regional- and reservoir-scale sequence stratigraphic framework.

A deeper understanding of the Cretaceous sequence will not only improve reservoir characterization but also optimize resource exploitation. A solid sequence stratigraphic framework for the southwestern Llanos Basin will provide additional insights to further improve our understanding of the geodynamic events that occurred during the Upper Cretaceous period in the northwestern corner of South America.

1.6. Dataset

The main dataset for this thesis revolves around seven cored well locations (W-2, W-4, W-7, W-8, W-9, W-10, and W-11; Table 1), some of which (W-2, W-7, W-8, W-9, W-11) contain microresistivity image logs. In addition, some of these well locations also contain palynological data. These cored wells almost cover the entire Cretaceous sequence. The main seven well

dataset was complemented with additional well locations that include gamma ray logs and occasional formation pore pressure data.

Table 1-1. Data inventory. Core logging of W-4 was performed indirectly (more details in Chapter 2).

Well	Gamma Ray log	Core	Palynology	Micro-resistivity images	Formation Pressure points
W-1	*		*		
W-2	*	*	*	*	
W-3	*		*		
W-4	*	-	*		
W-5	*		*		
W-6	*		*		
W-7	*	*		*	*
W-8	*	*		*	
W-9	*	*		*	*
W-10	*	*			*
W-11	*	*		*	
W-12	*				
W-13	*				
W-14	*				*
W-15	*				*
W-16	*				*
W-17	*				
W-18	*				*
W-19	*				*
W-20	*				
W-21	*				*

1.7. Methods

We address the sequence stratigraphic framework of the Cretaceous succession through the construction of a chronostratigraphic framework using palynological data sampled exclusively from cored intervals, as this data provides more reliable information regarding stratigraphic position compared to wellbore cuttings. Since palynology does not solely give information about relative dates, but also paleoecological information, a palynological marine index (MI) curve was

constructed using two broad groups, the total marine elements versus total continental elements. After establishing the chronostratigraphic framework, core-logging/description was conducted on seven core locations to correlate sedimentary structures and depositional environments. Core logging also included the construction of a bioturbation-index (BI) curve, which complements and refines our interpretation of possible depositional environments. Additionally, paleocurrent measurements were obtained from the interpretation of microresistivity images on highly reliable intervals, verified through the direct comparison with core data foot by foot.

Finally, we synthesize our results with additional wellbore locations and formation pore pressure data to build a robust sequence stratigraphic framework for the Southwestern Llanos Basin.

1.8. Organization

This thesis is presented in paper format, with its chapters following the standard stratigraphic workflow. Chapter One provides an overview of the general geological setting, including tectonics and stratigraphy. Chapter Two summarizes a core-based facies analysis, complemented by organic-walled microfossil and bioturbation index analyses, which refine the interpretation of the depositional environments. This chapter also incorporates sediment transport directions derived from the interpretation of microresistivity image logs. Finally, Chapter Three presents a sequence stratigraphic framework for the entire Upper Cretaceous wedge in the southwestern Llanos Basin. It integrates new observations from core and well data to explain the Cretaceous succession as a product of the interaction between accommodation and sedimentation. Last but not least, Chapter Four presents a discussion of the main conclusions of this effort, along with recommendations for future work.

1.9. References

Aspden, J.A., McCourt, W. J., and Brook, M. (1987). Geometrical control of subduction-related magmatism: the Mesozoic and Cenozoic plutonic history of western Colombia. Journal of the Geological Society. Vol. 144. p. 893-905.

Bayona, G., Cortes M., Jaramillo, C., Ojeda, G., Aristizabal, J.J., and Reyes-Harker, A. (2008). An integrated analysis of an orogen-sedimentary basin pair: Latest Cretaceous-Cenozoic evolution of the linked Eastern Cordillera orogen and the Llanos foreland basin of Colombia. GSA Bulletin. 120. p. 1171-1197. doi: https://doi.org/10.1130/B26187.1

Bayona, G., Bustamante, C., Nova, G., and Salazar-Franco, A.M. (2020). Jurassic evolution of the northwestern corner of Gondwana: Present knowledge and future challenges in studying Colombian Jurassic rocks. In: Gomez J., and Pinilla-Pachon A. O. (editors). The Geology of Colombia, Vol. 2 Mesozoic. Servicio Geológico Colombiano. Publicaciones Geológicas Especiales N. 36. p. 171-207. Bogotá. https://doi.org/10.32685/pub.esp.36.2019.05

Blakey, R.C. (2008). Gondwana paleogeography from assembly to breakup—A 500 m.y. odyssey. *In:* Fielding, C.R., Frank T.D., and Isabell, J.L., eds., Resolving the Late Paleozoic Ice Age in Time and Space. Geological Society of America Special Paper 441. p. 1-28 doi:10.1130/2008.2441(01)

Caballero, V., Naranjo, J., De La Parra, F., Mora, A., and Reyes-Harker, A. (2015). Estratigrafía de secuencias de los principales reservorios de la cuenca Llanos. XV Congreso Colombiano de Geología. Bucaramanga. Colombia.

Caballero, V.M., Rodríguez, G., Naranjo, J.F., Mora, A. and De La Parra, F. (2020). From facies analysis, stratigraphic surfaces, and depositional sequences to stratigraphic traps in the Eocene – Oligocene record of the southern Llanos and northern Magdalena Basin. In: Gómez J. and Mateus–Zabala, D. (eds). The Geology of Colombia. Vol. 3 Paleogene – Neogene. Servicio Geológico Colombiano. Publicaciones Geológicas Especiales 37. 48 p. Bogotá. https://doi.org/10.32685/pub.esp.37.2019.10

Carvajal Torres, J.S. (2021). The role of tectonism in the development of stratigraphic surfaces in the Colombian Llanos Foreland Basin. MSc Thesis 221 p.

Cooper, M., Addison, F., Alvarez, R., Coral, M. Graham, R. et al., (1995). Basin development and tectonic history of the Llanos basin, Eastern Cordillera, and Middle Magdalena Valley, Colombia. *AAPG Bulletin*. *Vol. 79*. No 10. p. 1421-1143.

Fajardo, A., Rojas, L., and Cristancho, J., (2000), Definición del modelo estratigráfico en el intervalo cretáceo tardío a mioceno medio en la cuenca llanos orientales y piedemonte llanero: Bucaramanga, Instituto Colombiano del Petróleo, Internal Report, p. 200.

Gelvez, J., Villamizar, C., Velasquez, A., Mora, A., Caballero V., De La Parra F., Ortiz J., and Cardozo, E. (2016). Re-thinking reservoirs: The case of the T2 sands in the southern Llanos basin of Colombia. AAPG ICE Conference paper. Search and discovery article No. 80559.

Guerrero, J. and Sarmiento, G. (1996). Estratigrafía Física, Palinología, Sedimentológica y Secuencial del Cretácico Superior y Peleoceno del Piedemonte Llanero. Implicaciones en Exploración Petrolera. Geología Colombiana No. 20 p 3-66 Bogotá.

Guerrero, J. Sarmiento, G. and Navarrete, R. (2000). The stratigraphy of the W side of the Cretaceous Colombian basin in the Upper Magdalena Valley. Reevaluation of selected areas and type localities including Aipe, Guaduas, Ortega, and Piedras. Geología Colombiana. Vol. 25. Bogotá. p. 45-110.

Hoorn, C., Wesselingh, F.P., ter Steege, H., Bermudez, M.A., Mora, A., Sevink, J., Sanmartín I., Sanchez-Meseguer, A., Anderson C.L., Figueiredo, J.P., Jaramillo, C., Riff, D., Negri F.R., Hooghiemstra, H., Lundberg, J., Stadler, T., Särkinen, T., and Antonelli, A. (2010). Through Time: Andean Uplift, Climate Change, Landscape Evolution, and Biodiversity. Science. Vol. 330.

Horton, B.K., Saylor, J.E., Nie, J., Mora, A., Parra, M., Reyes-Harker, A., and Stockli, D.F. (2010). Linking sedimentation in the northern Andes to basement configuration, Mesozoic extension, and Cenozoic shortening: Evidence from detrital zircon U-Pb ages, Eastern Cordillera, Colombia. Bulletin of Geological Society of America. Vol. 122. No 9-10. p. 1423-1442. https://doi.org/10.1130/B30118.1

Hubach, E. (1957). Contribución a las unidades estratigráficas de Colomba. Informe No. 1212 Instituto Geológico Nacional. Bogotá 166 p.

ICP, (2012). W-1. Internal report 08-12. Ecopetrol-ICP. Piedecuesta, Colombia.

ICP, (2013). W-6. Internal report 11-13. Ecopetrol-ICP. Piedecuesta, Colombia.

ICP, (2014a). Sagu Creek, las Blancas Creek and wells W-3 and Ctal-1. Internal report 20-14. Ecopetrol-ICP. Piedecuesta, Colombia.

ICP, (2014b). W-5. Internal report 08-14. Ecopetrol-ICP. Piedecuesta, Colombia.

ICP, (2015). W-2. Internal report 13-15. Piedecuesta, Colombia.

ICP, (2021). W-4. Internal report 01-21. Ecopetrol-ICP. Piedecuesta, Colombia.

Kerr, A.C. (1998). Oceanic Plateau formation: A cause of mass extinction and black shale deposition around the Cenomanian-Turonian boundary? Journal of the Geological Society. Vol. 155. p. 619-626.

Kerr, A.C. (2005). Oceanic LIPs: The kiss of Death. Elements. Vol. 1. p. 289-292.

Leckie, R.M., Bralower, T.J., and Cashman, R. (2002). Oceanic anoxic events and plankton evolution: Biotic response to tectonic forcing during the mid-Cretaceous. Paleoceanography. Vol. 17. No. 3. https://doi.org/10.1029/2001PA000623

Montes, C., Rodriguez-Corcho, A.F., Bayona, G., Hoyos, N., Zapata, S., and Cardona, A. (2019). Continental margin response to multiple arc-continent collisions: The northern Andes-Caribbean margin. Earth-Science Reviews. Vol. 198. p. 1-19. https://doi.org/10.1016/j.earscirev.2019.102903

Mora, A., Gaona, T., Kley, J., Montoya, D., Parra, M., Quiroz, L.I., Reyes, G., and Strecker, M.R. (2009). The Role of inherited extensional fault segmentation and linkage in contractional orogenesis: a reconstruction of Lower Cretaceous inverted rift basin in the Eastern Cordillera of Colombia. Basin Research. Vol. 21. p. 111-137. https://doi.org/10.1111/j.1365-2117.2008.00367.x

Moreno, C.J., Horton, B.K., Caballero, V., Mora, A., Parra, M., and Sierra, J. (2011). Depositional and provenance record of the Paleogene transition from foreland to hinterland basin evolution during Andean orogenesis, northern Middle Magdalena Valley Basin, Colombia. Journal of South American Earth Sciences. Vol 32. p. 246-263. https://doi.org/10.1016/j.jsames.2011.03.018

Parravano, V., Teixell, A., and Mora, A. (2015). Influence of salt in the tectonic development of the frontal thrust belt of the Eastern Cordillera, Guatiquía area, Colombian Andes. Interpretation 3, p. SAA17-SAA27. https://doi.org/10.1190/INTe2015e0011.1.

Poulsen, C.J., Gendaszek, A.S., and Jacob, R.L. (2003). Did the rifting of the Atlantic Ocean cause the Cretaceous thermal maximum? Geological Society of America. Vol. 31. No. 2. p. 115-118.

Sarmiento-Rojas, L.F. (2001). Mesozoic rifting and Cenozoic basin inversion history of the Eastern Cordillera Colombian Andes inferences from tectonic models. PhD. Thesis Univ. of Amsterdam. 295 p.

Sarmiento-Rojas, L.F. (2011) Llanos Basin. Geology and hydrocarbon potential. In: Cediel F. and Ojeda G. Y. (eds). Petroleum geology of Colombia, Vol 9. Universidad Eafit for ANH, Medellín, p 192.

Sarmiento-Rojas, L.F. (2019). Cretaceous stratigraphy and paleo-facies maps of northwestern South America. In: Cediel F and Shaw R. P eds. Geology and Tectonics of Northwestern South America: The Pacific-Caribbean-Andean Junction. Frontiers in Earth Sciences. p. 673-747. https://doi.org/10.1007/978-3-319-76132-9_10

Reyes-Harker, A., Ruiz Valdivieso, C.F., Mora, A., Ramirez-Arias, J.C., Rodriguez, G., De la Parra F., Caballero, V., Parra, M., Moreno, N., Horton, B.K., Saylor, J.E., Silva, A., Valencia, V., Stockli, D., and Blanco, V. (2015). Cenozoic paleogeography of the Andean foreland and retroarc hinterland of Colombia. AAPG Bulletin. Vol. 99. No. 8. p. 1407-1453.

Valderrama, Y., and Catuneanu, O. (2024). The Upper Cretaceous rock record in the Southwest of Llanos Basin, Colombia: An integrated Facies Analysis. In preparation.

Villagomez, D., Spikings, R., Magna, T., Kammer, A. Winkler, W. and Beltran, A. (2011). Geochronology, geochemistry and tectonic evolution of the Western and Central cordilleras of Colombia. Lithos Vol. 125. p. 875-896.

Villamil, T. (1999). Campanian-Miocene Tectonostratigraphy, depocenter evolution and basin development of Colombia and western Venezuela. Palaeo. Vol. 153. p. 239-275.

Villamil, T. (2003). Regional hydrocarbon systems of Colombia and western Venezuela: Their origin, potential, and exploration, *in* Bartolini C, Buffler, R. T. and Blickwede, J. eds., The Circum-Gulf of Mexico and the Caribbean: Hydrocarbon habitats, basin formation, and plate tectonics: AAPG Memoir. vol. 79, p. 697-734.

Chapter 2. The Upper Cretaceous rock record in the Southwest of Llanos Basin, Colombia: An integrated Facies Analysis.

Abstract

The Upper Cretaceous sequence of the Southwestern Llanos Basin (SWLB), Colombia, consists of three formations: Une, Chipaque, and a portion of the Lower Guadalupe. Previous studies have primarily focused on the Eastern Cordillera, where the depositional settings differ from those in more landward areas such as the SWLB. A more precise understanding of these depositional environments is still needed to support ongoing exploration and production in the SWLB. To uncover the hidden characteristics of these formations, we used an integrated approach combining sedimentology, stratigraphy, palynology, and ichnology, focusing on core data from the SWLB.

Conglomeratic sandstones with subangular clasts capped by paleosols constitute sparse alluvial deposits on top of the Paleozoic sequence. They may correspond to remnant deposits from the bypass and erosional periods between the Upper Cretaceous sequence and the Paleozoic basement.

Within the Une Formation, organic microfossil content reveals the presence of marine palynomorphs within the fine-grained beds interbedded within the 'massive' multistory deposits. These observations support a marine influence on the sedimentation of this Formation. Similar results are observable within the Lower Guadalupe Formation. The Chipaque Formation has the highest total marine counts among the three Upper Cretaceous units. However, there are some intervals within the Chipaque Formation where the continental palynological content is also significant, suggesting that some intervals corresponds to continental marine-influenced depositional settings at the study location.

The multistory channel deposits of the Une Formation are interpreted to have been deposited in a coastal setting at the study location. From base to top, there is a progressive change in its depositional environment, a continental-dominated setting at the bottom to a continental marine-influenced setting in the middle and upper segments. The middle and upper segments of Une are frequently punctuated by marine invasions, likely related to autogenic processes.

A strong cyclic imprint within the rock sequence suggests that this area underwent significant tidal conditions, especially notorious during the sedimentation of the Chipaque Formation (Middle Turonian- Middle-Campanian). Anoxic and/or dysoxic conditions at the bottoms can be inferred from the lack of bioturbation in the dark gray mudrocks of the Chipaque Formation. Constant fluctuation in water salinity, provoked by tidal action, may have intensified the stressful conditions for benthic organisms. Bioturbation primarily occurred as an opportunistic behavior, increasing seaward (northwest), and decreasing landward (southeast).

An environmental-response subdivision for the Chipaque Formation is presented here: at the base a transgressive brackish-water setting (estuarine complex), and at the top, a muddy regressive proximal offshore/embayed area with a strong aggrading component, although with an increase in coarse-grained interbedding in the last section.

Robust lithological evidence supports the interpretation of an Intra-Campanian unconformity, that separates the fine-grained rocks of the Chipaque Formation from the coarse-grained rocks of the Lower Guadalupe Formation.

The fraction of the Lower Guadalupe Formation present at the study location is interpreted to have been deposited in a delta plain to a delta front setting.

Image-log interpretation backed by core data indicates that during the Middle Cenomanian – Middle Turonian (Une Formation), rivers transported sediment from the southeast and deposited into the sea in a northwest direction, whereas during the Middle Campanian (Lower Guadalupe Formation), rivers transported sediment towards the west-northwest.

2.1. Introduction

Since humans were not present at the time of sedimentation of ancient rocks, we appeal to the observation of modern processes to decipher the past events. In that sense, facies analysis plays a fundamental role in unraveling the responses captured in the rock fabric in a particular location, providing key elements for the interpretation and reconstruction of past depositional settings (Catuneanu, 2006).

This paper provides a summary of integrated sedimentological research conducted on the Upper Cretaceous sedimentary wedge of the southwestern Llanos Basin (SWLB), Colombia. The Cretaceous wedge consists of three formations: Une, Chipaque, and part of the Lower Guadalupe. The Une and the Lower Guadalupe formations are conventional reservoir rocks, while the Chipaque Formation is mainly a source rock.

Previous studies have significantly improved our understanding of the depositional settings of these formations, however, these investigations have been conducted on outcrops along the Eastern Cordillera (e.g., Julivert, 1962; Perez and Salazar, 1978; Guerrero and Sarmiento, 1996; Montoya and Reyes, 2005), where their depositional settings depart from what can be observed at landward locations such as the SWLB (Fig. 2-1).

By focusing on this region, we aim to contribute to enhance understanding of the sedimentological response to the physical processes that the Upper Cretaceous sediments underwent during their sedimentation in the area of SWLB, and properly connect them to their corresponding depositional settings.

To achieve this objective, we implemented an integrated approach combining sedimentology, stratigraphy, ichnology, and palynology on seven cores that span nearly the entire Upper Cretaceous interval. Unlike outcrop data from Eastern Cordillera, core data from the subsurface of SWLB offer the advantage of having fresh rock samples in a relatively structurally quiet area.

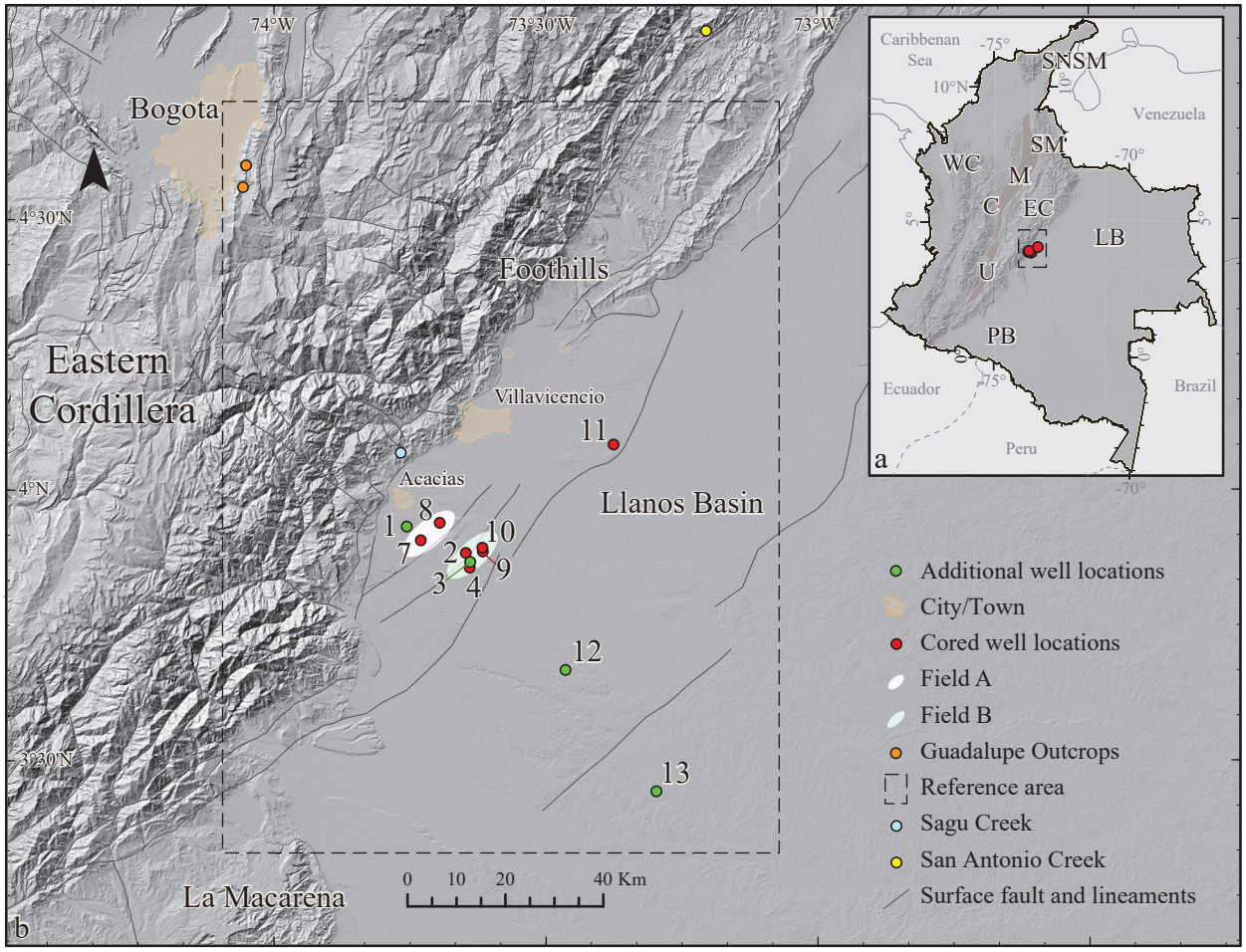

Figure 2-1. Regional topographic maps. **a**) Regional topographic map of Colombia showing the main topographic landmarks. Western Cordillera (WC); Central Cordillera (C); Middle and Upper Magdalena Valley (M and U); Eastern Cordillera (EC); Sierra Nevada de Santa Marta (SNSM); Santander Massif (SM); Llanos Basin (LB); Putumayo Basin (PB). **b**) Zoom in southwestern Llanos Basin, and adjacent areas. Red dots correspond to the analyzed cored well locations; green dots represent additional non-cored and cored well locations; orange dots are part of the studied outcrops of the Guadalupe Group by Perez and Salazar, 1978; blue dot indicates the Sagu Creek - a study location by the ICP, 2014; yellow dot correspond to the San Antonio Creek - a study location by Guerrero and Sarmiento, 1996. Topographic data from NASA, (2000).

2.2. Geological setting

2.2.1. Tectonic setting

The Cretaceous Basin in the northwestern area of South America underwent two distinct tectonic stages. During the early Cretaceous, the region experienced the continuation of a rifting period associated with the separation of the North and South American continents (Cooper et al., 1995). During the late Cretaceous the region experienced contraction marked by the transport, subduction, and accretion of allochthonous terrains from western locations to the northwestern side of the South American plate (Cooper et al., 1995; Villamil, 2003; Villagomez et al., 2011; Fig. 3-2a). Among these allochthonous terrains were large masses of volcanic oceanic plateaus, which, during their formation, possibly contributed to elevated atmospheric levels of CO2 concentrations, the acidification of oceanic water, and oceanic anoxia (Kerr, 1998; Leckie et al., 2002; Kerr, 2005; Fig. 3-2b).

2.2.2. Stratigraphy

From a regional perspective, part of the Upper Jurassic sequence, the entire Cretaceous sequence, and part of the Lower Paleogene is classified as a mega depositional sequence (Sarmiento-Rojas, 2001) with a maximum transgression close to the Early Turonian (Villamil, 2003), including smaller transgressive-regressive cycles (e.g., Guerrero et al., 2000; Sarmiento-Rojas, 2001). In some areas of the Cretaceous Basin, especially in the depo-centers (the ancient areas of Eastern Cordillera and Middle Magdalena Valley), sedimentation was locally continuous from the uppermost Jurassic to the Cretaceous without any apparent discontinuity (Sarmiento-Rojas, 2001); however, most of the Cretaceous sequence rests unconformably on older rocks, and the sequence becomes thinner outside of the depo-center areas (Sarmiento-Rojas, 2001), such as the Upper Magdalena Valley Basin or the Llanos foreland Basin (Fig. 2-2a).

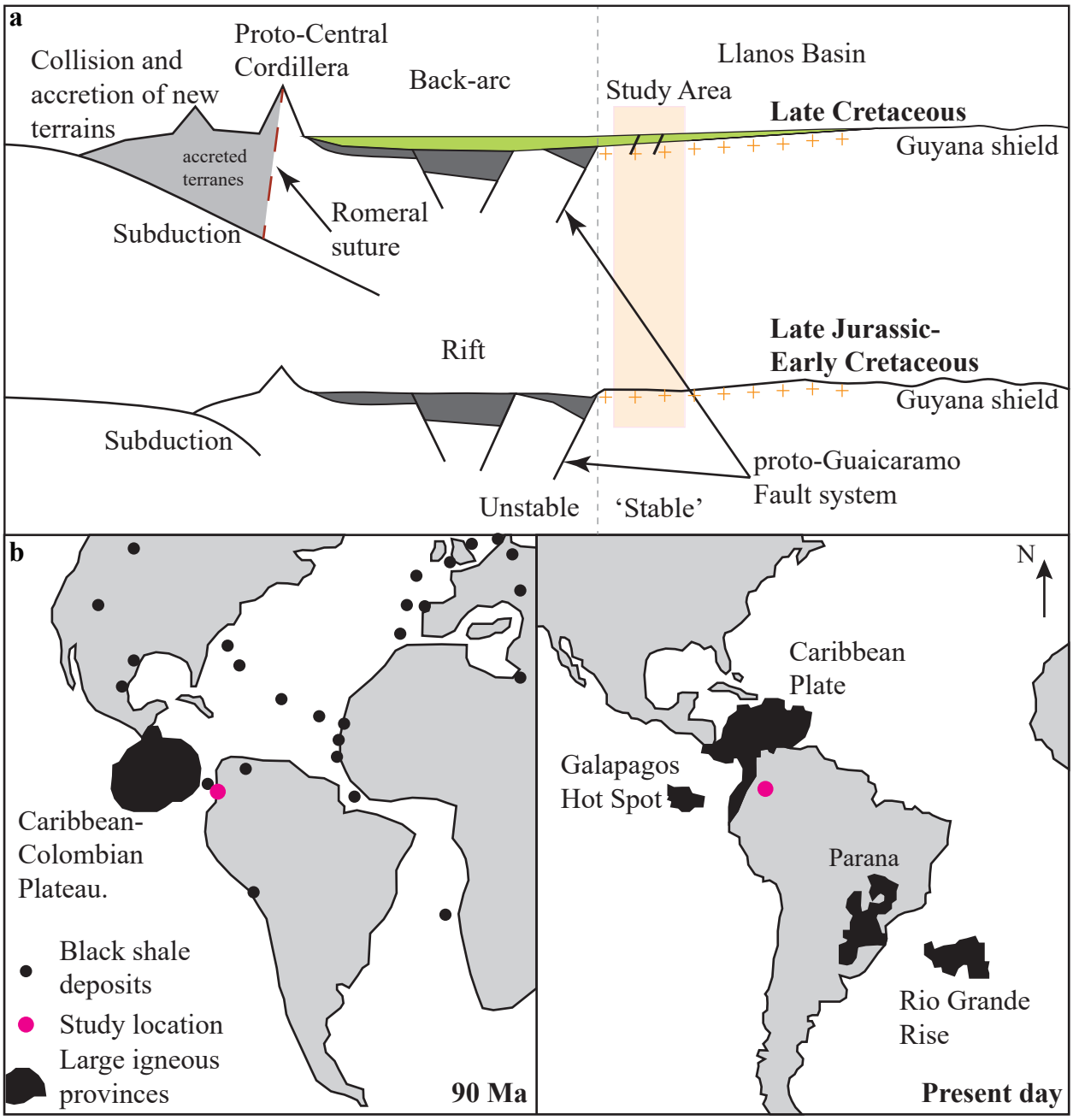

Figure 2-2. Geological setting. **a**) Schematic basin evolution in cross-section. (Modified from Horton et al., 2010). Two basin systems for the Cretaceous period - a rift and a back-arc. For the study area, the Early Cretaceous was a period of exposure and sediment bypass, whereas for the Upper Cretaceous some sedimentation, but also erosion, took place. **b**) Eastern Pacific large igneous provinces during the Turonian and their present-day locations. Part of the igneous material was transported and accreted to the western margin of Northern-South American plate. (Modified from Kerr, 1998).

The Cretaceous rock record toward the west of the study area (Fig. 3-3) begins with the Brechas de Buenavista Formation, succeeded by the mudstones of Macanal and Caqueza Formations. These formations are overlain by the Villeta Group which comprises the Fomeque, Une and Chipaque formations. Moving further east of Guaicaramo fault-system (Fig. 3-3) only Une and Chipaque formations are present as part of the Villeta Group. For that reason, the term Villeta Group is not recommended for use eastward of this major fault system (Guerrero and Sarmiento, 1996).

Overlying the Villeta Group, is the Guadalupe Group, composed of three formations Lower, Middle and Upper Guadalupe, (also known in the Eastern Cordillera as Dura, Plaeners and Labor-Tierna respectively). Similarly to the Villeta Group, the Guadalupe Group is not completely present to the east of the Guaicaramo fault-system as erosion in this area took place in several stages, leaving incomplete parts of the upper Cretaceous (Fig. 2-3).

In the southwestern side of Llanos Foreland Basin, the Cretaceous rock record comprises three Formations: Une, Chipaque, and a small portion of Lower Guadalupe. These formations are bounded by regional subaerial unconformities, which separate them from the underlying Paleozoic, and the overlying Cenozoic rocks (Fig. 2-3). The analyzed core data indicates that internally, the Lower Guadalupe and Chipaque Formations are separated by another erosive surface, referred to here as the Intra-Cretaceous subaerial unconformity (Fig. 2-3). Similarly, the analyzed core and log data revealed the occasional occurrence toward the base of the Cretaceous wedge, of some sparse deposits trapped among erosional periods and in turn separating the Une Formation from the Paleozoic sequence (Fig. 2-3).

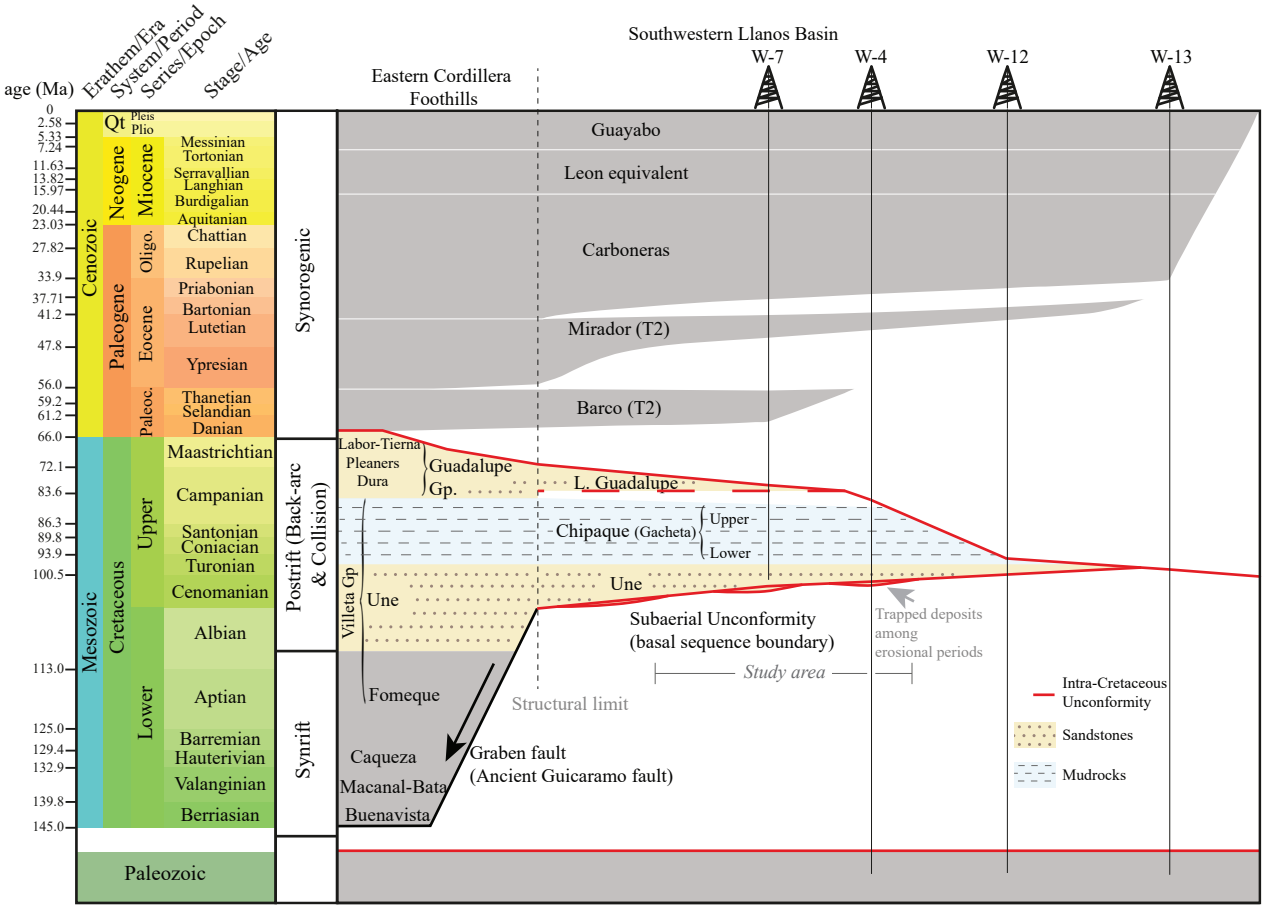

Figure 2-3. Schematic stratigraphic chart for the southwestern Llanos Basin. Rock ages for the study area based on relative palynological dates from internal reports (ICP, 2012, 2013, 2014a, 2014b, 2015). Sedimentological data points out the occurrence of Intra-Campanian unconformity. Sequence stratigraphic analysis links it with a forced regressive event that took place during the Middle Campanian (Valderrama and Catuneanu, 2024). It is expected that this subaerial unconformity may have extended basinward up to the fault rift system. Sedimentological evidence and well logs data support the interpretation of a basal unit consisting of sparse alluvial deposits trapped during erosional periods between the base of the Une Formation and the Paleozoic rocks (e.g., W-4, Fig. 2-7). Specific well locations can be found in figure 2-1b. Gray colored formations were not part of this study. Stratigraphic chart modified from Sarmiento-Rojas, 2011; Reyes-Harker et al., 2015; Sarmiento-Rojas, 2019).

2.3. Methodology

Seven cored wells (W-2, W-4, W-7, W-8, W-9, W-10, and W-11; Fig. 2-1b) were sedimentologically analyzed with the goal of unveiling their sedimentation process and properly linking to their depositional environment. These cored wells almost cover the entire Upper Cretaceous wedge of the southwestern Llanos Basin, Colombia

Six of the seven cores were logged in detail, unfortunately, one core (W-4) was not available for in-person examination, however, based on its 'acceptable' core-photo set, it was possible to estimate the grain-size curve, identify some of the sedimentary structures, the clasts shape, and detect the possible presence of biogenic structures such as rhizoliths.

For each cored-well location, a Bioturbation-Index (BI) curve was created to observe the trace-fossil distribution along the rock record. They were constructed by comparison with the schematic BI developed by Bann et al., (2008). BI values range from 0 to 6, where BI 0 corresponds to an unbioturbated layer, and BI 6 indicates full layer homogenization caused by the organisms (Gingras et al., 2011).

In addition to sedimentological and basic ichnological observations, a set of palynological data was incorporated to aid in environmental interpretation. This data set correspond to different stratigraphic intervals and wells, covering almost the entire span of study (Fig. 2-4).

Core-logging was initially conducted in the core depth domain and subsequently adjusted to the open-hole gamma ray log using core gamma and image logs. Most cored locations have microresistivity image logs (W-2, W-7 W-8 W-9 W-10, and W-11; Fig. 2-1b) which were also interpreted as part of this study.

The electrical raw image logs from field were processed using commercial software program, following standard procedures for environmental quality and corrections (e.g., Lai et al., 2018). Once the static and dynamic images were obtained, the interpretation step began. Bedding and crossbedding surfaces were picked solely from reliable readings supported by core data (e.g.,

Fig. 2-5a). This validation step was performed foot-by-foot, by simultaneously comparing the electrical images with core photos (compare Figs. 2-5a vs 2-5b). Afterward, the structural tilt was removed from the crossbeddings to obtain the true dip directions of sediment transport. Additionally, coarser-grained cored intervals, especially those with larger dip magnitudes in their internal stratification were oriented (e.g., Fig. 2-5a). Conversely, fine-grained cored intervals remained unoriented due to the lack of complete certainty in their orientation.

For confidentiality reasons, the initial digit of each log or core depth is coded alphabetically, and the true well names were replaced with simple numbers.

2.4. Palynological analysis

Despite the limited palynological data, characterized by few sampling locations and often low temporal resolution, the Cretaceous rock record in the study area has a fair palynological data set for the most part. Since some of the available palynological results have discriminated the total continental palynomorph counts from the total marine counts, this afforded a preliminary approach to determine their depositional settings. Based on the palynological yield and marine index ratio, the Upper Cretaceous sequence can be classified into the following gross depositional settings:

1. Continental settings: Composed exclusively of continental palynomorphs (i.e., pollen and spores).
2. Continental marine-influenced settings: Composed of a mix of continental and marine palynomorphs. However, the number of continental palynomorphs is relatively high in comparison to the number of marine palynomorphs (i.e., foraminiferal linings, dinocysts, copepod eggs, and acritarchs). To quantify this, a ratio of marine to continental elements (M/C ratio) was implemented. A simple visual inspection was used to define the value of two (2), as the maximum threshold for the marine index ratio of this group (M/C ratio < 2). Note that any chosen value will be an arbitrary value; however, there is some correlation between this limit and the dominant lithology type (Fig. 2-4).

3. Marine to marginal marine settings: also characterized by a mix of continental and marine elements. For marine and marginal marine settings, the ratio of marine palynomorphs in comparison to the previous group is larger (M/C ratio > 2) (Fig. 2-4).

From the bottom of the Une Formation, three pollen- and spores-rich samples without any marine elements were reported from W-4 (c103.25, c107.25, and c174.92 ft md plus core shift; green arrows in Fig. 2-4). This result indicates that the lower part of the section in W-4 was deposited in a fully continental setting without direct marine contact. However, this classification cannot be generalized to the entire base of the Une Formation, as this palynological data in W-4 may represent a sheltered location.

From the intermediate section of the Une Formation, the palynological study of W-2 (c474.5-c661.8 ft md plus core shift; Fig. 2-4) identified marine elements (e.g., foraminifers, dinocysts, copepod eggs, and acritarchs) within the muddy layers interbedded with the large-stacked sandstone beds of the Une Formation (horizontal blue lines in Fig. 2-4). These marine elements suggest proximity to/influence of the sea on the sedimentation of this unit. However, the ratio of marine to continental counts was low to very low (M/C < 2). Based on the presence of marine elements in relatively low proportions, this unit could be classified as a continental marine-influenced setting, where the fine-grained intervals with marine elements are the result of high-frequency transgressions and/or autogenic processes like lobe abandonment.

Moving upwards in the sedimentary sequence to the fine-grained lithologies of the Chipaque Formation (i.e., W-3, W-2, and W-1; b626-b818, b870-c015, f345-f360 ft md respectively; Fig. 2-4), the marine counts are (in most cases) significantly higher compared to those in the Une Formation. The ratios of marine to continental counts are notably higher in Chipaque than in the Une Formation (M/C >>2) for most sampled intervals, suggesting that the coastline may have been further away during sedimentation of the Chipaque Formation than during the sedimentation of the Une Formation. However, some intervals within the Chipaque Formation present similar total marine counts and marine ratios (e.g., W-3, b804-b817 ft md, Fig. 2-4) to those in the Une Formation, indicating that the coastline may have been closer during certain intervals/periods. Based on the elevated but variable marine indices observed, the Chipaque

Formation at the study location is interpreted to be mainly deposited in a marine to marginal marine setting.

Within the fine-grained beds of the Lower Guadalupe in W-1, just below the Paleocene subaerial unconformity (f240-f265, Fig. 2-4), the palynological yield exhibits similar marine-to-continental ratios to some intervals within the Chipaque Formation. This palynological yield suggests probable sedimentation in a marine to marginal marine setting. However, it's worth noting that the (fine-grained) sample interval may overrepresent the entire unit, hence the sandier packages of this formation may have been deposited in a continental marine-influenced setting similar to the Une Formation.

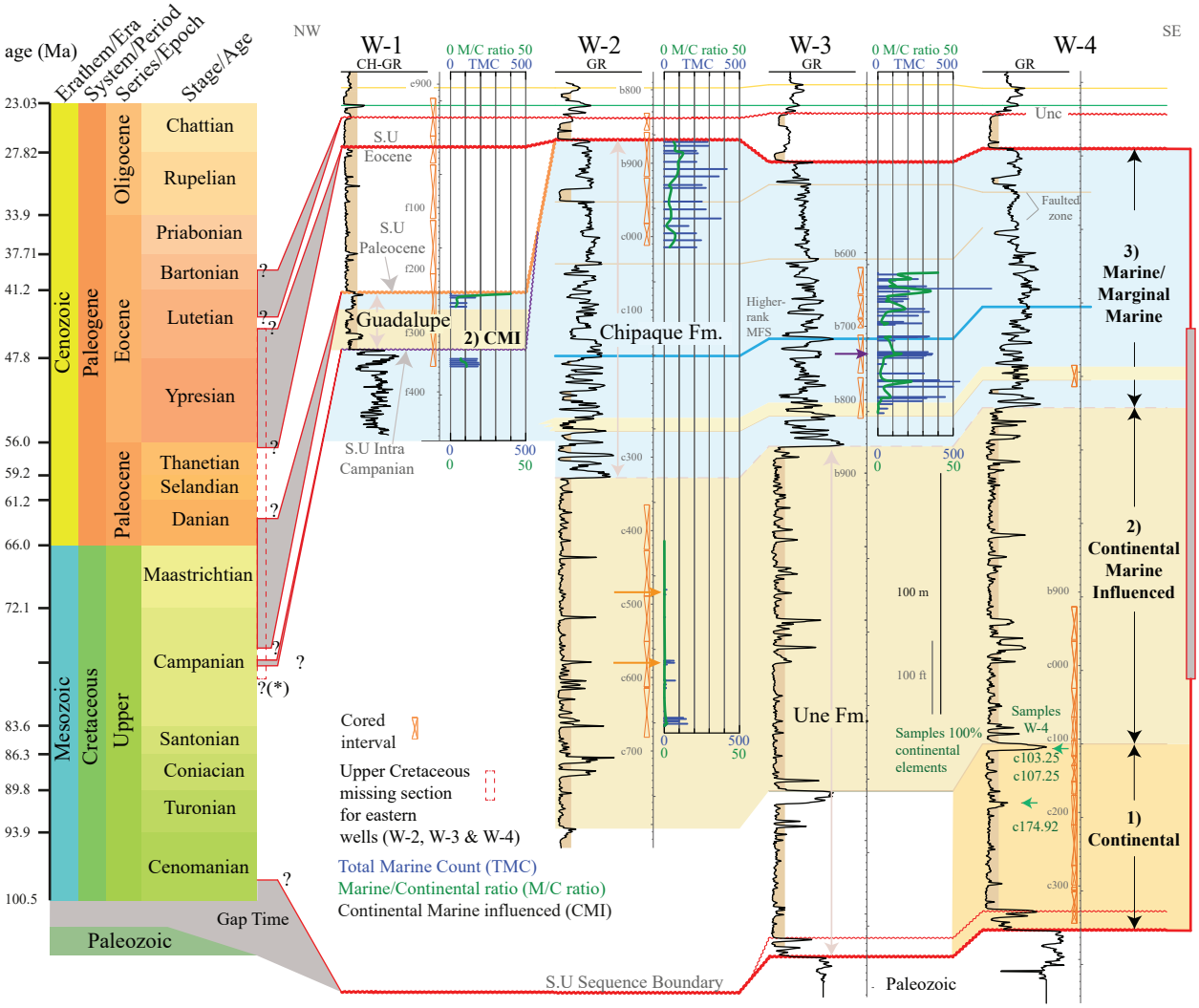

Figure 2-4. Upper Cretaceous Palynological yield and Marine/Continental ratio for the southwestern Llanos Basin. Horizontal blue bars (in W-1, W-2 and W-3) represent the total marine counts reported for each sample. Green polylines superimposed over the total marine counts represent the marine index ratio (marine to continental total counts). Green arrows within the lower part of W-4 indicate the sampling depths with 100% continental yield. This location and interval could be either interpreted as deposited landward of the bayline (*sensu* Bhattacharya, 2010) marked by a complete occurrence of continental palynomorphs or sheltered from the direct marine influence.

Locations/intervals of W-1, W-2 and W-3, are interpreted to be deposited seaward of the bayline, characterized by the incorporation of marine elements. The Chipaque Formation (e.g., W-2 and W-3) exhibits the larger total marine counts and marine index ratios. At western locations (i.e., W-1) the Upper Cretaceous is affected by the Paleocene subaerial unconformity and by the Intra-Campanian subaerial unconformity; (light gray areas represent the gap time or missing section). (*) At eastern locations (i.e., W-2, W-3, and W-4), the Middle Eocene unconformity puts Eocene rocks in direct contact on top of Middle/Lower Campanian rocks (dashed box line next to the chronostratigraphic chart represent the gap time from the Campanian up to the Eocene).

All samples reported here correspond to cored intervals*;* depths were shifted based on open hole gamma ray or in the case of W-1 based on the cased hole gamma ray (CH-GR). The initial digit of each log or core depth is coded alphabetically, and the true well names were replaced with simple numbers. Total marine and/or continental counts for wells W-1 W-2 W-3 and W-4 were taken from the following internal reports: ICP, 2012, 2015, 2014 20-14 and 2021, respectively.

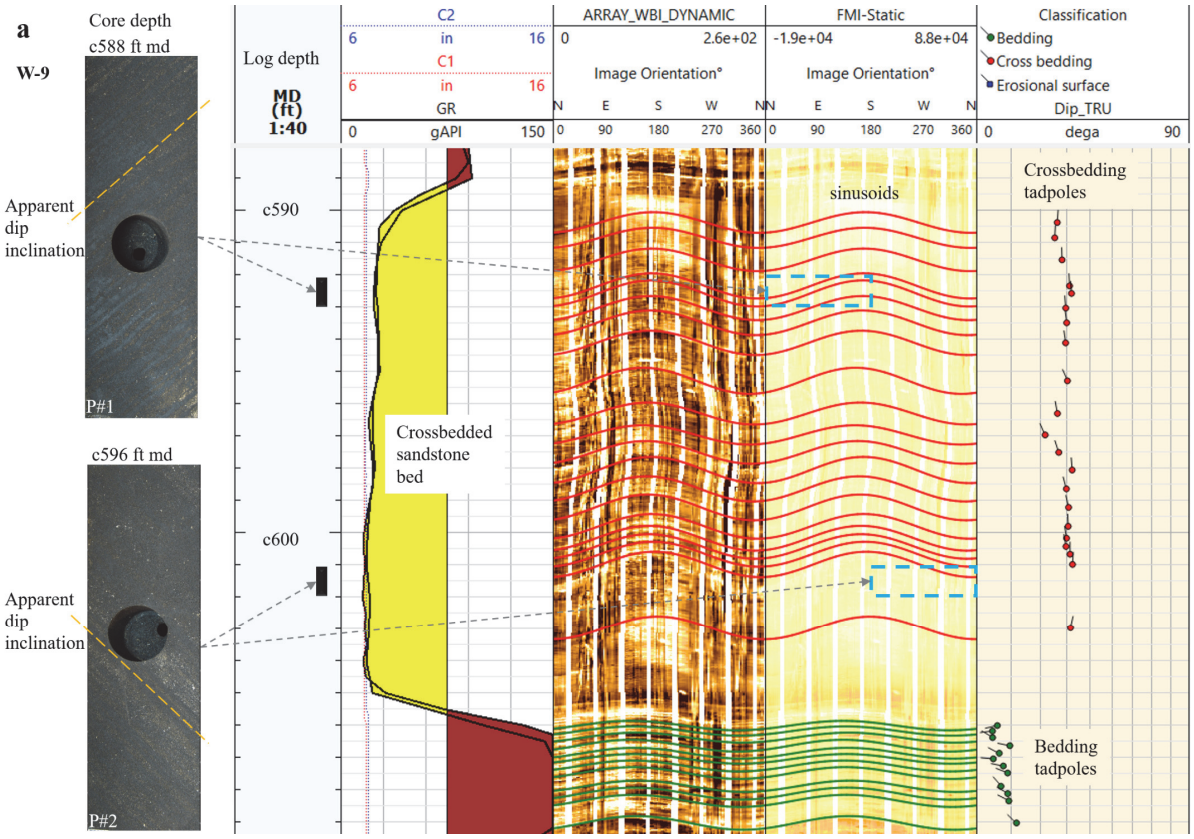
a
W-9
Core depth
c588 ft md
Log depth
MD
(ft)
1:40
C2
6 in 16
C1
6 in 16
GR
0 gAPI 150
ARRAY_WBI_DYNAMIC
0 2.6e+02
Image Orientation°
N E S W N
0 90 180 270 360
FMI-Static
-1.9e+04 8.8e+04
Image Orientation°
N E S W N
0 90 180 270 360
Classification
Bedding
Cross bedding
Erosional surface
Dip_TRU
0 dega 90
Apparent
dip
inclination
P#1
c590
Crossbedded
sandstone
bed
sinusoids
Crossbedding
tadpoles
c596 ft md
Apparent
dip
inclination
P#2
c600
Bedding
tadpoles

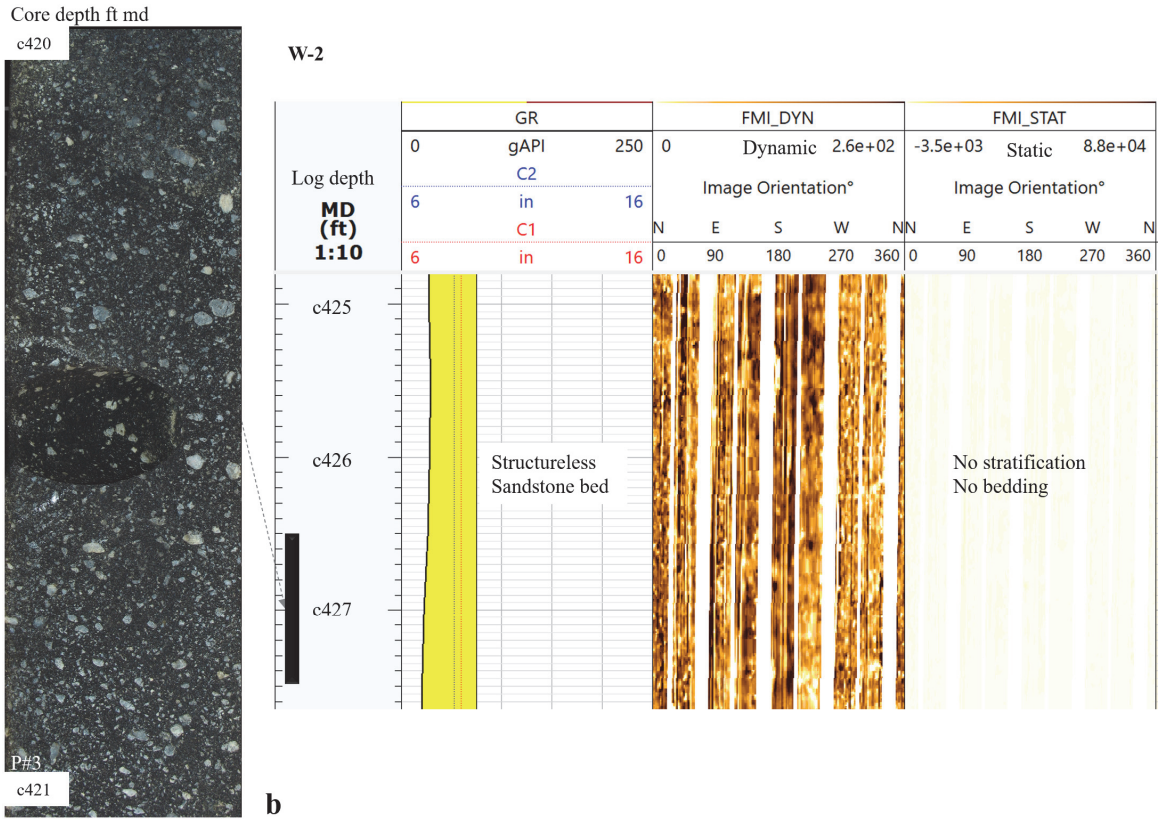
Core depth ft md
c420
P#3
c421
W-2
Log depth
MD
(ft)
1:10
GR
0 gAPI 250
C2
6 in 16
C1
6 in 16
FMI_DYN
0 Dynamic 2.6e+02
Image Orientation°
N E S W N
0 90 180 270 360
FMI_STAT
-3.5e+03 Static 8.8e+04
Image Orientation°
N E S W N
0 90 180 270 360
c425
c426
c427
Structureless
Sandstone bed
No stratification
No bedding
b

Figure 2-5. Core and image log data. **a**) Crossbedded sandstone bed photos and electrical image log interpretation for W-9. On the left, two core photos (P# 1 and 2) for the same bed with apparent opposite internal stratifications. On the center two electrical image logs (electrical image-logs are false-color images that represent the electrical conductivity (Fox and Vickerman, 2015)), one dynamic and one static displayed as unwrapped view of the borehole. The difference between these two images is just the color-normalization window (Fox and Vickerman, 2015). For the static images, the entire logged interval is color normalized, whereas for the dynamic images, the color normalization is done for small depth windows (commonly 2 or 3 feet), and the purpose of that is to enhance the visualization of the internal features (Fox and Vickerman, 2015). Over these two images are displayed the sinusoids and on the right two-color groups of tadpoles, the green ones corresponding to bedding planes (dipping to the West) and red ones, cross-stratification (dipping to the North). Notice the apparent opposite dip directions on the core photographs, this is caused by internal rotation during or after core acquisition, getting opposite sides of the core after the slabbing process. Orientation of the two photographs on the static image is indicated by discontinuous box lines. True core photographs depths are indicated by dashed gray arrow lines pointing to corresponding shifted depths. **b**) Conglomeratic sandstone bed and electrical image log for W-2. Both core photograph (P# 3) and image log have no internal stratification. In this case, the lack of internal stratification can be associated with autogenic resedimentation processes (e.g., Martin and Turner, 1998) or by an abrupt sedimentation. Notice on the electrical image log the presence of coarser grains dispersed along the dynamic image in a similar fashion to in the core photograph.

2.5. Facies Analysis

Each rock or sediment segment contains information about the physico-chemical processes that occurred during its sedimentation or immediately afterward. The identification of these intervals introduces the term facies, whose meaning has evolved over time to serve both descriptive and interpretive purposes (Dalrymple, 2010a).

Based primarily on the sedimentological analysis, complemented by basic ichnological control and palynological data where available, a total of eighteen recurring facies has been

identified across the three formations (Une, Chipaque, and Lower Guadalupe) that comprise the Upper Cretaceous wedge, as well as from a basal remanent unit among the Paleozoic rocks and the Une Formation (photo plates Figs. 2-6, 2-9 and 2-13; Table 2-1).

2.5.1. Facies Description

Facies 1 (F1). Conglomeratic sandstones to sandy conglomerates with rounded to subrounded clasts

Sedimentology

Its principal characteristic is the presence of subrounded and rounded clasts. Some gravel clasts may exceed pebble size (1.6 cm). The thickness of these deposits varies from a few centimeters to a few decimeters. Basal contacts are erosive. It is common to observe normal grading and occasionally imbrication, but also large clasts floating in a sandier matrix in a random distribution. Sorting varies from poor to moderate. No bioturbation is observed. (Fig. 2-6, F1 W-9).

Interpretation

In the overall grain-size context of this study, this facies contains the largest clast size, reflecting high-energy conditions like channel floor or the product of floodwaters, which may drag and dump coarser material outside of main channels onto finer-grained deposits.

Facies 2 (F2). Conglomeratic sandstones with angular to subangular clasts

Sedimentology.

This particular facies is present solely at the base of the entire sequence, specifically in core W-4, overlying the discordant contact with Paleozoic rocks (Fig. 2-7, at log depths c346-c358 ft md). It consists of thin (3-10 cm) to medium (10-30 cm) beds of conglomeratic

sandstones with a sandy to clayish matrix. The main distinctive characteristic is its angular- to subangular-shaped clasts of variable sizes (ranging from less than 1 cm up to 5 cm) reflecting a poor selection. Basal contacts are commonly erosional. No bioturbation is observed. (Fig. 2-6, F2 W-4).

Interpretation

Since sorting and clast roundness are functions of transport history (Nichols, 2009), this facies, unlike the previous facies, indicates a more proximal bedrock source. Similar to the previous facies, the presence of large clasts suggests high-energy systems or events, such as channel floors or the result of abrupt floodings that promotes the displacement of bedload clasts. However, the sedimentological properties of this facies differ from the overlying packages of the proper Une Formation. Additionally, well correlations indicate a discontinuous occurrence of this subunit, suggesting these deposits may represent isolated remnant deposits from erosional periods, likely corresponding to a pre-Une alluvial fan.

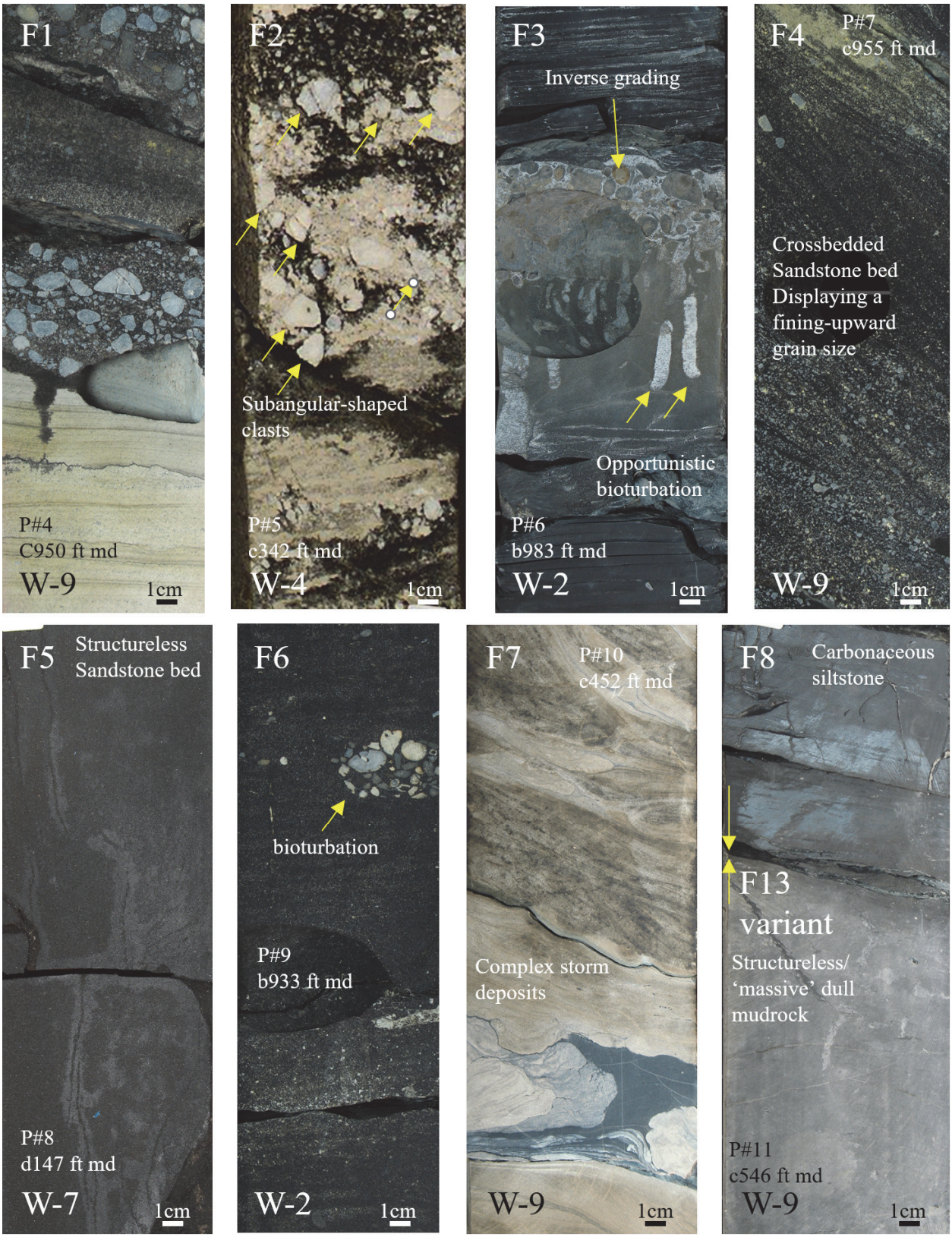
F1
P#4
C950 ft md
W-9
1cm
F2
Subangular-shaped clasts
P#5
c342 ft md
W-4
1cm
F3
Inverse grading
Opportunistic bioturbation
P#6
b983 ft md
W-2
1cm
F4
P#7
c955 ft md
Crossbedded Sandstone bed Displaying a fining-upward grain size
W-9
1cm
F5
Structureless Sandstone bed
P#8
d147 ft md
W-7
1cm
F6
bioturbation
P#9
b933 ft md
W-2
1cm
F7
P#10
c452 ft md
Complex storm deposits
W-9
1cm
F8
Carbonaceous siltstone
F13 variant
Structureless/ 'massive' dull mudrock
P#11
c546 ft md
W-9
1cm

Figure 2-6. Photo plate 1 of facies classification. Examples for facies 1 to 8 (F1…F8). F1 Displaying a sandier gravel bed eroding a finer-grained sandstone bed; F2. Subangular-shaped clast indicating a more proximal bedrock source; F3. Conglomeratic lag and associated bioturbation (event bed), displaying an inverse grading and an opportunistic bioturbation behavior with low diversity and intensity; F4. Tabular and trough cross-bedded sandstones representative of Une Formation, displaying high foresets inclinations and normal grading. Black color due to the oil saturation; F5. Unstructured sandstone bed. Microresistivity images confirmed lack of internal stratification; F6. Bioturbated coarse-grained sandstone bed. Yellow arrow pointing to a larger bioturbation feature. Internal stratification altered by the living-organism activity; microresistivity image logs confirmed the bioturbation; F7. Complex hummocky cross stratification; F8. The upper half of picture corresponds to Carbonaceous siltstones to coals facies. The ‘massive’ mudstone below corresponds to a variant of mudrocks of facies 13 and is interpreted to be deposited in a supratidal or intertidal environment.

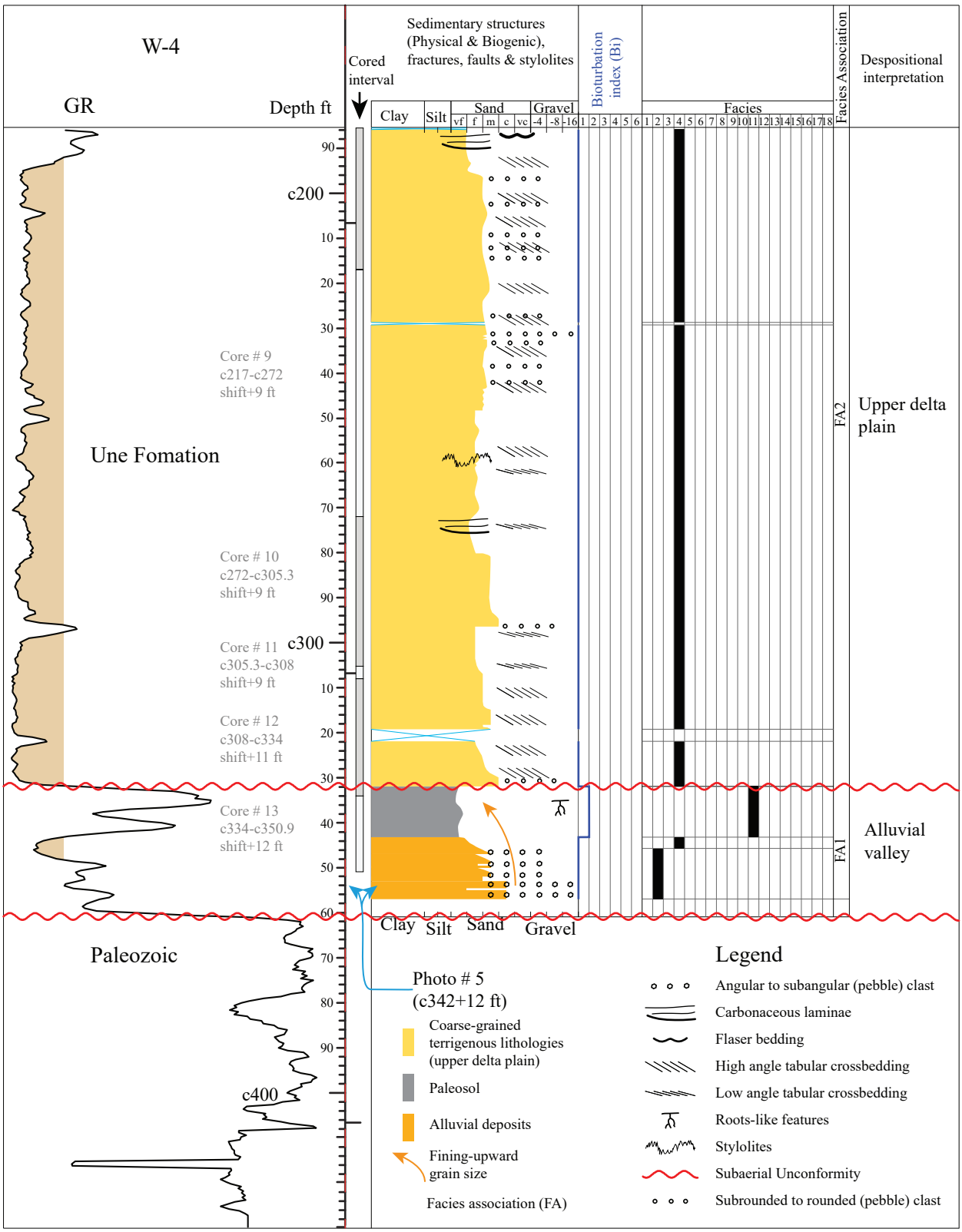
W-4
GR
Depth ft
Cored interval
Sedimentary structures (Physical & Biogenic), fractures, faults & stylolites
Clay
Silt
Sand
Gravel
vf f m c vc
Bioturbation index (Bi)
Facies
Facies Association
Despositional interpretation
c200
c300
c400
Core # 9
c217-c272
shift+9 ft
Core # 10
c272-c305.3
shift+9 ft
Core # 11
c305.3-c308
shift+9 ft
Core # 12
c308-c334
shift+11 ft
Core # 13
c334-c350.9
shift+12 ft
Une Fomation
Paleozoic
FA2
FA1
Upper delta plain
Alluvial valley
Photo # 5
(c342+12 ft)
Coarse-grained terrigenous lithologies (upper delta plain)
Paleosol
Alluvial deposits
Fining-upward grain size
Facies association (FA)
Legend
Angular to subangular (pebble) clast
Carbonaceous laminae
Flaser bedding
High angle tabular crossbedding
Low angle tabular crossbedding
Roots-like features
Stylolites
Subaerial Unconformity
Subrounded to rounded (pebble) clast

Figure 2-7. Core logging lower section of Une Formation and basal unit in W-4. The basal subunit has a sparse occurrence and is bounded at the top and base by unconformities. No bioturbation was observed except in the interpreted paleosol where some features that resemble roots are found.

Facies 3 (F3). Conglomeratic lags and associated bioturbation (Event beds)

Sedimentology

This facies occurs mostly in beds of few centimeters thick, exclusively within the Chipaque Formation. Clasts are rounded to semirounded with less than 1 cm in diameter, although occasionally there are larger tabular-shaped intraformationally eroded fragments. Grading varies, with some beds displaying normal grading, while others exhibit reverse grading with floating clasts in the upper part of the beds. One of the most notable characteristics of this facies is the presence of features associated with organic-living activity, however, its diversity and intensity are low. (Fig. 2-6, F3 W-2).

Interpretation

This facies represents an abrupt interruption to the underlying finer-grained interval successions. A high-energy depositional mechanism can be deduced from the contrasting lithologies, as well as the presence of rip-up clasts and the sharp-based contacts. The floating clasts in the upper part of the beds, with no apparent internal order, suggest that this abrupt and high-energy deposits may be the result of some type of density flow events (e.g., hyperpycnal, debris or turbiditic flows) that disrupt the continuum fallout sedimentation. These events may be related to seasonal floods or the collapse of some nearby coarser deposits. Interestingly, most of these thin deposits are accompanied by a notable bioturbation, which reflect an opportunistic behavior of the benthic community.

Facies 4 (F4). Tabular and trough cross-bedded sandstones

Sedimentology

This facies consists mainly of sandstone beds with trough and tabular stratification. Their thickness varies from thin (3-10 cm) to very thick (>1 m), and the grain size ranges from medium to coarse-grained sand, although other grain sizes are also present. Generally, but not exclusively, the foreset inclinations of the crossbeddings are higher in beds with the larger grain sizes and lower in those with finer-grain sizes. Commonly, larger clasts are located at the base of each crossbedding set, marking reactivation surfaces. Carbonaceous detritus, visible to the naked eye if the rock is not stained by black oil (a condition mostly occurring in finer-grained beds), also helps to distinguish reactivation surfaces. In some cases, the clasts at the bed boundaries are altered to clay minerals, reflected occasionally as high gamma ray values. Sorting varies from poor to moderate with a direct relationship to grain size —the smaller the grain size, the better the sorting, and vice versa. Grading is generally normal, however, occasionally appears as inverse. Notably, finer-grained layers lack oil stain, even when located above the oil-water contact. Another representative feature of the finer-grained beds is the presence of compaction structures, which increase in occurrence with depth. These thin features are composed of carbonaceous-organic detritus and are generally oriented parallel to the bed boundaries, indicating that the principal stress in this area is vertical. In terms of biological-activity record, this facies, commonly lacks trace fossils evidence (Fig. 2-6, F4 W-9).

Interpretation

This facies is interpreted to reflect sandy dune-scale bedforms indicating quasi-unidirectional flows at the level of crossbedding sets or, in some cases, cosets. Several characteristics support a high-energy depositional environment interpretation, such as (1) constant reworking and scouring evidenced from the erosive and sharp-base bounding surfaces; (2) the lack of a regional or semi-regional fine-grained interbedding beds (which belong to other facies classification); and (3) the lack of trace-fossils.

The palynological content from the fine-grained interbedding beds that separates the sandy bedforms varies from 100% continental to a mix of continental and marine elements. This content suggests proximity to the sea, indicating a coastal depositional setting (Fig. 2-4).

Finally, the clasts at the bed boundaries displaying alteration to clayish minerals, as mentioned in the description, reflect an additional process known as weathering, indicating short periods of exposure to climatic factors. In other words, they represent small and immature paleosols (which are grouped here as Facies 11).

Facies 5 (F5). Unstructured sandstones and irregular stratification

Sedimentology

This facies comprises a group of thin (3-10 cm) to medium (10-30 cm) sandstone beds characterized by either a lack of apparent internal structure or grading (observed in both oil-saturated and non-oil-saturated beds), or a series of interrupted arcs composed mainly of finer-grain material. Grain size generally varies from fine to medium-grained sand. No apparent bioturbation is observed. (Fig. 2-6, F5 W-7) Microresistivity images from this facies confirm the internal structureless appearance (Fig. 2-5b).

Interpretation

Paleozoic and Triassic rocks exhibiting similar structureless features to those described in this facies, were documented by Martin and Turner (1998). In their work, the origin of these 'massive-type' sandstones is ascribed to autogenic resedimentation processes, such as the collapse of channel bank or bar that abruptly cover previous sediments. Structureless appearance is also linked to high depositional rates which suppress the grain traction (Jelby et al., 2019).

For those beds displaying diffuse and non-continuous lamination, the evidence of water-scape structures suggest an increase in pore pressure as consequence of rapid sedimentation (Miall, 2016), as might occur in crevasse splay deposits. During the pressure-stabilization process, water-escape structures such as pillar-and-dish, flames, and diapirs may form, as

pressurized fluids move to a more equilibrate level, dragging or displacing sediment in the process (Miall, 2016). Overall, this facies is interpreted to correspond to autogenic resedimentation processes and/or abrupt sedimentation.

Facies 6 (F6). Bioturbated sandstones

Sedimentology

This facies encompasses medium (10-30 cm) to very thick (>1 m) beds with fine- to coarse-grained sand but its main characteristic is the notable bioturbation, which in some cases obscures or obliterates the internal sedimentary structures. Bioturbation intensity varies. Microresistivity images from this facies show a chaotic pattern reflecting the bioturbation. (Fig. 2-6, F6 W-2; Fig. 2-8).

Interpretation

From a regional perspective, the coarser-grained sand beds are interpreted as corresponding to coastal regressive events within the Upper Chipaque. Supporting aspects for this hypothesis include: (1) detail gamma-ray log correlations indicating individual points of source as distributary channel geometry; and (2) a regional shift marked by the gamma ray log, showing an increase in grain size basinward. Conversely, bioturbation in finer-grained beds suggest opportunistic behaviors, indicating that these beds could be interpreted as event beds.

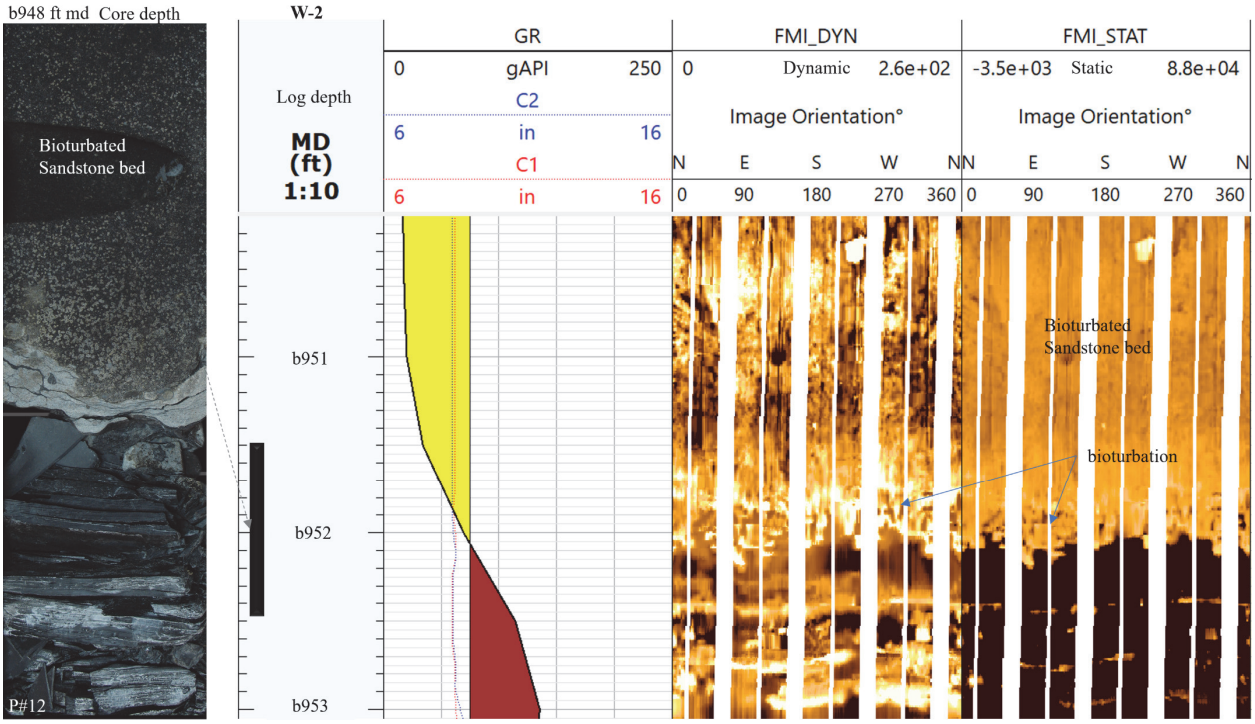

Figure 2-8. Bioturbated sandstone bed core W-2. Biological activity obliterated the physical stratification, impeding its identification on both electrical image logs, dynamic and static.

Facies 7 (F7). Complex hummocky- and swaley-like cross-stratification (wavy ripple cross-lamination, soft sediment deformation structures, rip-up clast and fluid muds)

Sedimentology

This facies encompasses a group of sedimentary structures, primarily consisting of laminae sets of wave ripple cross-lamination, and less commonly, soft sediment deformation structures and rip-up clast. Most of the structures display lamina downlap and conspicuous bidirectional cross-sets. Occasionally, some lamina sets exhibit a thin and thicken shape in opposite directions. Notorious erosional truncations between lamina sets are common. Rip-up clasts display irregular shapes and are finer-grained than the host interval. No bioturbation is observed. (Fig. 2-6, F7 W-9).

Interpretation

This facies is interpreted as the product of storm deposits (tempestites). It is important to note that storm deposits are not solely represented by hummocky and swaley cross-stratification structures but include a wide range of additional sedimentary structures. The magnitude and dominance of storm-linked process (including waves, currents, density flows, among others) determine the type of sedimentary structures that occur, ranging from the traditional hummocky cross-stratification (HCS) to the swaley cross-stratification (SCS) (Jelby et al., 2020). For instance, storms often increase river discharge, resulting in larger amounts of sediment being transported basinward as hyperpycnal flows. During the storm lulls, finer-grained lithologies are prone to be deposited, while during storm peaks currents may augment wave action (Jelby et al., 2020). Given the observed dominance of wave and bidirectional current structures, this facies is interpreted as tempestites and more specifically as the 'complex' type of HCS *sensu* Jelby et al., 2020.

Facies 8 (F8). Carbonaceous Siltstones to Coals

Sedimentology

Although this facies occurs as beds of few centimeters thick, its stratigraphic and environmental relevance makes it a crucial element to incorporate in any analysis. This facies ranges from carbonaceous siltstone to pure coal, with colors varying from black to very dark gray and a luster ranging from dull to bright. Occasionally, some grains of pyrite are present. These beds or laminae are commonly capped erosively by coarser materials. Some layers present root-like features. (Fig. 2-6, F8 W-9).

Interpretation

This facies could be interpreted to have formed in restricted peat-forming environments. Peat, the precursor of coal, is the accumulation product of decomposed organic matter, mainly from plants but also from microbes, fungi, algae, and other animal remains, under the balance of biochemical process and physical conditions such as a high-water table and low external-sediment supply (Flores, 2014).

Coal seams have been recognized as a high-resolution proxy, particularly for solving lower-order events owing to their high reactivity to environmental variations (Diessel, 2007). Nevertheless, the extension, continuity, and preservation of the peatland areas was likely limited, primarily controlled by the highly dynamic surrounding environment, which is reflected in the reworking and/or the high sedimentation rates imposed mainly by the coarser-grained sediments.

Facies 9 (F9). Current and wavy rippled sandstones

Sedimentology

Its principal characteristic is the presence of oscillation and current ripple structures. This facies is composed of thin (3-10 cm) to thick (30-100 cm) beds, occasionally interbedded with mud drapes. Grain size ranges from silt to medium sand. Bioturbation is sporadic and typically consists of small-size forms (Fig. 2-9, F9 W-8).

Interpretation

Oscillatory-generated structures indicate a subaqueous depositional environment above the fair-weather wave base. The numerous muddy laminae capping the individual ripple sets suggest a relatively quiet setting, consistent with the lower flat regime typical of these bedforms. The presence of interbedded asymmetrical ripples suggests alternations in the driving mechanism, shifting from wave to current.

Facies 10 (F10). Variable stratification, cross-bedded sandstones current ripples and bidirectional-like stratification

Sedimentology

It consists of medium to thin sandstone beds of medium- to coarse-grained sand, interbedded with thin beds to thick laminae of claystone or siltstone, often with significant

scouring. Some intervals display bidirectional stratification (herringbone-like). Cross-stratification is also common in coarser beds. These beds frequently contain clayish-semirounded rip-up clasts. No bioturbation is observed. (Fig. 2-9, F10 W-9).

Interpretation

This facies may correspond to tidal bars deposits. It is important to note that tidal current directions can be flood or ebb dominated depending on the location (Dalrymple, 2010b). The lack of bioturbation, the herringbone-like structures, and the presence of clayish rip-up clasts, suggest a highly dynamic depositional setting under a cyclic control.

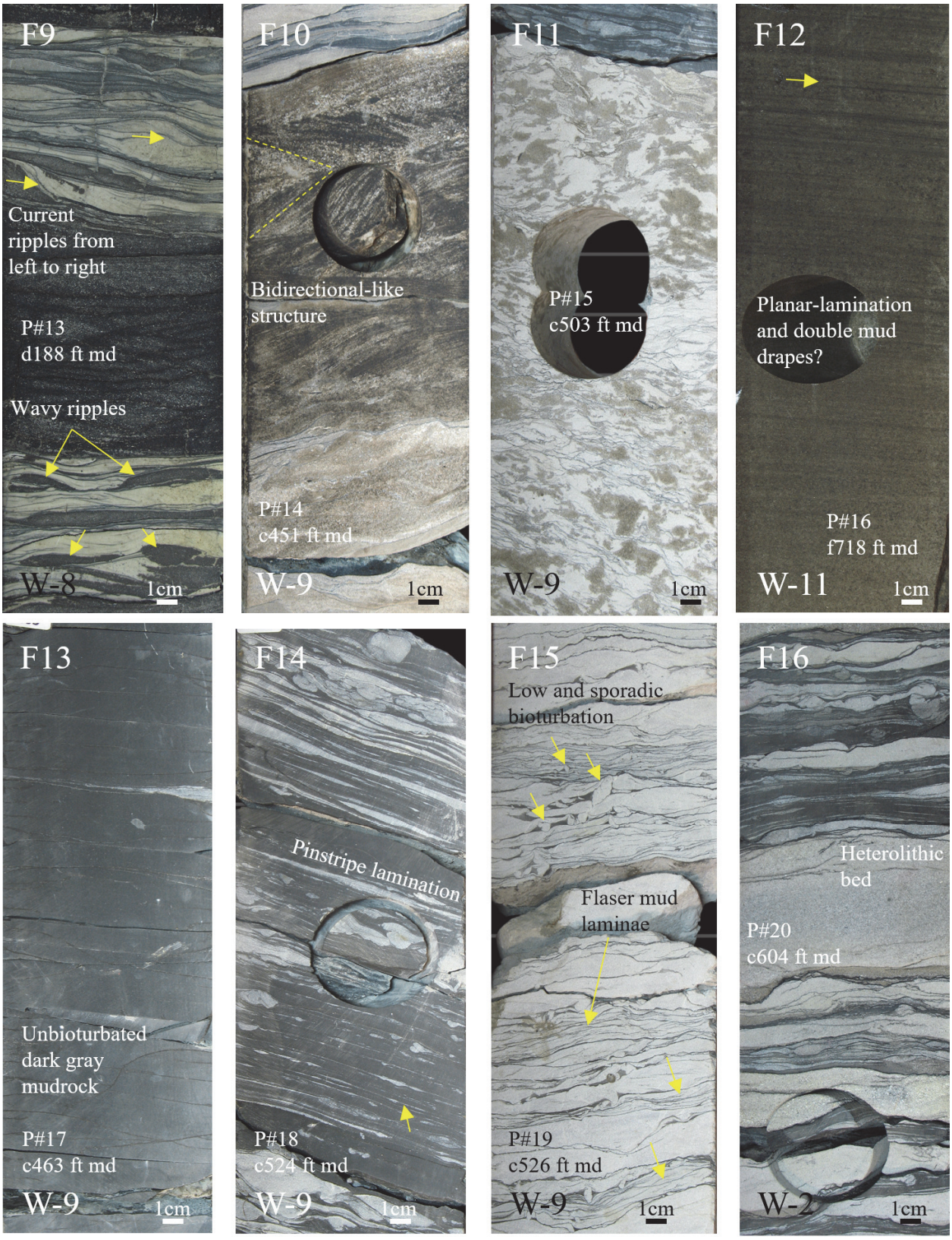
F9
Current ripples from left to right
P#13
d188 ft md
Wavy ripples
W-8
1cm
F10
Bidirectional-like structure
P#14
c451 ft md
W-9
1cm
F11
P#15
c503 ft md
W-9
1cm
F12
Planar-lamination and double mud drapes?
P#16
f718 ft md
W-11
1cm
F13
Unbioturbated dark gray mudrock
P#17
c463 ft md
W-9
1cm
F14
Pinstripe lamination
P#18
c524 ft md
W-9
1cm
F15
Low and sporadic bioturbation
Flaser mud laminae
P#19
c526 ft md
W-9
1cm
F16
Heterolithic bed
P#20
c604 ft md
W-2
1cm

Figure 2-9. Photo plate 2 of facies classification. Examples for facies 9 to 16 (F9…F16). F9. Displaying some current ripples in the upper part and wavy ripples in the lower part. F10. Sandstone bed displaying bidirectional-like stratification. F11. Kaolinitic sandstone bed resulting from weathering action. F12. Planar-lamination sandstone bed. Some internal laminae set resembles to display double mud drapes in a cyclic pattern. F13. Dark gray mudrock; unbioturbated interval meaning a stressful setting for benthic organism. F14. Dark gray siltstone with sandy lenses and pinstripe lamination. F15. Flaser bedded sandstone bed with variable bioturbation dominated by diminutive forms. F16. Wavy heterolithic bed with current ripples with low to absent bioturbation.

Facies 11 (F11). Silty to clayish Sandstones

Sedimentology

This facies comprises beds that generally lack internal structure, occasionally, some minor features resembling planar stratification are observed. Its color is milky white (Fig. 2-9, F11 W-9). Notably in W-4 (Fig. 2-7; W-4, log depth c332-c343 ft md), this facies seems to display root-like features. This facies also encompasses the clayish and altered intervals that mark some of the bedding planes in between beds of Facies 4.

Interpretation

This facies is interpreted as the product of pedogenic or weathering action over the sediments at that times. Most of the paleosols identified in this study were formed during the base-level rise leg and were primary affected by high sedimentation rates and reworking action—factors that impeded robust soil development; although, the interpreted paleosol at core W-4 may have greater significance (Fig. 2-7; W-4, log depths c332-c343 ft md). Notably, this paleosol is not directly on top of the contrasting Paleozoic finer-grained lithology, instead, it is below a series of amalgamated multistory channel deposits of Cretaceous age. Additionally, the thickness of this paleosol-like interval is larger than the other paleosol beds commonly found within the Une Formation. Thus, this paleosol may be attributed to a more subregional to

regional nondepositional and/or erosive event that took place before the sedimentation of the proper Une Formation.

Facies 12 (F12). Planar-lamination Sandstone beds

Sedimentology

This facies consists of medium beds of sandstone ranging from very fine- to medium-grained size, with planar lamination as its main characteristic. In some cases, it displays cyclic patterns. Low to absent bioturbation is observed (Fig. 2-9, F12 W-11).

Interpretation

This facies is interpreted to has been deposited within a sheltered setting, allowing for the recording of cyclic sedimentation (e.g., Dalrymple 2010b). The observed cyclicity suggests some degree of tidal modulation.

Facies 13 (F13). Dark gray mudrocks

Sedimentology

This facies consist predominantly of dark gray siltstones with a smaller proportion of claystones. It comprises thick to very thin beds that commonly display planar lamination, with occasional sandy lenses revealing a wavy and/or current origin. Its BI is variable, generally tending towards low values (0-1). Trace-fossil diversity is low with diminutive forms dominating the record (Fig. 2-9, F13 W-9). A variant of this facies are thin to medium beds of dull dark gray to brownish color lacking internal stratification or exhibiting a massive appearance (Fig. 2-6, lower section of photo # 11, W-9).

Interpretation

As a product of the addition of palynological analysis, this facies can be interpreted as having been deposited into two different depositional settings. Samples from the lower section of the Une Formation indicate a continental setting with no marine influence, (landward from the bayline *sensu* Bhattacharya, 2010) marked by a complete yield of continental palynomorphs, while the rest of the sequence upwards (Middle- and upper-Une, Chipaque and Lower Guadalupe formations) shows at least some degree of marine influence (Fig. 2-4), however, the biological activity (trace fossils), indicates values ranging from low to absent—which has been linked to physico-chemical stressed settings (MacEachern et al., 2007; Gingras et al., 2011). Such marginal-marine settings (e.g., lagoons or bays) receive a mix of fresh and marine waters, and are characterized, in part, by low levels of oxygen and/or salinity, which affect the normal development of marine communities (MacEachern et al., 2007), a fact that is notoriously common of this facies within the Chipaque Formation. In addition, the variant of this facies is interpreted as to be deposited in tidal mud flats, in which the sediments undergoes a homogenization process as result of animals and/or plants actions. This muddy facies is commonly capped by carbonaceous beds or can be overlaid by erosive coarse-grained lithologies. This facies is mainly present within the estuarine complex deposits (or lower part of Chipaque Formation)

Apart from the sedimentological perspective, interestingly, this facies and the wavy-heterolithic attest to three major subaerial exposure periods. The intra-Campanian unconformity (S.U.2) located in core W-8 (Fig. 2-10 at core depth d241 ft md and Fig. 2-11, at log depth d252 ft md), separates Middle? Campanian from Middle -Upper? Campanian lithologies. The Paleocene unconformity (S.U.3), also observed in W-8 (Fig. 2-10 at core depth d150 ft md; Fig. 2-11, at log depth d161 ft md), puts in contact lithologies from the Upper? Campanian with Paleocene rocks. And the Eocene unconformity (S.U.4), (landward in W-2, Fig. 2-12, at log depth b868 ft md), puts in contact Middle-lower? Campanian fine-grained facies with Eocene coarse-grained facies. In all these cases, the rock 'freshness' is altered by weathering action, resulting in an opaque lithology with reddish hues associated with iron (Fe) oxidation (Fig. 2-

10). This characteristic change rapidly in just a few meters down from each unconformity, where rock recover its fresh appearance.

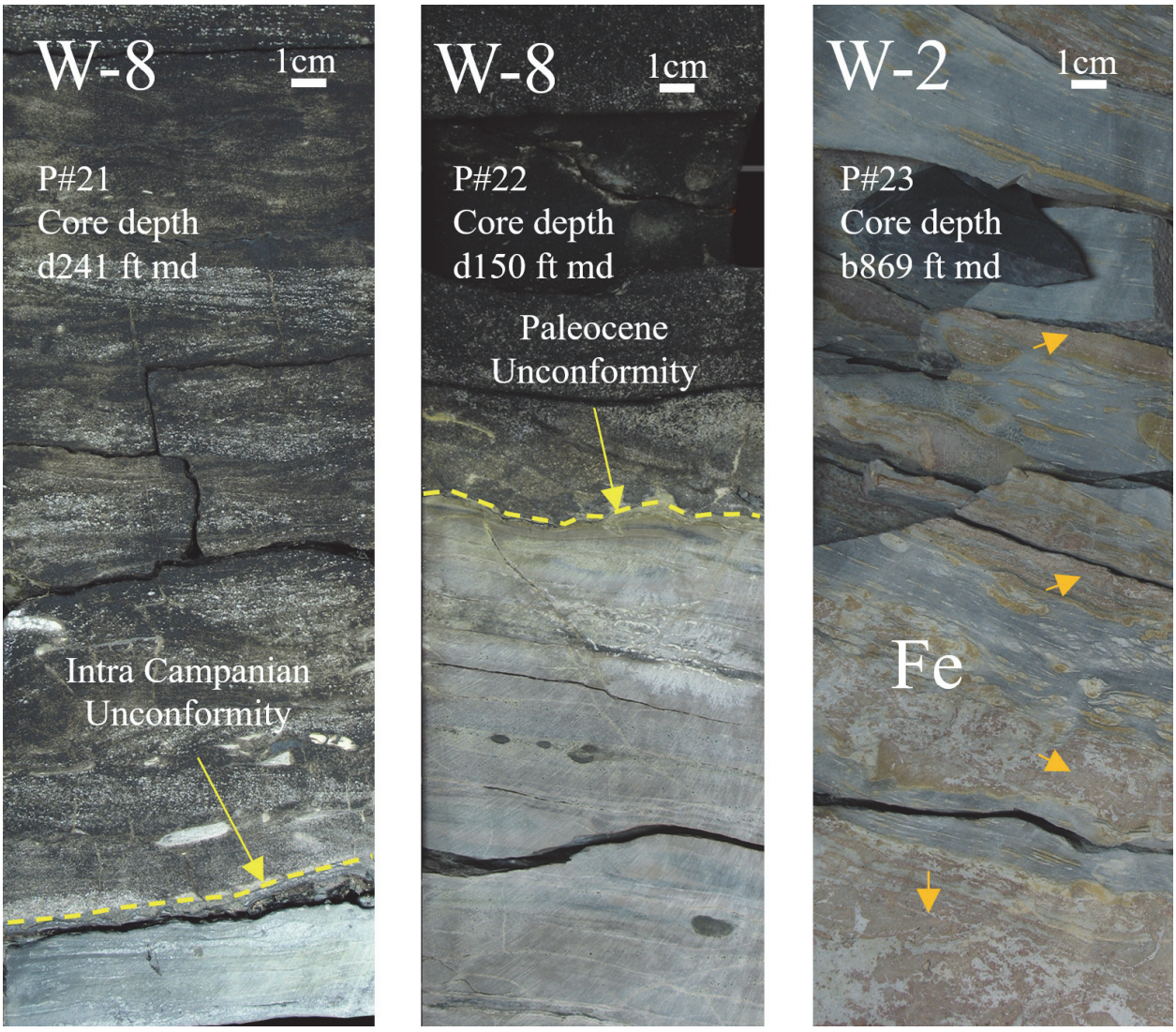

Figure 2-10. Photo plate 3. Subaerial unconformities. The fine-grained beds below of these subaerial unconformities have a dull color resulting from the weathering action. Oxidation process promotes the precipitation of iron oxides. Photo # 21 corresponds to the Paleocene subaerial unconformity (S.U.3). Photo # 22 corresponds to the Intra-Campanian unconformity (S.U.2). And photo # 23 exhibits iron oxides related to the Eocene unconformity (S.U.4).

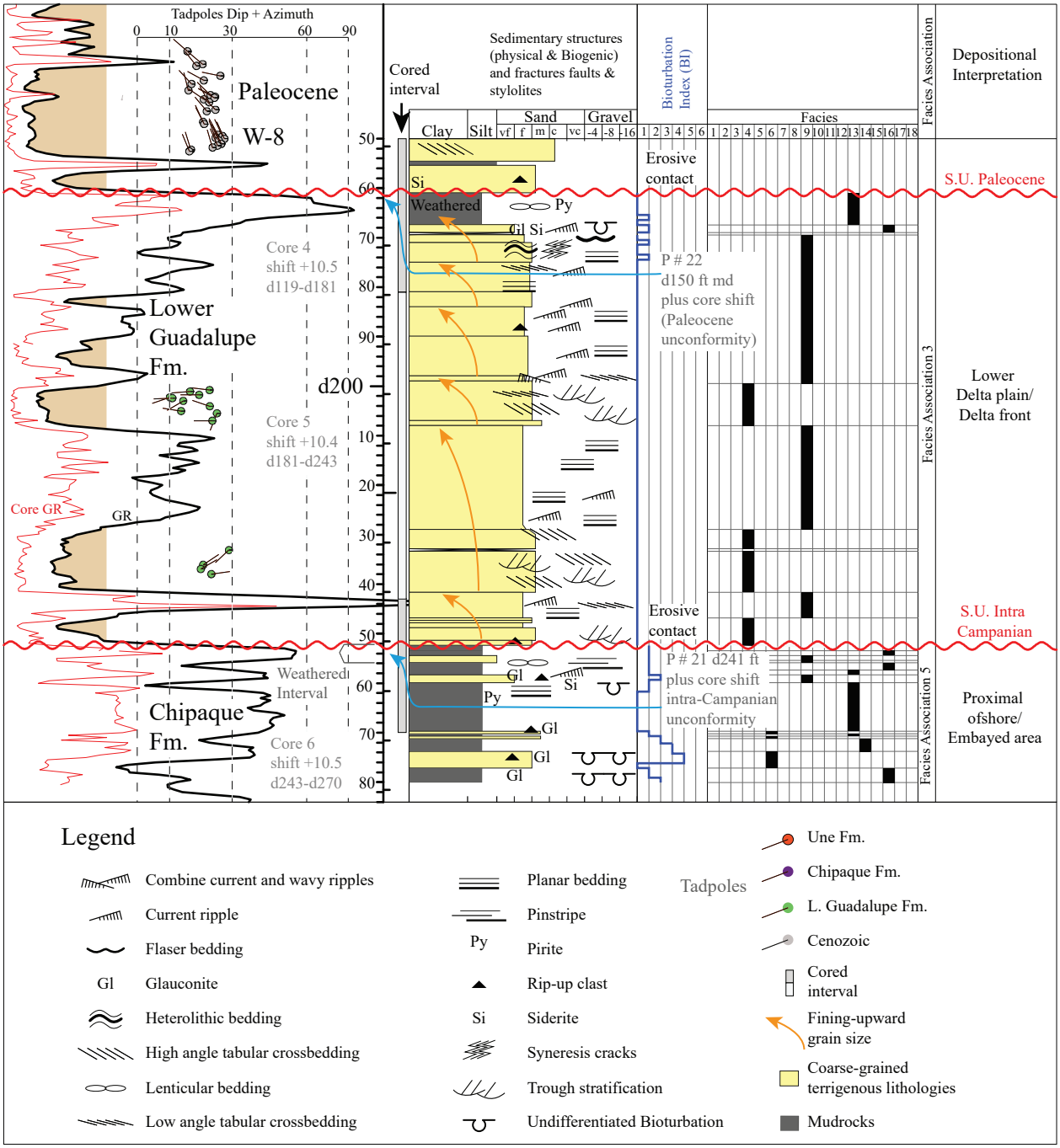

Figure 2-11. Core logging Lower Guadalupe W-8. Individual bed sets within Lower Guadalupe Fm., display a fining upward lithological trend in an amalgamated manner. Paleocene and Intra-Campanian subaerial unconformities limit the thickness of this unit. Below these unconformities the rock is altered and display dull colors (see Photos # 21 and 22 in Figure 2-10). Bioturbation in Chipaque Formation occurs mainly associated to coarse-grained beds. Middle dark gray interval of facies 13 (d260-d274 ft md at log depth) remains unbioturbated.

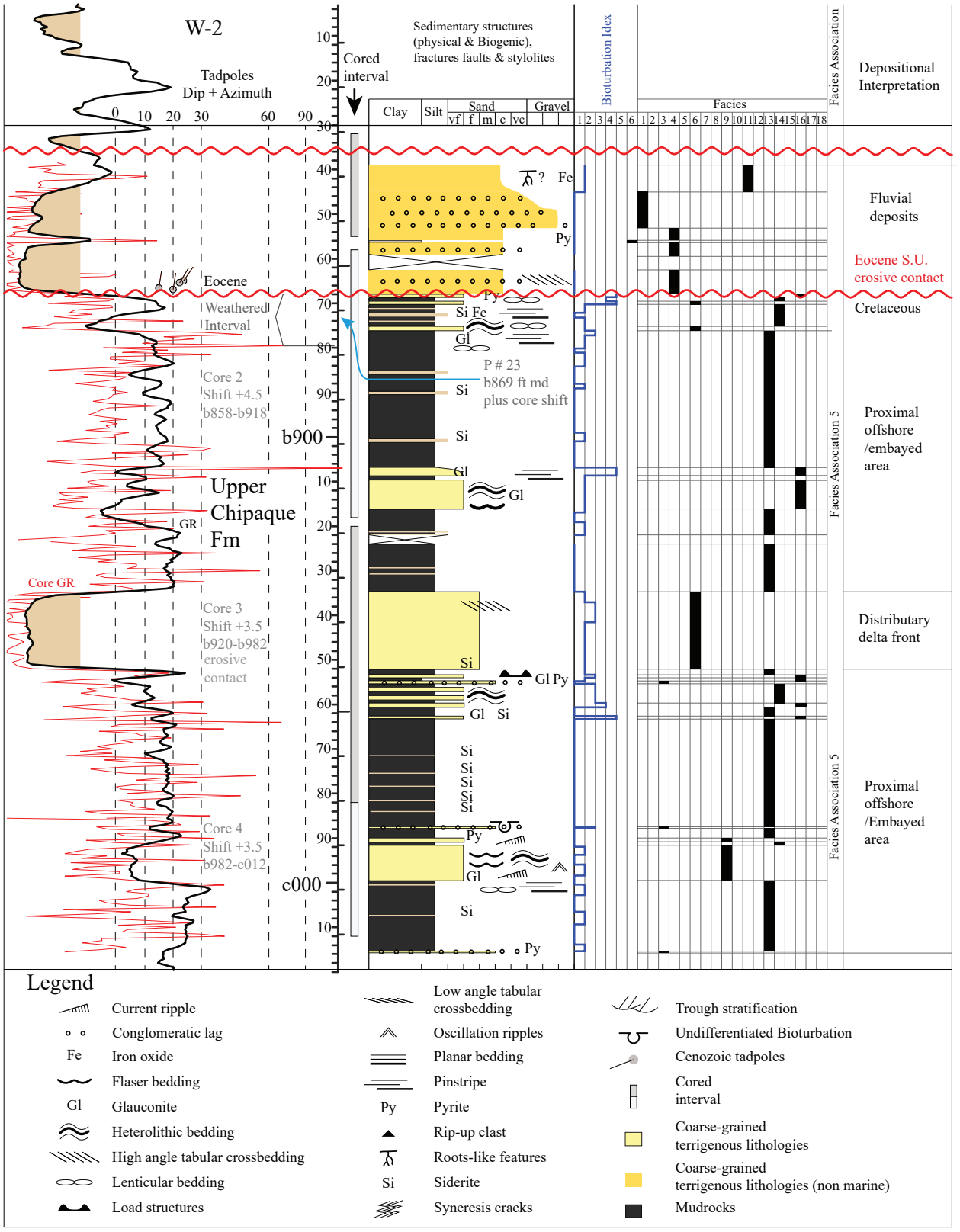
W-2
Tadpoles
Dip + Azimuth
0 10 20 30 60 90
Cored interval
Sedimentary structures (physical & Biogenic), fractures faults & stylolites
Clay
Silt
Sand
vf f m c vc
Gravel
Bioturbation Idex
Facies
Facies Association
Depositional Interpretation
Fluvial deposits
Eocene S.U. erosive contact
Cretaceous
Eocene
Weathered Interval
Core 2 Shift +4.5 b858-b918
Upper Chipaque Fm
GR
Core GR
Core 3 Shift +3.5 b920-b982 erosive contact
Core 4 Shift +3.5 b982-c012
b900
c000
P # 23 b869 ft md plus core shift
Proximal offshore /embayed area
Distributary delta front
Proximal offshore /Embayed area
Facies Association 5
Fe
Py
Si
Gl
Legend
Current ripple
Conglomeratic lag
Iron oxide
Flaser bedding
Glauconite
Heterolithic bedding
High angle tabular crossbedding
Lenticular bedding
Load structures
Low angle tabular crossbedding
Oscillation ripples
Planar bedding
Pinstripe
Pyrite
Rip-up clast
Roots-like features
Siderite
Syneresis cracks
Trough stratification
Undifferentiated Bioturbation
Cenozoic tadpoles
Cored interval
Coarse-grained terrigenous lithologies
Coarse-grained terrigenous lithologies (non marine)
Mudrocks

Figure 2-12. Core logging Upper Chipaque W-2. Along the sequence can be observed several unbioturbated mudrock intervals, probably associated to anoxic or dysoxic bottoms. Conversely, coarse-grained intervals are bioturbated, revealing an opportunistic behavior associated with more favorable oxygen levels. (See Photo # 23 in Figure 2-10 below to the Eocene subaerial unconformity).

Heterolithic Group

Facies 14 (F14). Dark gray Siltstone with sandy lenses and/or pinstripe lamination

Sedimentology

This facies shares some similarities with F13, however, unlike the previous one, it has a more significant presence of coarser-grained lenses. This facies is dominated by pinstripe lamination, although some oscillation and current ripples occur. Occasionally some load structures appear in the form of ball-and-pillow. Most intervals remain largely unborrowed. (Fig. 2-9, F14 W-9).

Interpretation

This facies represent the transition step into the heterolithic spectrum. Some intervals display regular-spacing patterns that support the idea for tidal modulation. The presence of load structures suggests variable sedimentation rates. In line with F13, the absence or the low bioturbation intensity points to a marginal-marine setting.

Facies 15 (F15). Flaser bedded sandstones to siltstones

Sedimentology

This facies is characterized by thin and isolated mud drapes within the very fine- to fine-grained sandstone cross-lamination. Some intervals exhibit a cyclic alternation of mud and sand

dominance. Some sandy units internally display a fuzzy to blurry lamination, which may be related to cryptoturbation. Bioturbation is variable and dominated by diminutive forms. (Fig. 2-9, F15 W-9).

Interpretation

This facies is interpreted to be the product of variable energy conditions. The changes in energy are reflected in the alternation of sediment types (sand versus silt/mud). Although heterolithic successions may or may not result from tidal action (Dalrymple 2010b), the cored intervals display some degree of cyclicity that support the idea of tidal modulation.

Facies 16 (F16). Wavy Heterolithic deposits

Sedimentology

This facies consists of heterolithic successions of medium beds to thick laminae of sandstones to siltstones interbedded with black mudrocks. The lower contacts of the dark gray mudrocks are occasionally as erosive as the sandstones bed boundaries. Overall, the proportion of sand to muddy intervals constantly fluctuates, however, some intervals display regular changes. The most common sedimentary structures are stationary and current ripples. Bioturbation intensities are generally low (0-2), and their occurrence is mostly sporadic, although some intervals may reach higher values. Commonly, trace fossils are composed of diminutive forms. (Fig. 2-9, F16 W-2; Fig. 2-13 photos # 30 and 31).

Interpretation

Heterolithic successions can result from various processes other than tidal action (Dalrymple 2010b), however, strong cyclic patterns can be observed, particularly, in the lower part of Chipaque Formation (e.g., Fig 2-9, F12 W-11; Fig. 2-13, W-7, photos 26 and 27). These short intervals are the clue to unveiling the tidal action that these rocks have undergone, as tidal-

signature identification has limitations such as intense bioturbation or the overlap of additional process like wave action, which can destroy the tidal evidence (Davis, 2012).

The Une Formation also records heterolithic intervals (e.g., Fig. 2-9, F16 W-2**)**. Unlike those in the Chipaque Formation, these intervals do not display strong evidence of tidal modulation; however, this process cannot be discarded. Davis (2012) highlights the Hudson River as an example of the challenges in identifying tidal processes. Despite the river recording tidal influence up to 100 km up from the sea, only a few kilometers reflect this influence in their sediments. As previously mentioned, some palynological samples from the fine-grained (also heterolithic) intervals of Une Formation's show combinations of marine and continental elements providing evidence of marine influence. (Fig. 2-4, W-2).

Facies 17 (F17). Heterolithic deposits with soft sediment deformation structures (SSDS)

Sedimentology

Heterolithic deposits with soft-sediment deformation structures (SSDS) are restricted to Chipaque Formation. These deposits are composed mainly of ball-and-pillow structures and convolute lamination, varying from a few millimeters to a few centimeters in scale. The load cast structures have a semi-circular shape, composed of sandier-grain size structures diving into the underlaying finer-grain units. Convolute lamination is less common but appears associated to the same intervals. Occasionally, within the beds and laminae, current, wave and combined ripples can be observed. Another interesting synsedimentary structure associated with this facies is the syneresis crack. Although, its occurrence is low along the rock record, it is in this facies where is most commonly present. Bioturbation is sporadic and ordinarily varies from low to none (Fig. 2-13, F17 W-9).

Interpretation

In some cases, the distribution and occurrence of SSDS can be linked to a fault system or an evaporitic-diapir displacement as the trigger mechanism for disturbing the sedimentation process (e.g., Novak and Egenhoff, 2019; Snyder et al., 2021). In other instances, the root cause is not tectonically associated. For instance, Greb and Archer, (2006) recorded the formation of SSDS in one night as a result of tidal-bore action in the Turnagain Arm estuary, Alaska. Another example of SSDS caused by non-tectonic activity is the reported SSDS intra-complex HCS by Jelby et al., (2020).

Beyond the tectonic or non-tectonic origin, the thixotropic properties of some sediments, combined with variations in densities among layers and sudden vibrations, are seen as potential mechanisms for the formation of load structures (Miall, 2016). This facies is interpreted to has been formed in a marine restricted environment, such as an embayment with variable current strengths resulting from tidal control. Facies 17 also display low to no BI values, a fact that has been linked as animal responses to environment-stress conditions, such as low salinity or high-sedimentation rates (Gingras et al., 2011).

Facies 18 (F18). Hyperpycnal flow deposits

Sedimentology

It consists of very thin to thick beds of mixtures of sandy, silty, and muddy particles. Convolute structures are also common, and the bases frequently contain rip-up clasts and lag deposits. Bioturbation is absent. (Fig. 2-13, F18 W-9). A variant of this facies exhibits a blurry or turbiditic appearance with chaotic internal structure, although seems to have some degree of cyclic control. For this variant, the proportion of fine-grained is larger than the coarse-grained particles (Fig. 2-13, F18 variant W-9).

Interpretation

These beds are commonly structureless, with irregular geometries at their bases, indicating significant density differences with the underlying fine-grained beds. Sedimentation

occurs abruptly as large mases or small flocculate balls, which depending on their size, may fold the underlying muddy layers, giving the false appearance of bioturbation (Fig. 2-13, F18 W-9 photo # 28).

This facies is interpreted to represent river sediment outflow into a marine setting, where the sediment outflow has denser properties than the surrounding marine waters. When the heavier sediments settle on top of the muddy bottoms, the contrasting density among the layers provokes a series of imbalances, resulting in the formation of soft sediment deformation structures (SSDS). These sedimentary structures are deformed during the early stages of sedimentation and before complete lithification (Allen, 1982). Additionally, the angle of deposition plays a significant role; unstable sediment accumulation can fail and cause internal layering to shear, promoting the generation of convolute bedding, folding, and faulting (Miall, 2016).

One important characteristic of this facies is the lack of bioturbation, which reflects rapid sedimentation processes that may kill, reduce, or modify the organism's community as consequence of the new conditions and/or by the low-oxygen levels (MacEachern et al., 2007). The muddy variant could be interpreted to have been deposited within the turbiditic maximum area among the fluvial-marine transition zone.

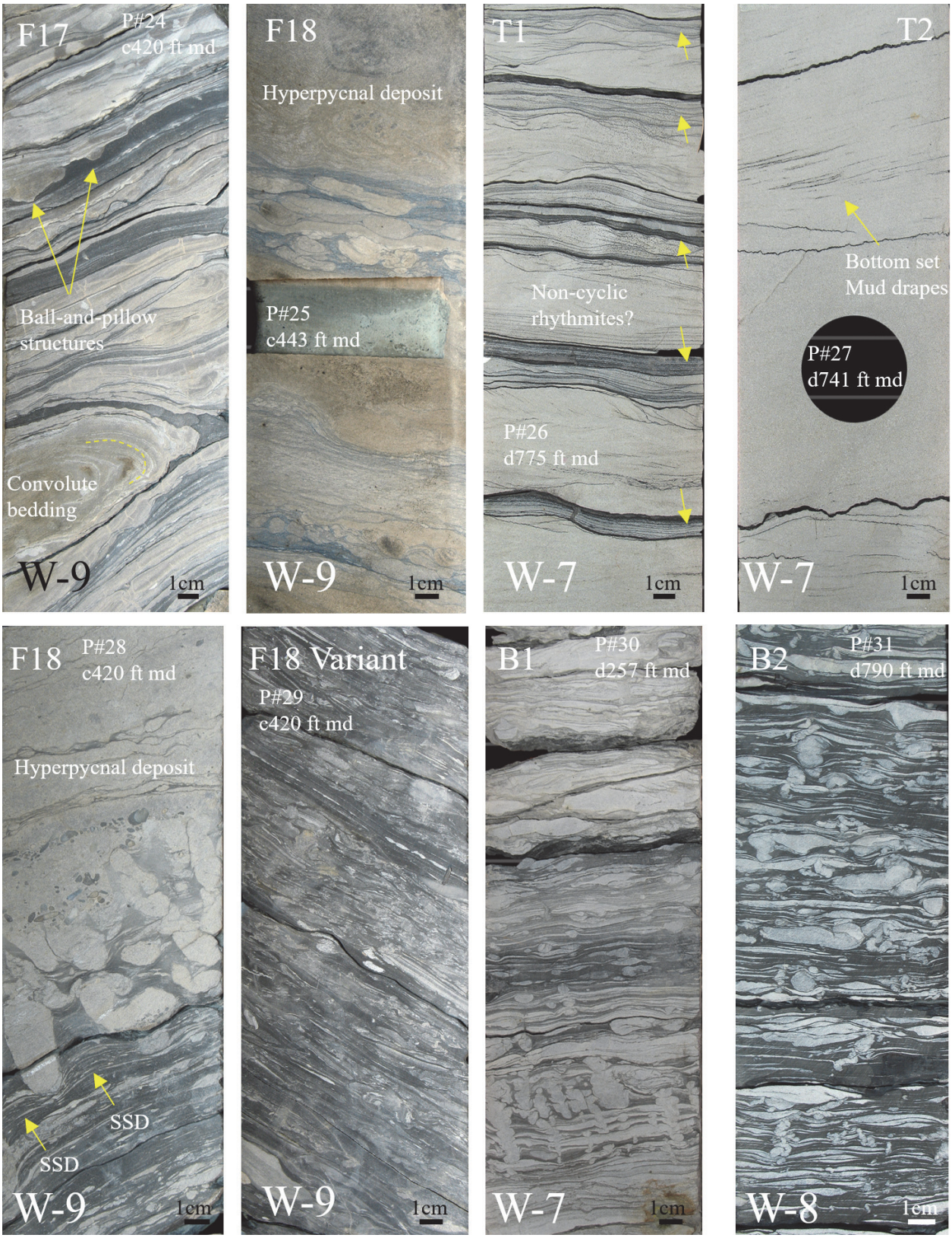
F17
P#24
c420 ft md
Ball-and-pillow structures
Convolute bedding
W-9
1cm
F18
Hyperpycnal deposit
P#25
c443 ft md
W-9
1cm
T1
Non-cyclic rhythmites?
P#26
d775 ft md
W-7
1cm
T2
Bottom set
Mud drapes
P#27
d741 ft md
W-7
1cm
F18
P#28
c420 ft md
Hyperpycnal deposit
SSD
SSD
W-9
1cm
F18 Variant
P#29
c420 ft md
W-9
1cm
B1
P#30
d257 ft md
W-7
1cm
B2
P#31
d790 ft md
W-8
1cm

Figure 2-13. Photo plate 4 of facies classification. Examples for facies 17 to 18 (F17 and F18), tidal signature and bioturbation. F17. Heterolithic bed with soft sediment deformation and convolute bedding. F18. Hyperpycnal flow deposits. Photo # 25 coarse-grained dominated interval, whereas photo # 29 fine-grained dominated (F18 Variant) shows a blurry or turbiditic appearance however also with a cyclic control. Photo # 28 exhibit a hyperpycnal deposit that folds the underlying fine-grained layers, creating a false bioturbation appearance. Photo # 26 (T1) exhibits some degree of cyclicity, affording its classification as rhythmites. Photo # 27 (T2) exhibits some bottom set mud drapes deposited during slack-water periods. Photos # 30 (B1) and # 31 (B2) show some examples of bioturbation activity found in the western logged cored sites; they correspond to small and diminutive forms with variable intensity.

Table 2-1. Facies summary.

Facies	Lithology	Primary sedimentary characteristics	(BI)	Variations	Hydrodynamic interpretation
1	Conglomeratic sandstones to sandy conglomerates with rounded to subrounded clasts	Occasional clast imbrication. Gravel clasts may exceed the pebble size	0		Channel floors. High-energy conditions. River currents
2	Conglomeratic sandstones with angular to subangular clasts	Angular to subangular clast floating in finer-grained matrix	0		Channelized and unchannelized debris flows. High-energy conditions. Abrupt floodings. Ephemeral streams
3	Conglomeratic lags and associated bioturbation (Event beds)	Very thin beds that interrupt the succession. Bioturbation is restricted to the event bed	0-2		Seasonal rain floodings increase river discharge. Density flow events. High-energy conditions. Below Fair-weather wave base (FWWB)

4	Tabular and trough cross-bedded sandstones	Trough and tabular internal stratification	0-1	River channel. High-energy conditions. Current flows
5	Unstructured sandstones and irregular stratification	Structureless beds	0	Rapid depositional rates suppressing grain traction, or resedimentation processes
6	Bioturbated sandstones	Bioturbation that obscure or affect the internal stratification	1-5	Wide range of deposits above of the FWWB outside of channels. Moderate-energy conditions
7	Complex hummocky- and swaley-like cross-stratification (wavy ripple cross-lamination, soft sediment deformation structures, rip-up clast and fluid muds)	HCS- and swaley-like stratification	0	High-energy conditions. Combined flows (wave and currents) with high aggradation rates characterized by periodic shifts
8	Carbonaceous siltstones to Coals	Carbonaceous luster	0-1	Low-energy conditions. Sheltered area. Swampy-subaerial conditions
9	Current and wavy rippled sandstones	Symmetrical ripples and unidirectional ripples	0-2	Moderate-energy conditions

10	Variable stratification, cross-bedded sandstones current ripples and bidirectional-like stratification	Bidirectional-like structures, crossbedding stratification	0-2		High-energy conditions
11	Silty to clayish Sandstones	Interbedding beds of silt and sand particles, with clayish and altered intervals	0-1		Variable conditions fluctuating between low- moderate-energy conditions
12	Planar-lamination Sandstone beds	Cyclic planar lamination of alternating finer and coarser grain sizes	0-1		Low- moderate-energy conditions. Controlled by periodic shifts. Sheltered area
13	Dark gray mudrocks	Dark gray mudrocks with planar lamination	0-3	Dull dark gray mudrock structureless internal stratification	Hemipelagic fallout in oxygen-poor water below FWWB. In the case of the variant tidal mud flats
14	Dark gray siltstone with sandy lenses and/or pinstripe lamination	Dark gray mudrocks with planar lamination alternated with sandy lenses which may exhibit some degree of cyclicity	0-3		Hemipelagic fallout in oxygen-poor water near FWWB. Frequently interrupted by minor deposition of silt and sand from fair-wave-base-generated oscillatory

15	Flaser bedded sandstones to siltstones	Current-rippled dominated structures with flaser lamination. Sometimes displaying cyclic alternations with finer-grained laminations	0-3		Variable energy conditions, characterized by periodic shifts. Sand flats
16	Wavy Heterolithic deposits	Interbedding of finer and coarser grain particles sometimes displaying a cyclic patterns	0-4		Variable energy conditions, characterized by periodic shifts. Mixed flat
17	Heterolithic deposits with soft sediment deformation structures (SSDS)	Interbedding of finer and coarser grain beds displaying soft sediment deformation structures, convolute bedding and synaeresis cracks. Sometimes exhibiting cyclic patterns	0		Variable energy conditions, characterized by periodic shifts. Mixed flat
18	Hyperpycnal flow deposits	Turbiditic appearance, sometimes displaying cyclic control	0	Fine-grained matrix with blurry coarser grained within it	Rapid and abrupt suspension fallout triggered by salinity and/or density contrasts; tidal action impose the imprint

2.5.2. Facies Associations

Collinson, (1969) stated that a facies association is formed by 'groups of facies genetically related to one another, and which have some environmental significance'. Bearing this in mind, five (5) facies associations (FA) were defined in this study, encompassing the diverse depositional settings along the interest column.

Facies Association 1 (FA1): Alluvial deposits

FA1 comprises three facies: 1) conglomerates of angular to subangular clasts (facies 2); 2) tabular and trough cross-bedded sandstones (facies 4); and 3) silty to clayish sandstones (facies 11). The first two facies reflect high-energy depositional settings, in which the presence of angular to subangular clasts is indicative of a proximal bedrock source, (as the edges of the clasts were not abraded enough to become more rounded). In addition, paleosols (facies 11) represent periods of exposure with pedogenic processes. These facies indicate a fully continental setting. FA1 is interpreted to be deposited in an alluvial valley that may have undergone significant subaerial exposure (Figs. 2-7, 2-15; Table 2-2). This facies succession exhibits a fining-upward trend, with coarser material at the base represented by facies 1 and 2, and finer material by facies 3, which contains root-like features; this succession is bounded by unconformities (Fig. 2-7).

Facies Association 2 (FA2): Multistory channel deposits above the bay line (Upper delta plain)

This association is composed by 1) conglomeratic sandstone to sandy conglomerate with rounded to subrounded clasts (facies 1); 2) tabular and trough cross-bedded sandstones (facies 4); 3) unstructured sandstones and irregular stratification (facies 5); 4) carbonaceous siltstones to coals (F8); 5) silty to clayish sandstones (facies 11**)**; (6) dark gray siltstones (facies 13); and **(**7) wavy heterolithic deposits (facies 16) intervals. FA2 caps either a paleosol (at the base of core W-4; Figs. 2-7), or Paleozoic rocks.

Multistory channel deposits are the most common element of this facies association, with facies 1, reflecting the channels bases, where the energy level is the highest, and facies 4, representing the continuum of the normal filling, (dune-scale bar channel deposits); and facies 5, reflecting episodic and autogenic processes of proximal deposits collapsing (resedimentation) or heightened amounts of sediment avoiding the grain traction, and sedimentation such as crevasse splay deposits. The fine-grained lithologies (of facies 8, 13, and 16) reflect sheltered settings like an abandoned oxbow, where sedimentation rates are lower than inside of channels. Finally, exposed areas are dominated by immature and/or within systems tract paleosols represented by facies 11.

Taking into account that the limit between the upper and lower delta plain is defined by the bayline, which essentially marks the presence or absence of marine or brackish-water organisms (Bhattacharya, 2010), the occurrence of continental palynomorphs in the lower levels of the Une Formation at the base of core W-4 (Fig. 2-4), versus the mix of continental and marine palynomorphs in W-2 (Fig. 2-4), also within the Une Formation but in an upper levels, allows for the differentiation of the upper from the lower delta plain setting. Locally for the Une Formation at W-4, FA2 consists mainly of stacked channel deposits in the upper delta plain setting (Figs. 2-7, 2-15; Table 2-2). In general, this facies succession commonly displays a blocky gamma ray motif on electrical logs (Fig. 2-15). However, core data often reveals a fining-upward trend, indicative of the channel hydrodynamics (higher at the bases and decreasing upward). These channel deposits are frequently interrupted by the bases of younger channel deposits, resulting in an overall amalgamated character. In this succession, coarser material is located at the base of the channel deposits, followed by finer-grained material, capped with some sparse thin, muddy layers and/or immature paleosols at the top (Fig. 2-7).

Facies Association 3 (FA3): Multistory channel deposits below the bay line (Lower delta plain and uppermost part of the delta front)

In terms of succession, this facies association has similar characteristics to the previous one. FA3 comprises nearly the same group of facies as FA2 (facies 1, 4, 8, 11, 13 and 16), with the addition of some small intervals of highly bioturbated sandstones (facies 6) and, notoriously,

fine-grained intervals whose palynological yield includes both continental and marine elements (Fig. 2-4). This simple but definitive characteristic establishes the basis for defining the lower delta plain setting. FA3 consist of stacked channel deposits in the lower delta plain setting (Figs. 2-15; Table 2-2), however, it may include the uppermost part of the delta front setting.

Facies Association 4 (FA4): Transgressive brackish water tidally modulated (Estuarine complex)

FA4 is composed of: 1) carbonaceous siltstones to coals (facies 8); 2) variable stratification, cross-bedded sandstones current ripples and bidirectional-like stratification (facies 10); 3) planar-lamination sandstones beds (facies 12); 4) dark gray siltstones (facies 13); 5) dark gray siltstone with sandy lenses and/or pinstripe-lamination (facies 14); 6) flaser-bedded sandstones to siltstones (facies 15); 7) wavy heterolithic deposits (facies 16); 8) heterolithic deposits with significant soft sediment deformation structures (SSDS) (facies 17).

In general, FA4 contains significant proportions of heterolithic rocks (e.g., Fig. 2-14) reflecting a cyclicity imprint (e.g., F12 W-11, Fig 2-9; Fig. 2-13, tidal structures T1 and T2 W-7). Additionally, these rocks display sporadic borrows characterized by diminutive forms and low diversity (e.g., Fig. 2-13, B1 and B2), aspects characteristics of variable energy conditions and stressful environments such as brackish-water settings (MacEachern et al., 2007; MacEachern et al., 2010; Gingras et al., 2011). This facies succession commonly exhibits a fining-upward trend, marked by an increasing mud-to-sand ratio toward the top (Fig. 2-15). Individual succession packages are frequently eroded by subsequent depositional events (Fig. 2-14). Overall, the succession is characterized by a strong heterolithic component, displaying a full range of dominance from sand to mud, and vice versa. When individual successions are complete, mudrocks and coal layers may appear at the top (Lower Chipaque section; Fig. 2-14). Based on these characteristics, and the overall depositional trend change, FA4 is interpreted to have been deposited in a transgressive marginal marine setting with some degree of tidal modulation, specifically within an estuarine complex setting (Fig. 2-15; Table 2-2).

Facies Association 5 (FA5): Regressive Proximal offshore or embayed area setting

This facies association is composed of: 1) conglomeratic lags and associated bioturbation event beds (facies 3); 2) blocky to coarsening upward bioturbated sandstones (facies 6); complex hummocky- and swaley-like cross-stratification (facies 7); 4) current and wavy rippled sandstones beds (facies 9); 5) dark gray siltstones (facies 13); 6) dark gray siltstone with sandy lenses and/or pinstripe lamination (facies 14); 7) flaser-bedded sandstones to siltstones (facies 15); 8) wavy heterolithic deposits (facies 16); 9) heterolithic deposits with soft sediment deformation structures (facies 17). Similar to the previous facies association descriptions, the bioturbation index remains low and sporadic, with an increase in values seaward (west-northwest). In general, the succession is sparsely punctuated by progradational events, although the muddy component remains high at the base and at the middle section (Figs. 2-12, 2-14, 2-15; Table 2-2). In general, this FA5 exhibits a coarsening-upward trend, which is observable in the gamma ray log (Fig. 2-15). The fine-grained mudrocks are increasingly punctuated by the deposition of coarser material beds, which erode the underlying muddy layers (Fig. 2-15). FA5 is interpreted to represent a regressive proximal offshore/embayed area setting.

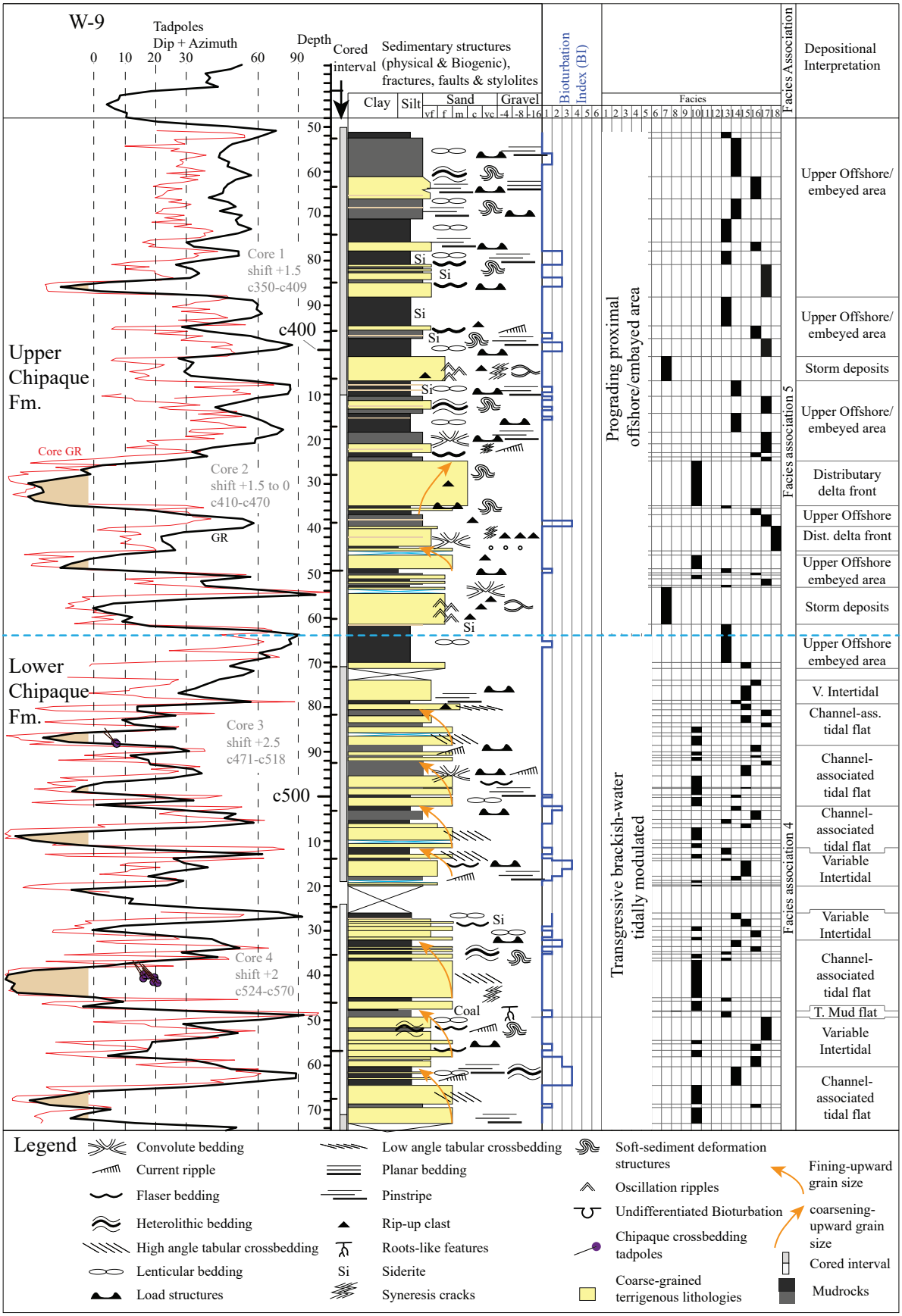
W-9
Tadpoles
Dip + Azimuth
0 10 20 30 60 90
Depth
Cored interval
Sedimentary structures (physical & Biogenic), fractures, faults & stylolites
Clay
Silt
Sand
Gravel
vf f m c vc -4 -8 -16
Bioturbation Index (BI)
1 2 3 4 5 6
Facies
1 2 3 4 5 6 7 8 9 10 11 12 13 14 15 16 17 18
Facies Association
Depositional Interpretation
Upper Chipaque Fm.
Lower Chipaque Fm.
Core 1 shift +1.5 c350-c409
Core 2 shift +1.5 to 0 c410-c470
Core 3 shift +2.5 c471-c518
Core 4 shift +2 c524-c570
Core GR
GR
c400
c500
Si
Coal
Prograding proximal offshore/embayed area
Transgressive brackish-water tidally modulated
Facies association 5
Facies association 4
Upper Offshore/ embeyed area
Upper Offshore/ embeyed area
Storm deposits
Upper Offshore/ embeyed area
Distributary delta front
Upper Offshore
Dist. delta front
Upper Offshore embeyed area
Storm deposits
Upper Offshore embeyed area
V. Intertidal
Channel-ass. tidal flat
Channel-associated tidal flat
Channel-associated tidal flat
Variable Intertidal
Variable Intertidal
Channel-associated tidal flat
T. Mud flat
Variable Intertidal
Channel-associated tidal flat
Legend
Convolute bedding
Current ripple
Flaser bedding
Heterolithic bedding
High angle tabular crossbedding
Lenticular bedding
Load structures
Low angle tabular crossbedding
Planar bedding
Pinstripe
Rip-up clast
Roots-like features
Si Siderite
Syneresis cracks
Soft-sediment deformation structures
Oscillation ripples
Undifferentiated Bioturbation
Chipaque crossbedding tadpoles
Coarse-grained terrigenous lithologies
Fining-upward grain size
coarsening-upward grain size
Cored interval
Mudrocks

Figure 2-14. Core logging Lower and part of Upper Chipaque W-9. The interpreted higher rank maximum flooding surface that separates the transgressive brackish water tidally modulated setting from the regressive proximal offshore/embayed setting above (dashed blue line) is established at the end of a fining upward lithological succession, also represented by the increase in gamma ray values. Individual packages exhibit a fining upward lithological trend, and the overall mud-to-sand ratio increases toward the top of the Lower Chipaque section.

Table 2-2. Depositional setting summary.

Unit	Subunit	Interpreted Depositional Setting	Lithology	Additional Characteristics	BI
Lower Guadalupe		Lower delta plain/ Upper Delta front	Sandstones Mudrocks	Continental and marine palynomorphs	0-1
	Upper Chipaque	Regressive proximal offshore/embayed area. Brackish water influenced and anoxic bottoms.	Mudrocks Sandstones	Heterolithic. Tidal imprint. High flocculation Continental and marine palynomorphs. Soft sediment deformation structures	Varies 0-5 Opportunistic behavior. Commonly black unbioturbated mudrocks
Chipaque					
	Lower Chipaque	Transgressive brackish water tidally modulated. (Estuarine complex deposits)	Sandstones Mudrocks Carbonaceous siltstones to coals	Heterolithic. Tidal imprint. Soft sediment deformation structures. Continental and marine palynomorphs	Varies 0-5 Opportunistic behavior.

Une	*Upper and Middle*	Lower delta plain. (Multistory channel deposits below the bay line)	Sandstones Mudrocks Carbonaceous siltstones to coals	Occasional heterolithic intervals. Immature paleosols. Continental and marine palynomorphs	Varies 0-3 Opportunistic behavior
	Lower	Upper delta plain (Multistory channel deposits above the bay line)	Sandstones Mudrocks	Immature paleosols. Continental palynomorphs	0-1
Basal Unit		Alluvial valley	Conglomerates. Conglomeratic sandstones. Siltstones and claystones	Mature and immature paleosols. Angular-shaped clasts. Rhizoliths	0-1

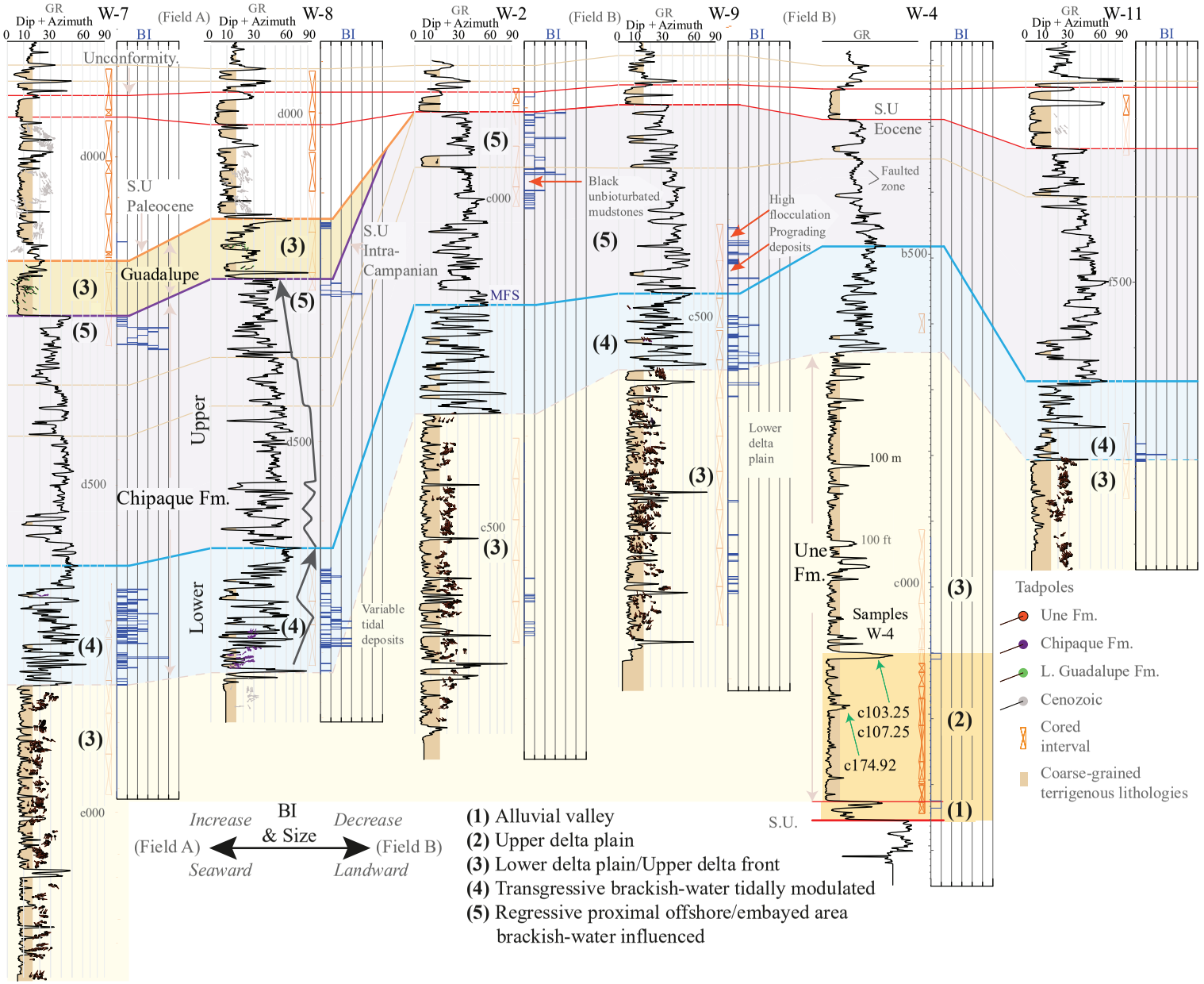
W-7
(Field A)
W-8
W-2
(Field B)
W-9
(Field B)
W-4
W-11
GR
Dip + Azimuth
0 10 30 60 90
BI
Unconformity.
S.U
Paleocene
Guadalupe
S.U
Intra-
Campanian
Upper
Lower
Chipaque Fm.
Variable
tidal
deposits
Black
unbioturbated
mudstones
High
flocculation
Prograding
deposits
Lower
delta
plain
S.U
Eocene
Faulted
zone
Une
Fm.
100 m
100 ft
Samples
W-4
c103.25
c107.25
c174.92
MFS
d000
d500
c000
c500
b500
f500
e000
(1)
(2)
(3)
(4)
(5)
Increase
BI
& Size
Decrease
(Field A)
(Field B)
Seaward
Landward
S.U.
(1) Alluvial valley
(2) Upper delta plain
(3) Lower delta plain/Upper delta front
(4) Transgressive brackish-water tidally modulated
(5) Regressive proximal offshore/embayed area
brackish-water influenced
Tadpoles
Une Fm.
Chipaque Fm.
L. Guadalupe Fm.
Cenozoic
Cored
interval
Coarse-grained
terrigenous lithologies

Figure 2-15. Summary of Bioturbation and depositional trends of Chipaque. Overall, the bioturbation-index curves exhibits several characteristics: For the Une Formation can be observed low to null bioturbation intensities. In this case it is associated exclusively with the fine-grained interbedding since the heightened levels of sedimentation within the coarse-grained intervals impeded the thriving of living communities. Bioturbation within Chipaque Formation increases in a seaward direction (west to northwest; Field A wells) and decreases in a landward direction (east to southeast; field B wells). Several unbioturbated black muddy intervals (red arrows) are observed along the regressive proximal offshore/embayed area setting (Upper Chipaque), they are associated to anoxic or dysoxic bottoms that impeded the development of benthic communities. Palynological samples depths with 100% continental elements in W4 are indicated by green arrows within Une Formation. Within the Chipaque Formation (e.g., W-8) two major vertical trends can be observed from the gamma ray, a fining upward for the Lower Chipaque and a coarsening upward for the Upper Chipaque, both punctuated by several lower rank events.

2.6. Paleocurrent data

As sedimentary structures can provide invaluable information about the processes involved in their creation and as per se in their depositional settings, paleocurrent data from physical sedimentary structures is essential not only defining the direction of sediment transport but also showing pathways of reservoir connectivity.

Paleocurrents from Une Formation (Middle Cenomanian – Middle Turonian)

Paleocurrent data from the Une Formation shows various distribution patterns. In wells W-9 and W-11, the net sediment transport direction consistently points toward the northwest. However, wells W-7 and W-2 exhibit more scattered distributions, in some cases showing opposite directions (Fig. 2-16). These differences in distribution may be linked to the paleogeographic location and the processes occurring at those sites. For instance, locations of W-9 and W-11 might represent areas around distributary river channels with minimal tidal influence, while locations at W-7 and W-2 likely experienced not only river sediment transport

but also other processes. This inference is supported by the presence of marine biota in the fine-grained intervals of the Une Formation (e.g., W-2, Fig. 2-4), which indicates that additional processes occurred at western (seaward) locations.

Paleocurrents from W-9 and W-11 in the Une Formation consistently point to the northwest. Assuming that coastlines are generally perpendicular to the sediment transport direction, the paleocoastline likely had a southwest northeast (SW-NE) orientation (Fig. 2-16). This suggests that rivers transported material predominantly from the southeast and deposited it into the sea toward the northwest.

Paleocurrents from Chipaque (Turonian - Middle Campanian)

For the Lower Chipaque (Upper Turonian- Lower Coniacian), it was possible to obtain some paleocurrent measurements from the coarse-grained beds. In general, these measurements point toward western directions. Unfortunately, for Upper Chipaque (Lower Coniacian – Middle Campanian) it was not possible to obtain a significant and confident number of paleocurrent measurements. The reasons for this are attributed to: 1) high biological activity in coarse-grained sediments, which obliterated the physical sedimentary structures (e.g., Fig. 2-8); 2) the impossibility of core orientation with total certainty; 3) lack of measurements, (e.g., Upper Chipaque, Fig. 2-15); and 4) low resolution or quality of the image logs.

Paleocurrents from Lower Guadalupe (Middle Campanian)

Rose diagrams from Lower Guadalupe Formation (W-7 and W-8; Fig. 2-16) display a general vector mean of sediment transport westward, however, with some northward component. The total measurements from W-7 show a unidirectionally dominated towards the west-northwest (WWN) direction. In contrast, W-8 has some measurements with a wider direction spectrum. This fact could be associated with the facies analysis, which indicates the presence of wave and current ripples in that location. This suggest that W-8 could be influenced by additional processes besides the unidirectional river sediment transport.

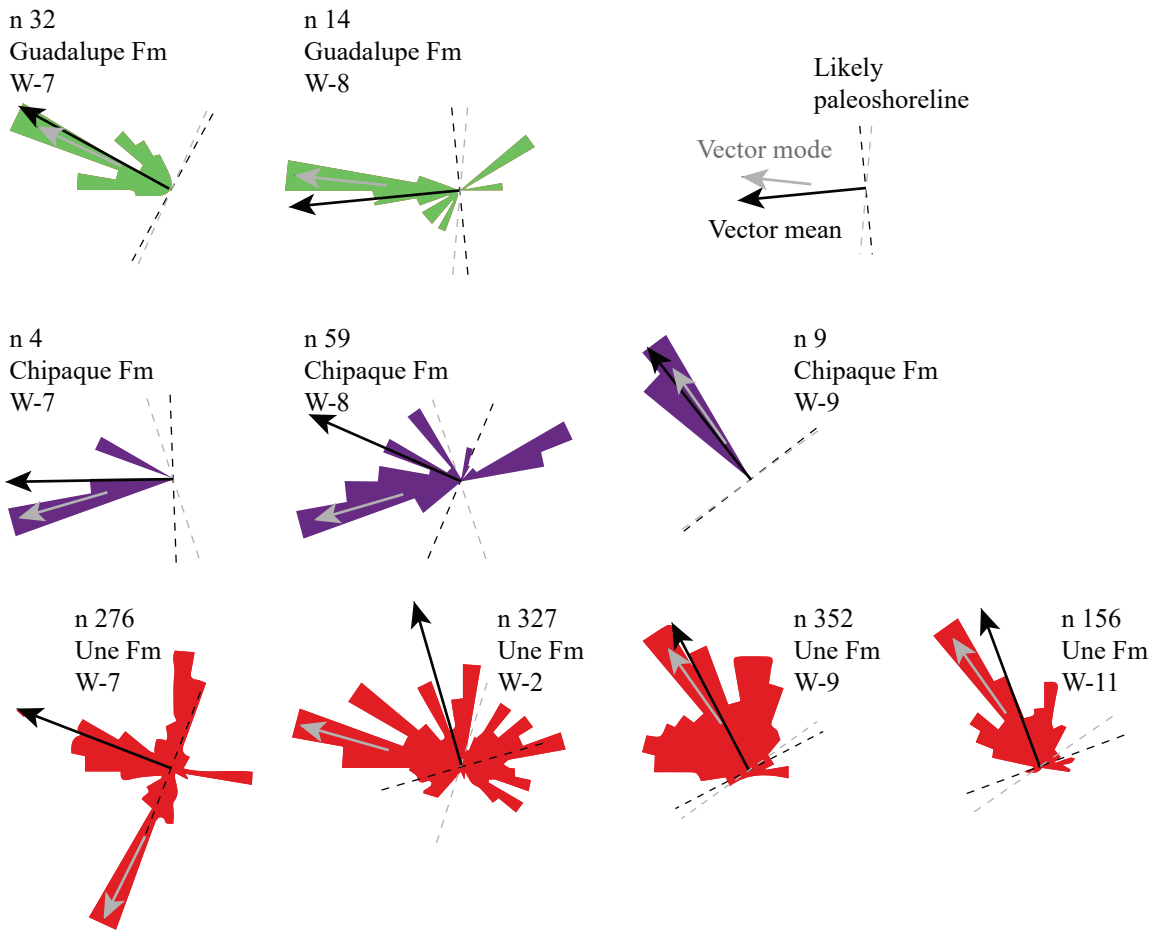

Figure 2-16. Rose diagrams paleocurrents and paleo coastlines directions. Rose diagrams from the sandier formations (e.g., W-9, W-11 for Une, and W-7, W-8 for Lower Guadalupe) display almost unidirectional patterns towards the NW and WNW, respectively. This can be interpreted as rivers bringing material from the southeast and east and depositing it into the sea towards the northwest and west in general. Consequently, coastlines were most likely oriented in NE and NNE directions, perpendicular to sediment transport directions. Paleocoastlines are interpreted to be perpendicular to the vector mean and/or to the vector mode sediment transport direction.

2.7. Integration and Interpretation

The following paragraphs contains the paleo environmental interpretation based on the core logging data and its integration with ichnology and palynology.

Remnants from the bypass and erosion period can be found on top of the Paleozoic sequence. They correspond to alluvial deposits characterized by large clast sizes and subangular edges, indicating proximity to the source and short transport distances (Figs. 2-6 F2; 2-7). This is followed by multistory channel deposits with a sandy massive appearance (the Une Formation). These high-energy deposits are marked by a lack of bioturbation, medium to coarse grain sizes, and erosive sharp-base bounding surfaces; however, the sparse fine-grained intervals reveal combinations of marine and continental palynomorphs, providing evidence of the unit's proximity to and connectivity with the sea (Figs. 2-4, 2-15).

Section up, the marine influence increases, reaching its peak expression in the fine-grained succession (of the Chipaque Formation). Based on a multi-proxy approach, including sedimentology and sequence stratigraphy, this unit can be divided into two subunits. The first or lower subunit was deposited in a transgressive brackish water tidally modulated environment (Fig. 2-15). Some packages of this lower unit display a fining-upward trend, starting at the base with sandy channel fills, followed by intertidal heterolithic deposits, and finally supratidal deposits of massive mudstone capped by coal beds (photo # 11, Fig. 2-6). Other packages present variable or incomplete tidal marginal marine sequences (Fig. 2-14). These deposits are interpreted to have been deposited in an estuarine complex setting, culminating in a higher rank maximum flooding surface (mfs).

The subsequent subunit is characterized by the progradation of small coarse-grained deposits, however, engulfed in a muddy matrix (Figs. 2-12; 2-14). This second subunit is also marked by heightened levels of flocculation (Fig. 2-13, F18 W-9). Notably, this subdivision is dominated by dark gray unbioturbated mudrocks (e.g., W-2, Figs. 2-12, 2-15).

The uppermost part of the second subdivision is characterized by a slight intensification in progradation rates, although the vertical component (aggradation) remains significantly high. In the wells of field B (Fig. 2-15), this intensification is marked by a notable increase in coarse-grained beds. Moving seaward (to Field A), the thickness and caliber of the possible correlative packages decrease as can be expected. The uppermost interval of the Chipaque Formation in

field A is continuously eroded southward and is absent in field B (Fig. 2-15). These deposits consist of black mudrocks, fine-grained sandstones, and heterolithic successions.

Bioturbation occurs as an opportunistic behavior within the sandier intervals, whereas the dark gray mudrocks remain unbioturbated throughout the entire logged intervals of the Chipaque Formation. This suggests that the black unbioturbated mudrocks were likely deposited in anoxic or dysoxic environments, with benthic communities able to thrive solely when coarse-grained, oxygenated sediments were deposited. In general, across all subdivisions of the Chipaque Formation, bioturbation increases seaward (Field B) and decreases landward (Field A). (Fig. 2-15).

The final part (the fraction of Lower Guadalupe) is mainly typified by stacked coarse-grained beds. Bioturbation is absent in the sandstone beds and very low in the mudrocks (e.g., W-8, Fig. 2-15). Additionally, the marine to continental ratio is relatively low, resembling some intervals of the Chipaque Formation. Unfortunately, this unit is eroded by an unconformity, limiting the capacity to observe and deduce further details about it. This unit is ultimately interpreted to have been deposited in a delta plain and/or uppermost delta front setting.

2.8. Discussion

A significant limitation of palynology data is related to the transport effect that the palynomorphs may undergo; for instance, continental palynomorphs such as pollen, spores, fungi, and small plant-remains, can be transported over long distances by wind, water, or by animals, far from their sources into the marine realm. These potential transportation vectors introduce uncertainty regarding the probable depositional setting, particularly for two of the three gross classifications (i.e., 2) continental marine-influenced, and 3) marine to marginal marine). However, this challenge has been addressed previously by using relative ratios (marine vs continental counts) and assuming a decrease in continental influence with increasing seaward distance. This mathematical approach mitigates, to some extent, the error introduced by continental palynomorphs transported into the marine realm. This technique has been demonstrated to be a reliable indicator for the relative influence of continental over the marine

elements (e.g., de Vernal and Giroux, 1991; de Vernal, 2009) and as per se, in the setting differentiation in terms of distance.

The ratio between marine and continental palynomorphs observed in the study area (Fig. 2-4; represented by the green curve above the total marine counts) provides a solution for the primary objective of gross depositional setting differentiation. For instance, there is a notable contrast between the low M/C ratio values in the Une Formation (Fig. 2-4; continental marine-influenced; W-2) and the higher M/C ratio values observed in the Chipaque Formation, (Fig. 2-4, marine to marginal marine). In the Une Formation, most M/C ratio values are close to zero, indicating a prevalence of continental counts over marine counts, suggesting a closer association with continental environments. Conversely, in the Chipaque Formation, the majority of marine counts exceeds twice or more the continental counts, indicating a predominance of marine elements over continental ones. Consequently, it is inferred that the coastline (at some moments) during the sedimentation of Chipaque was farther away than during the sedimentation of Une or Lower Gudalupe formations.

While most palynological samples in the vertical domain may provide sufficient insight into the gross depositional settings of the Upper Cretaceous sequence, some intervals are limited spatially. For example, samples from W-4 at the bottom section of the Une Formation suggest a continental setting without any direct marine contact. However, this interpretation could be erroneous from a regional perspective if this site were located in a sheltered area from the sea but surrounded by it. Additional lateral delineation of this unit would help refine paleo depositional interpretations of the bottom of the Une Formation.

Similar to the palynological analysis, the paleocurrent direction results presented here may contain several biases, specifically due to the low spatial density and irregular distribution of sampling points. From a spatial perspective, this is true. However, the vertical sampling is somewhat redundant, especially for the Une and Lower Guadalupe Formations, which are dominated by coarse-grained lithologies and unidirectional patterns, where most of the measurements were obtained. Our results indicate two broad group of sediment transport directions, northwest and west-northwest for the Une and Lower Guadalupe formations, respectively (Fig. 2-16). This variation could be related to a possible reconfiguration of the basin

over time. This is, during the Cenomanian-Turonian (Une Formation), the basin depocenter may have been located more towards the northwest of the study area, whereas for the Middle Campanian (Lower Guadalupe Formation), the basin depocenter axis was situated more towards the west of the study area, as proposed by Villamil (1999).

In terms of depositional settings for the Chipaque Formation, the findings from this study indicate a marginal-marine depositional setting, contrasting with interpretations from the Eastern Cordillera, where the Chipaque Formation is interpreted to have been deposited in more marine conditions (e.g., Guerrero and Sarmiento, 1996; Montoya and Reyes, 2005). Our findings are supported by the low bioturbation intensities, small faunal sizes, and low diversity of trace fossils observed. Additionally, the presence of black unbioturbated mudrocks and bioturbated event beds suggests that bioturbation occurred as an opportunistic behavior linked to oxygen levels. These characteristics could have been related to, or exacerbated by, the tidal action experienced in this marginal area. Likewise, the Une and Lower Guadalupe formations exhibit a larger continental affinity and lower marine influence than those studied in the Eastern Cordillera locations (e.g., Julivert, 1962; Perez and Salazar, 1978; Guerrero and Sarmiento, 1996; Montoya and Reyes, 2005), this difference has a direct relationship with distance; indeed, the corrected distance to those sites may be greater than it appears on a simple map. Structural reconstructions indicate that the Eastern Cordillera and Magdalena Valley have undergone significant shortening due to tectonic activity (e.g., 68 km, Cooper et al., 1995; 70 km, Cortes et al., 2006; 100 km, Bayona et al., 2008).

Unlike outcrop data from the Eastern Cordillera, core data from the subsurface of the southwestern Llanos Basin offers the advantage of fresh rock samples in a relatively structurally quiet area, allowing the distinction of these subaerial periods in the rock record. The analyzed core data contains clear evidence not only of the unconformity between Lower Guadalupe and Chipaque formations but also of additional subaerial exposure periods, including the Paleocene and Eocene unconformities. The absence of the unconformity between the Lower Guadalupe and Chipaque formations in western locations (e.g., Perez and Salazar, 1978; Guerrero and Sarmiento, 1996; Montoya and Reyes, 2005), can be explained by the probable extent of the unconformity. In other words, the extension of this unconformity toward the west is likely

limited by the position of the proto-Guaicaramo fault system or by the weathering conditions of the analyzed outcrops.

2.9. Conclusions

The sparse occurrence of a basal unit and its lithological differences compared to overlying unit suggest they corresponds to remnant bodies from the bypass period between the Paleozoic and the Upper Cretaceous.

The general lack of bioturbation within most of the dark gray mudrocks of Chipaque Formation suggests a stressful environment for benthic organisms. A possible cause may contribute to this situation are anoxic or poorly oxygenated bottoms, as can be deducted from the dark gray muddy rocks.

The tidal imprint is present not solely within the Chipaque Formation but also within the Une and Lower Guadalupe Formations. The inferred fluctuations in water salinity due to tidal action, along with the heightened levels of sedimentation during the deposition of the Une and Lower Guadalupe Formations, may have exacerbated the stressful conditions for living organisms, fact that is reflected by the increase of bioturbation intensity and size seaward and conversely decreasing in landward direction.

Paleocurrent measurements suggest a subtle change in net sediment transport from northwest during the Cenomanian-Turonian to west-northwest during the Middle Campanian, which could be related to basin reconfiguration over time.

2.10. References

Allen, J.R.L. (1982). Sedimentary structures: their character and physical basis. V2 Elsevier. New York 663p.

Bann, K.L., Tye, S.C., MacEachern, J.A., Fielding, C.R., and Jones, B.G. (2008). Ichnological and sedimentologic signatures of mixed wave-and storm-dominated deltaic deposits:

Examples from the Early Permian Sydney Basin, Australia. *In*: G.J. Hampson, R.J. Steel, P.B. Burgess, R.W. Dalrymple (Eds.), Recent Advances in Models of Siliciclastic Shallow-Marine Stratigraphy, SEPM Spec. Publ., vol. 90 (2008), p. 293-332.

Bayona, G., Cortes, M., Jaramillo, C., Ojeda, G., Aristizabal, J.J., and Reyes-Harker, A. (2008). An integrated analysis of an orogen-sedimentary basin pair: Latest Cretaceous-Cenozoic evolution of the linked Eastern Cordillera orogen and the Llanos foreland basin of Colombia. GSA Bulletin. Vol. 120. No. 9/10. p. 1171-1197. doi: 10.1130/B26187.1

Bhattacharya, J.P. (2010). Deltas. in James, N.P., and Dalrymple, R.W., eds, Facies Models 4: GEOtext 6, Geological Association of Canada, St. John's, Newfoundland, 233-264.

Catuneanu, O. (2006). Principles of Sequence Stratigraphy. 1st Ed. Elsevier, Amsterdam, 375p.

Collinson, J.D. (1969). The sedimentology of the Grindslow shales and the Kinderscout grit: A deltaic complex in the Namurian of northern England. *Journal of Sedimentary Petrology*, Vol. 39, p. 194-221.

Cooper, M., Addison, F., Alvarez, R., Coral, M. Graham, R. et al., (1995). Basin development and tectonic history of the Llanos basin, Eastern Cordillera, and Middle Magdalena Valley, Colombia. *AAPG Bulletin*. *Vol. 79*. No 10. p. 1421-1143.

Cortes, M., Colleta, B. and Angelier, J. (2006). Structure and tectonics of the central segment of the Eastern Cordillera of Colombia. Journal of South American Sciences. Vol. 21. p. 437-465. doi:10.1016/j.jsames.2006.07.004

Dalrymple, R.W. (2010a). Interpreting sedimentary successions: facies analysis and facies models, in James, N.P., and Dalrymple, R.W., eds, Facies Models 4: GEOtext 6, Geological Association of Canada, St. John's, Newfoundland, 3-18.

Dalrymple, R.W. (2010b). Tidal depositional systems, *in*: James, N.P., and Dalrymple, R.W., eds, Facies Models 4: GEOtext 6, Geological Association of Canada, St. John's, Newfoundland, 201-231.

Davis, R.A. (2012). Tidal signatures and their preservation potential in stratigraphic sequences. *in*: Davis R.A. and Dalrymple R.W. (eds.), Principles of Tidal Sedimentology. https://DOI10.1007/978-94-007-0123-6_3

Diessel Claus, F.A. (2007). Utility of coal for sequence-stratigraphy analysis. International Journal of Coal Geology, 70, 3-34. https://doi:10.1016/j.coal.2006.01.008

Flores, R.M. (2014). Coal and coalbed gas: fueling the future. 1st Ed. Elsevier, Waltham, MA. 697p.

Fox, A. and Vickerman, K., (2015). The value of borehole image logs. Reservoir, Canadian Society of Petroleum Geologist. January, p. 30-34.

Gingras, M.K., MacEachern, J.A., and Dashtgard, S.E. (2011). Process ichnology and the elucidation of physico-chemical stress. Sedimentary Geology, 237, 115-134. https://doi:10.1016/j.sedgeo.2011.02.006

Guerrero, J., and Sarmiento, G. (1996). Estratigrafía Física, Palinología, Sedimentológica y Secuencial del Cretácico Superior y Peleoceno del Piedemonte Llanero. Implicaciones en Exploración Petrolera. Geología Colombiana No. 20 p 3-66 Bogotá.

Guerrero, J., Sarmiento, G. and Navarrete, R. (2000). The stratigraphy of the W side of the Cretaceous Colombian basin in the Upper Magdalena Valley. Reevaluation of selected areas and type localities including Aipe, Guaduas, Ortega, and Piedras. Geología Colombiana. Vol. 25. Bogotá. p. 45-110.

Greb, S.F., and Archer, A.W. (2007). Soft-sediment deformation produced by tides in meizoseismic area, Turnagain Arm, Alaska. The Geological Society of America. 35, 5, 435-438. https://doi:10.1130/G23209A.1

Horton, B.K., Saylor, J., E., Nie, J., Mora, A., Parra, M., Reyes-Harker, A., and Stockli, D.F. (2010). Linking sedimentation in the northern Andes to basement configuration, Mesozoic extension, and Cenozoic shortening: Evidence from detrital zircon U-Pb ages, Eastern Cordillera, Colombia. Bulletin of Geological Society of America. Vol. 122. No 9-10. p. 1423-1442. https://doi.org/10.1130/B30118.1

ICP, (2012). W-1. Internal report 08-12. Ecopetrol-ICP. Piedecuesta, Colombia.

ICP, (2014a). Sagu Creek, las Blancas Creek and wells W-3 and Ctal-1. Internal report 20-14. Ecopetrol-ICP. Piedecuesta, Colombia.

ICP, (2015). W-2. Internal report 13-15. Piedecuesta, Colombia.

ICP. (2021). W-4. Internal report 01-21. Ecopetrol-ICP. Piedecuesta, Colombia.

Jelby, M.E., Grundvåg, S.-A., Helland-Hansen, W., Olaussen, S., and Stemmerik, L., (2020). Tempestite facies variability and storm-depositional processes across a wide ramp: Towards a polygenetic model for hummocky cross-stratification. Sedimentology 67, 742-781. https://doi.org/10.1111/sed.12671

Julivert, M. (1962). La Estratigrafía de la formación Guadalupe y las estructuras por gravedad en la serranía de Chía (Sabana de Bogotá). Boletín de Geología UIS. No. 11. p. 5-21 Bucaramanga. Colombia.

Kerr, A.C. (1998). Oceanic Plateau formation: A cause of mass extinction and black shale deposition around the Cenomanian-Turonian boundary? Journal of the Geological Society. Vol. 155. p. 619-626.

Kerr, A.C. (2005). Oceanic LIPs: The kiss of Death. Elements. Vol. 1. p. 289-292.

Lai, j., Wang, G., Wang, S., Cao, J., Li, M., Pang, X., Han, C., Fan, X., Yang, L., He, Z., and Qin, Z. (2018). A review on the applications of image logs in structural analysis and sedimentary characterization. Marine and petroleum geology. Vol 95. p. 139-166.

Leckie, R.M., Bralower, T.J., and Cashman, R. (2002). Oceanic anoxic events and plankton evolution: Biotic response to tectonic forcing during the mid-Cretaceous. Paleoceanography. Vol. 17. No. 3. https://doi.org/10.1029/2001PA000623

MacEachern, J.A., Pemberton, S.G., Bann, K.L. and Gingras, M.K. (2007). Departures from the archetypal ichnofacies: effective recognition of physico-chemical stresses in the rock record, *in*: MacEachern, J.A., Bann, K.L., Gingras, M.K., and Pemberton, S.G., eds., 2007. Applied Ichnology, SEPM Short Course Notes #52, 380p.

MacEachern, J.A., Pemberton, S.G., Gingras, M.K. and Bann, K.L. (2010). Ichnology and facies models, *in*: James, N.P., and Dalrymple, R.W., eds, Facies Models 4: GEOtext 6, Geological Association of Canada, St. John's, Newfoundland, 201-231.

Martin, C.A.L. and Turner, B.R. (1998). Origins of massive-type sandstones in braided rivers systems. Earth-Science Reviews, 44, 15-38

Miall, A. (2016). Stratigraphy: A modern synthesis. Springer. 454p. https://doi:10.1007/978-3-319-24304-7

Montoya, D. and Reyes, G. (2005). Geología de la Sabana de Bogotá. Ingeominas. Bogota. Colombia. 104 p.

NASA. (2000). Suttle radar topography mission. https://www.earthdata.nasa.gov/sensors/srtm

Nichols, G. (2009). Sedimentology and stratigraphy 2nd ed. Wiley-Blackwell. 419 p.

Novak, A., and Egenhoff, S. (2019). Soft-sediment deformation structures as a tool to recognize synsedimentary tectonic activity in the middle member of the Bakken Formation, Williston

Basin, North Dakota. Marine and Petroleum Geology, 105, 124-140. https://doi.org/10.1016/j.marpetgeo.2019.04.012

Perez, G., and Salazar, A. (1978). Estratigrafía y facies del Grupo Guadalupe. Geología Colombiana No. 10. p. 1-116 Bogotá. Colombia.

Reyes-Harker, A., Ruiz Valdivieso, C.F., Mora, A., Ramirez-Arias, J.C., Rodriguez, G., De la Parra, F., Caballero, V., Parra, M., Moreno, N., Horton, B.K., Saylor, J.E., Silva, A., Valencia, V., Stockli, D., and Blanco, V. (2015). Cenozoic paleogeography of the Andean foreland and retroarc hinterland of Colombia. AAPG Bulletin. Vol. 99. No. 8. p. 1407-1453.

Sarmiento-Rojas, L.F. (2001). Mesozoic rifting and Cenozoic basin inversion history of the Eastern Cordillera Colombian Andes inferences from tectonic models. PhD. Thesis Univ. of Amsterdam. 295 p.

Sarmiento-Rojas, L.F. (2011) Llanos Basin. Geology and hydrocarbon potential. In: Cediel F. and Ojeda G. Y. (eds). Petroleum geology of Colombia, Vol 9. Universidad Eafit for ANH, Medellín, p 192.

Sarmiento-Rojas, L.F. (2019). Cretaceous stratigraphy and paleo-facies maps of northwestern South America. In: Cediel F and Shaw R. P eds. Geology and Tectonics of Northwestern South America: The Pacific-Caribbean-Andean Junction. Frontiers in Earth Sciences. p. 673-747. https://doi.org/10.1007/978-3-319-76132-9_10

Snyder, M.E. and Waldron, J.W.F. (2021). Deformation of soft sediments and evaporites in a tectonically active basin: Bay St. George sub-basin, Newfoundland, Canada. Atlantic Geology, 57, 275-304. https://doi:10.4138/atlgeol.2021.013

Valderrama, Y., and Catuneanu, O. (2024). High-resolution Sequence Stratigraphy for the Cretaceous in the Southwestern side of the Llanos Basin, Colombia: implications for exploration and production. *In preparation (following Chapter)*.

Villagomez, D., Spikings, R., Magna, T., Kammer, A. Winkler, W., and Beltran, A. (2011). Geochronology, geochemistry and tectonic evolution of the Western and Central cordilleras of Colombia. Lithos Vol. 125. p. 875-896.

Villamil, T. (1999). Campanian-Miocene tectonostratigraphy, depocenter evolution and basin development of Colombia and western Venezuela. Palaeogeography, Palaeoclimatology, Palaeoecology Vol. 153. Iss. 1-4. p. 239-275. https://doi.org/10.1016/S0031-0182(99)00075-9

Villamil, T. (2003). Regional hydrocarbon systems of Colombia and western Venezuela: Their

origin, potential, and exploration, *in* Bartolini C, Buffler, R. T. and Blickwede, J. eds., The Circum-Gulf of Mexico and the Caribbean: Hydrocarbon habitats, basin formation, and plate tectonics: AAPG Memoir. vol. 79, p. 697-734.

Chapter 3. High-resolution Sequence Stratigraphy for the Cretaceous in the southwestern side of the Llanos Basin, Colombia: Implications for exploration and production.

Abstract

The Llanos foreland basin stands out as one of the most prolific hydrocarbon basins in Colombia, in particular, the southwestern area contains two of the major Colombian oil fields, which produce from both Cretaceous and Cenozoic rocks. A thorough understanding of the Cretaceous sequence is essential to continue with the exploration and production in this and other areas. In this context, a robust sequence stratigraphic framework is still needed. By applying an integrative approach that combines sedimentology, palynology, ichnology and stratigraphy, on core and wellbore data, allowed us to reveal the hidden characteristics of the rock record and built a sequence stratigraphic framework that explains the Upper Cretaceous sequence of the southwestern region of Llanos Basin, Colombia, in terms of relative sea-level changes and sedimentation, and subsequently, providing valuable insights for exploration and production processes in the area. This framework encompasses five distinct stages, starting at the base with a Lowstand Systems Tract (1) represented by Une Formation, followed by a Transgressive Systems Tract (2), which solely comprises the lower section of Chipaque Formation, and a Highstand Systems Tract (3), which span the remaining upper section of Chipaque Formation. After that, towards the eastern side of the ancient proto-Guaicaramo fault system, a period of erosion occurred during a fraction of the Middle Campanian, however, at the same time, sedimentation continues westward of this fault system, these two coetaneous events constitute the Falling-Stage Systems Tract (4); finally, a return of the normal regression conditions to the area, with a Lowstand Systems Tract (5), represented by the partial occurrence of Lower Guadalupe eastward of the Guaicaramo fault system.

3.1. Introduction

At a regional level, one of the most iconic studies on the Cretaceous evolution of Colombia is the work done by Etayo-Serna et al., (1969). Using ammonites for large-scale correlations, they produced stage-by-stage maps of the Colombian Cretaceous Basin. Following this line of research, Villamil (1996, 1998), in his PhD research, detailed the Albian-Santonian interval in the southern part of the basin, employing geochemical and paleontological tools while also integrating data from other areas of the basin. Another significant integrative study was conducted by Sarmiento-Rojas (2001), his PhD research focused on the evolution and inversion of the Eastern Cordillera, area that could be envisaged as the principal depositional axis of the Colombian Cretaceous Basin.

This current research aims to continue contributing to advance in the Colombian Cretaceous succession understanding, however, from the southwestern area of the Llanos foreland Basin (Figs. 3-1). This is done by integrating facies analysis, biostratigraphy, and borehole information corresponding to the Upper Cretaceous in a sequence stratigraphic framework.

During the Lower Cretaceous the study area was subject to sediment bypass and erosion, while during the Upper Cretaceous, sedimentation and erosion took place. Given that the southwestern Llanos foreland Basin during the Upper Cretaceous was situated in a marginal marine setting (Figs. 3-2), it becomes an ideal location for study, as these places are highly susceptible to record fluctuations in accommodation and sedimentation.

One of the main advantages of sequence stratigraphy is its independence of lithology, nevertheless, affording the lithological prediction (Catuneanu et al., 2011). Since the purpose of sequence stratigraphy is to provide a stratigraphic framework that represents the variations in accommodation and sedimentation, however, at the same time reflecting the interplay of local and global controls (Catuneanu et al., 2011), sequence stratigraphy emerges as an ideal tools to decipher and to understand the interactions among the variables that controlled the rock succession during its deposition, and consequently filling the knowledge gap in understanding the Cretaceous record in the area.

3.1. Geologic setting

3.1.1. Tectonic setting

The Cretaceous period was characterized by elevated levels of CO2 (Barron and Washington, 1985), warm conditions (Haywood et al., 2019), highly dynamic tectonic activity, such us the continued rifting of South America and Africa (Poulsen et al., 2003), the creation of new oceanic plateaus (Kerr, 1998, 2005; Fig. 3-2), and the expansion and contraction of several interior sea ways (Blakey and Ranney, 2018; Fig. 3-2).

In particular, the northwestern area of South America experienced active tectonism (e.g., Aspden et al., 1987; Cooper et al., 1995; Villamil, 1999; Sarmiento-Rojas, 2001; Fig. 3-2). This condition along with the aforementioned global context, implicitly, triggered conditions recorded in the rock succession.

The tectonic history of the Cretaceous basin is represented by two different stages, a Lower Cretaceous rifting stage (that began in the Triassic), and an Upper Cretaceous back-arc basin stage (Cooper et al., 1995, Horton et al., 2010; Fig. 3-2). The rifting stage was characterized by the creation of grabens and associated large vertical faults, such as the proto-Guaicaramo fault-system (Figs. 3-2 and 3-3), which controlled the creation of accommodation and later were inverted during the contractional phases (Sarmiento-Rojas., 2001; Villamil, 2003; Mora et al., 2009). The final stage is characterized by the onset of active subduction along the western margin and the uplift of the ancestral Central Cordillera (Villamil, 1999, 2003). The subduction at the western margin progressively transported large mases of oceanic crust, which were subsequently accreted to the margin along the 'suture' represented by the Romeral fault system (Cooper et al., 1995; Villamil, 2003; Villagomez et al., 2011; Fig. 3-2). As a result of this ongoing subduction and accretion process, the seaway was closed by the Late Cretaceous and/or Early Paleocene (Montes et al., 2019; Fig. 3-2), giving place to a new basin configuration. This new basin configuration formed a vast foreland basin that extended from the ancient eastern side of the proto-Central Cordillera to a significant portion of the eastern Amazon (Hoorn et al., 2010); however, the subsequent uplift of the Eastern Cordillera further modified the internal

basin configuration. With the definitive uplift of the Eastern Cordillera, two new physiographic landmarks were created - a hinterland, located between two mountain systems (Central and Eastern Cordillera), known as Magdalena Valley and the current foreland basin, located eastward of the Eastern Cordillera, known as Llanos Basin (Cooper et al., 1995; Moreno et al., 2011).

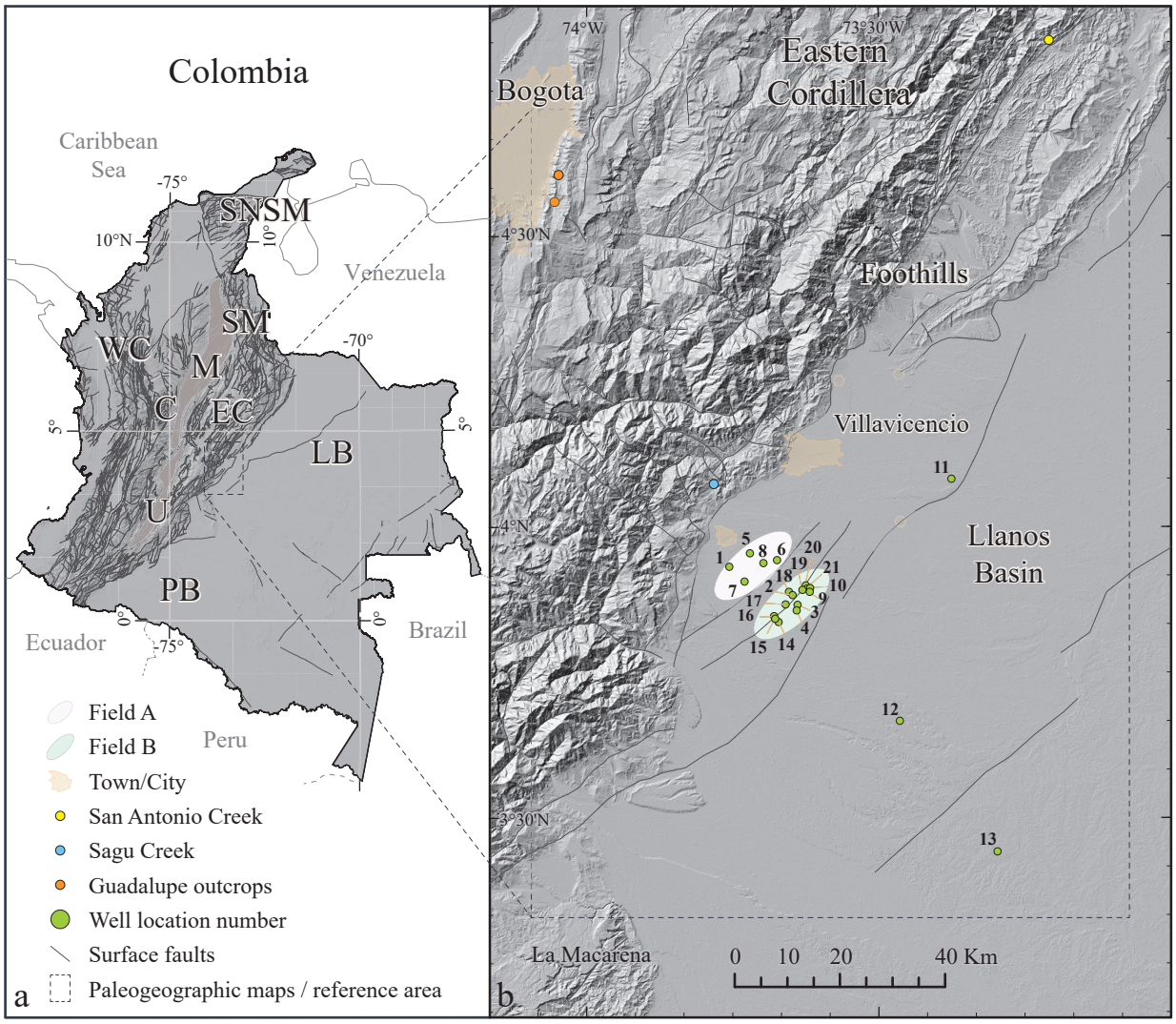

Figure 3-1. Study Location and well distribution. a) Colombian map and major surface fault systems and lineaments. Western areas depict a larger tectonic deformation than eastern areas. Western Cordillera (WC), Central Cordillera (C), Middle and Upper Magdalena Valley Basin (M and U) respectively. Santander Massif (SM). Eastern Cordillera (EC). Llanos Basin (LB). Putumayo Basin (PB). Sierra Nevada de Santa Marta (SNSM). b) Zoom in study area, detailing

the well location distribution, surface fault systems and lineaments, and major towns as reference. Topographic base map from NASA, (2000).

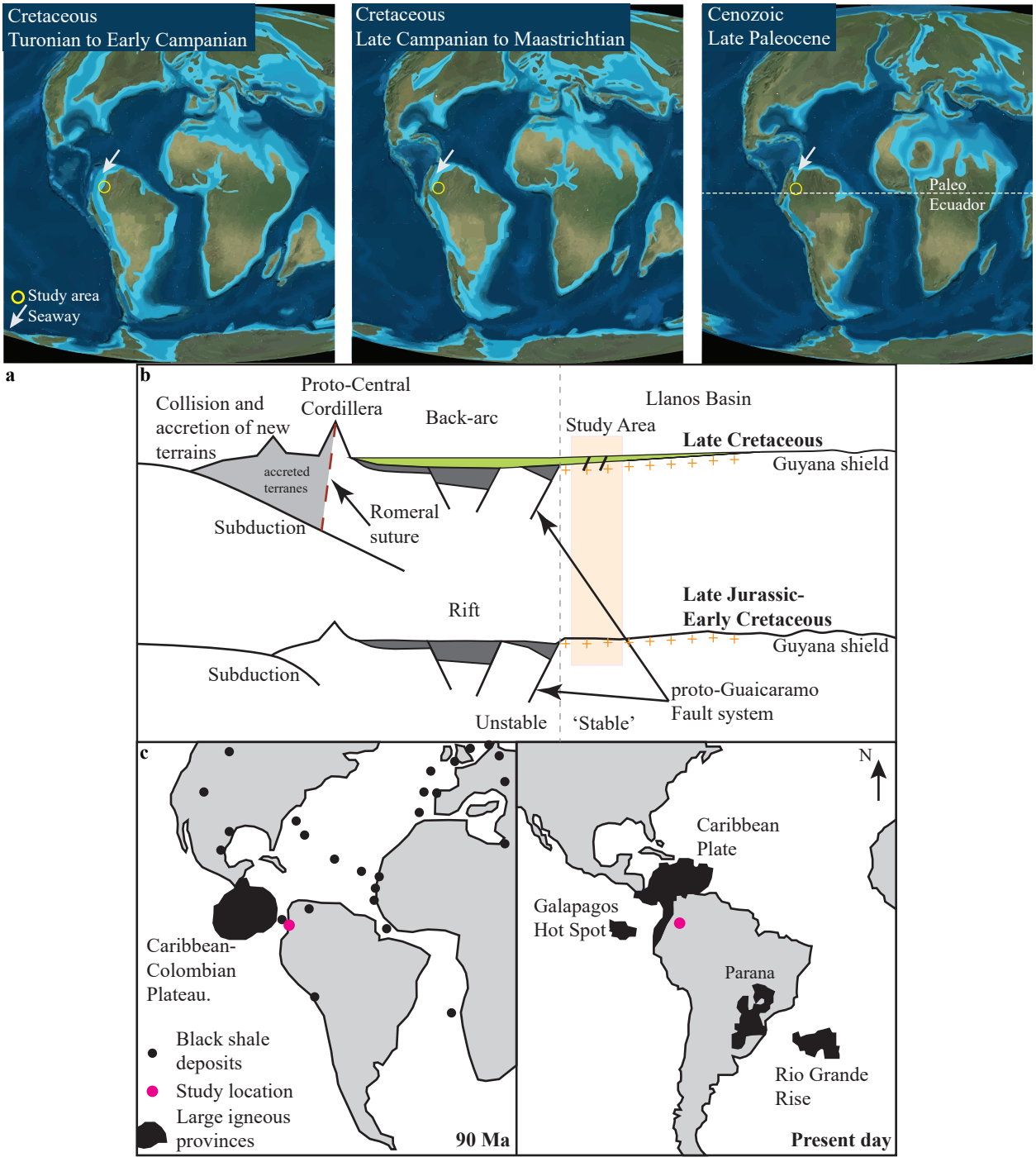

Figure 3-2. Tectonic Setting Summary. **a**) Approximate paleogeographic location for the study area at three stages (Turonian, Late Campanian/Maastrichtian, and Late Paleocene). The orange arrow indicates the ancient epicontinental sea that covered part of the Northwestern side

of South America; Over time, the influence area of this sea diminished due to the accretion of new terrains at the western border. The black circle denotes the approximate location of the study area, initially interpreted to be situated in a coastal to shallow marine environment (during the Upper Cretaceous) and eventually transitioning to a continental setting (during the Late Paleocene). Maps modified from Blakey, (2008). **b**) Eastern pacific large igneous province during the Turonian and its present-day location. Part of the igneous material was transported and accreted to the western margin of Northern South American plate. Modified from Kerr, (1998). **c**) Schematic basin evolution in cross-section for the Cretaceous period. For the study area, the Early Cretaceous was a period of exposure and sediment by-pass, whereas for the Late Cretaceous sedimentation (but also erosion) occurred. Guaicaramo fault system marks the limit among tectonically 'unstable' and 'stable' terrains. Modified from Horton et al., (2010).

3.1.2. Stratigraphy

The main units of interest in this study are the Une, Chipaque, and Lower Guadalupe formations - units that partially appears to the east of Guaicaramo fault-system by action of erosion and/or non-deposition (Fig. 3-3). The Une and Lower Guadalupe formations belong to the conventional reservoir group, composed mainly of sandy packages. In contrast, Chipaque formation mostly corresponds to a source rock, although some encased coarser-grained beds commonly occur at the study location. Basinward, La Luna and Villeta formations, are the partial equivalents to the Chipaque Formation (Villamil, 2003), however, these formations have a larger areal and vertical extent and are less influenced by the continental input.

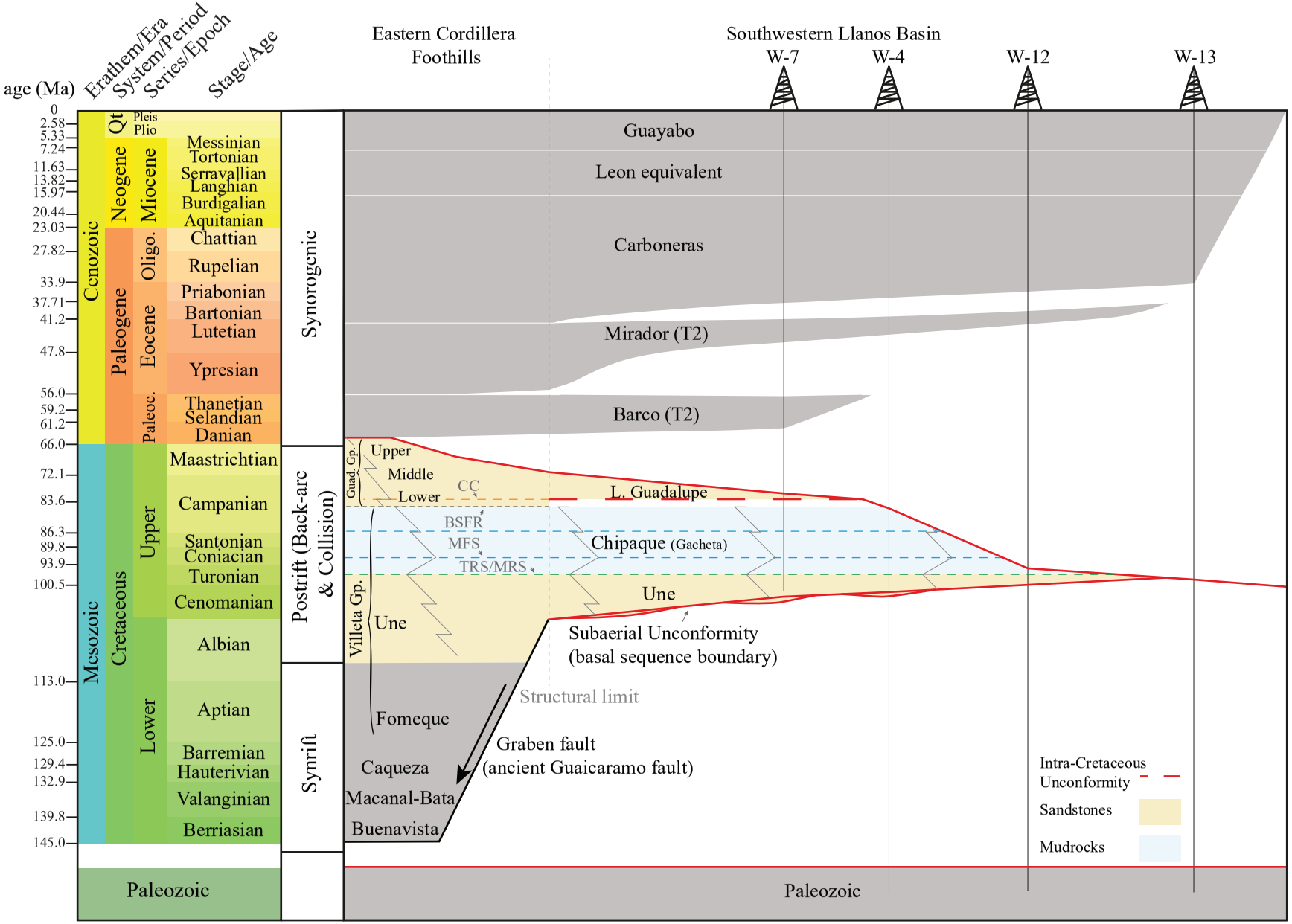
age (Ma)
Erathem/Era
System/Period
Series/Epoch
Stage/Age
Eastern Cordillera
Foothills
Southwestern Llanos Basin
W-7
W-4
W-12
W-13
0
2.58
5.33
7.24
11.63
13.82
15.97
20.44
23.03
27.82
33.9
37.71
41.2
47.8
56.0
59.2
61.2
66.0
72.1
83.6
86.3
89.8
93.9
100.5
113.0
125.0
129.4
132.9
139.8
145.0
Cenozoic
Mesozoic
Paleozoic
Qt
Pleis
Plio
Neogene
Miocene
Paleogene
Oligo.
Eocene
Paleoc.
Cretaceous
Upper
Lower
Messinian
Tortonian
Serravallian
Langhian
Burdigalian
Aquitanian
Chattian
Rupelian
Priabonian
Bartonian
Lutetian
Ypresian
Thanetian
Selandian
Danian
Maastrichtian
Campanian
Santonian
Coniacian
Turonian
Cenomanian
Albian
Aptian
Barremian
Hauterivian
Valanginian
Berriasian
Synorogenic
Postrift (Back-arc & Collision)
Synrift
Guayabo
Leon equivalent
Carboneras
Mirador (T2)
Barco (T2)
Guad. Gp.
Upper
Middle
Lower
CC
L. Guadalupe
BSFR
MFS
TRS/MRS
Chipaque (Gacheta)
Villeta Gp.
Une
Une
Subaerial Unconformity
(basal sequence boundary)
Structural limit
Fomeque
Graben fault
(ancient Guaicaramo fault)
Caqueza
Macanal-Bata
Buenavista
Intra-Cretaceous
Unconformity
Sandstones
Mudrocks
Paleozoic
Paleozoic

Figure 3-3. Schematic stratigraphic chart for the southwestern Llanos Basin. Rock ages for the study area based on relative palynological dates (Biostratigraphic internal reports: ICP, 2012, 2013, 2014a, 2014b, 2015). The maximum regressive surface (MRS) which separates the Une and Chipaque Fms, is interpreted to have occurred around Middle Turonian. Towards the lower part of Chipaque Fm., the maximum flooding surface (MFS) is interpreted to have occurred during the Middle of Coniacian, *however, future adjustments from absolute or relative data could modify this estimation*. Sedimentological data indicates the occurrence of Intra-Campanian unconformity; sequence stratigraphic analysis from this study links it with a force regressive event that took place during the Middle Campanian. It is expected that this subaerial unconformity may have extended basinward up to the eastern bounding fault rift system (proto-Guaicaramo fault system). Two surfaces, the basal surface of the forced regression (BSFR) and the correlative conformity (CC) are interpreted to correlate the onset and the end of this exposure period respectively. (Stratigraphic chart modified from Guerrero and Sarmiento, 1996; Sarmiento-Rojas., 2011; Reyes-Harker et al., 2015; Sarmiento-Rojas, 2019). Specific well locations can be found in Figure 3-5.

3.1.3. Depositional settings and paleoshoreline directions

For Une Formation, two depositional settings are recognized, an upper delta plain and lower delta plain. In the case Chipaque Formation, two depositional settings are interpreted (an estuarine complex at the base, and a proximal offshore or embayed area, both tidally modulated); and finally, for the Lower Guadalupe Formation, a lower delta plain and/or upper delta front are interpreted (Valderrama and Catuneanu, 2024; Figure 3-4).

Paleocurrent analysis performed on wells within the area (W-2, W-7, W-8, W-9, and W-11), indicates that the sediment transport direction during the Middle Cenomanian to Middle Turonian (Une Fm.) was towards the NW, and during Middle Campanian (Lower Guadalupe Fm.) was towards the WNW. The paleo coastline during Une deposition likely had a NE-SW direction, while the paleocoastline during Lower Guadalupe deposition likely had a NNE - SSW direction (Valderrama and Catuneanu, 2024; Fig. 3-5).

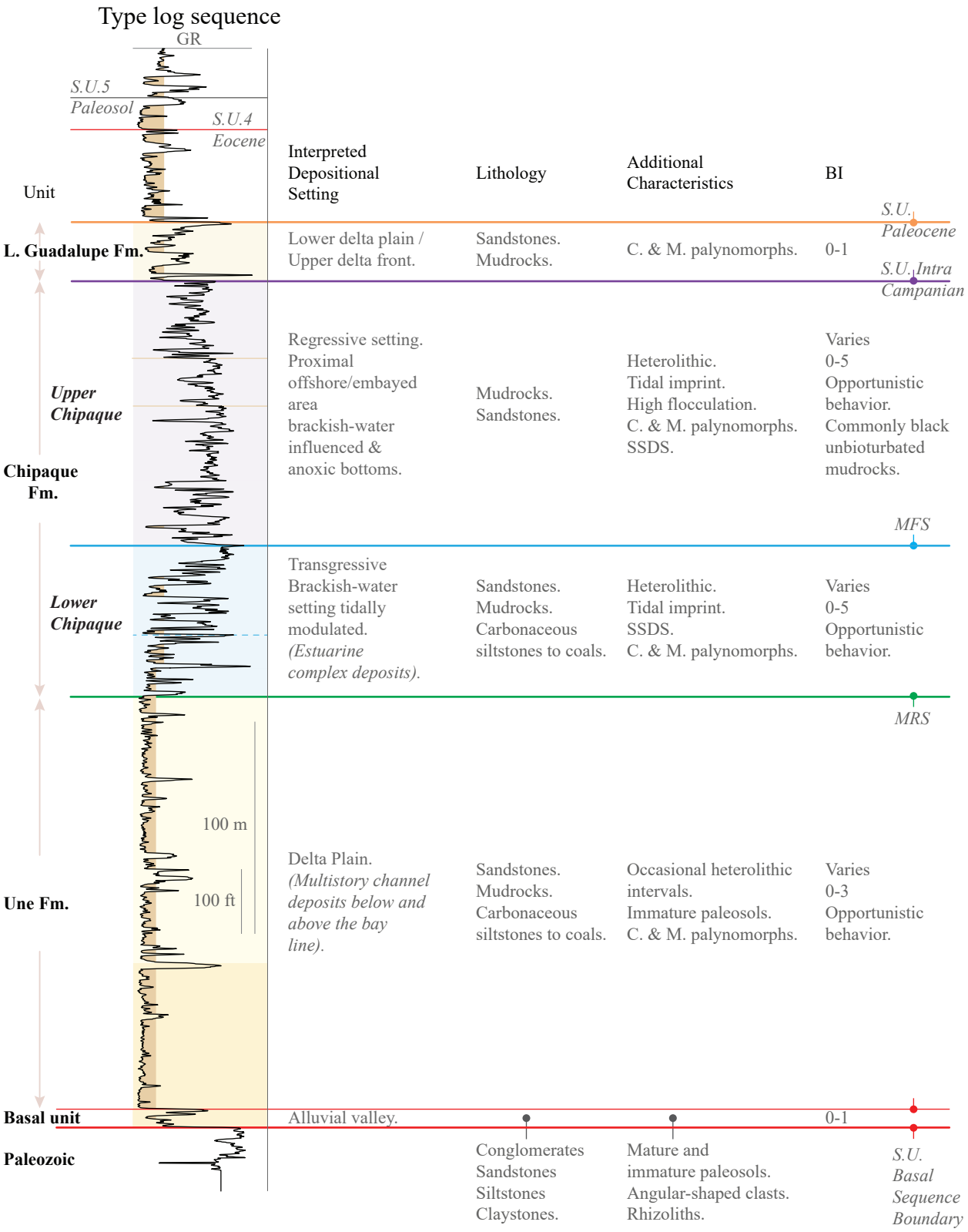
Type log sequence
GR
S.U.5
Paleosol
S.U.4
Eocene
Unit
Interpreted Depositional Setting
Lithology
Additional Characteristics
BI
S.U. Paleocene
L. Guadalupe Fm.
Lower delta plain / Upper delta front.
Sandstones. Mudrocks.
C. & M. palynomorphs.
0-1
S.U. Intra Campanian
Upper Chipaque
Chipaque Fm.
Regressive setting. Proximal offshore/embayed area brackish-water influenced & anoxic bottoms.
Mudrocks. Sandstones.
Heterolithic. Tidal imprint. High flocculation. C. & M. palynomorphs. SSDS.
Varies 0-5 Opportunistic behavior. Commonly black unbioturbated mudrocks.
MFS
Lower Chipaque
Transgressive Brackish-water setting tidally modulated. (Estuarine complex deposits).
Sandstones. Mudrocks. Carbonaceous siltstones to coals.
Heterolithic. Tidal imprint. SSDS. C. & M. palynomorphs.
Varies 0-5 Opportunistic behavior.
MRS
100 m
100 ft
Une Fm.
Delta Plain. (Multistory channel deposits below and above the bay line).
Sandstones. Mudrocks. Carbonaceous siltstones to coals.
Occasional heterolithic intervals. Immature paleosols. C. & M. palynomorphs.
Varies 0-3 Opportunistic behavior.
Basal unit
Paleozoic
Alluvial valley.
0-1
Conglomerates Sandstones Siltstones Claystones.
Mature and immature paleosols. Angular-shaped clasts. Rhizoliths.
S.U. Basal Sequence Boundary

Figure 3 4. Depositional setting summary. Typical gamma-ray log signature. Bioturbation index (BI). Subaerial unconformity (SU). Maximum flooding surface (MFS). Maximum regressive surface (MRS). Soft sediment deformation structures (SSDS). Continental (C). Marine (M). Modified from Valderrama and Catuneanu, (2024). Some wells in the area record the occurrence of a basal unit with sedimentological characteristics that differ from the typical lithological standard of the Une Formation. Sedimentological analysis indicates that this unit was probably deposited in an alluvial valley. The discontinuous presence of this unit is interpreted as remnant bodies from the bypass period.

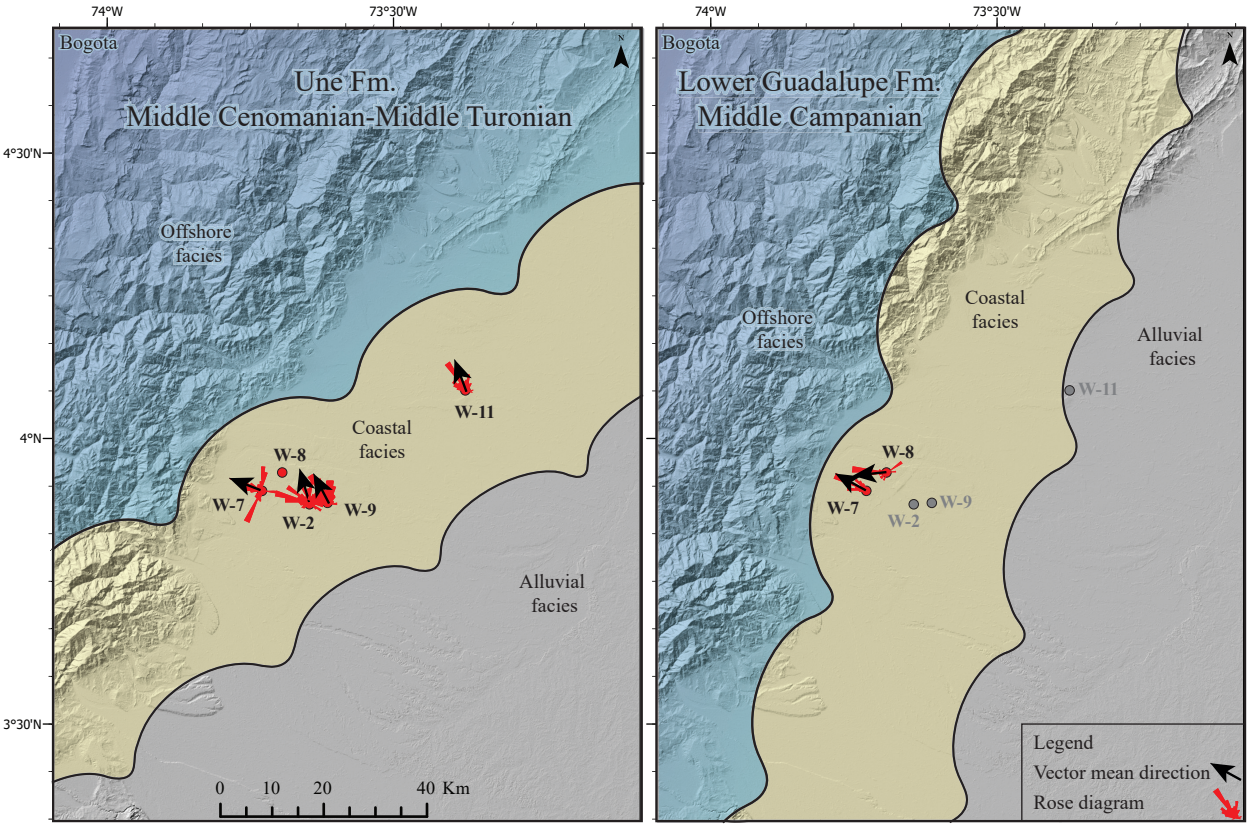

Figure 3 5. Paleoshoreline directions from Middle Cenomanian up to Middle Campanian. Paleocurrent direction extracted from micro-resistivity image logs backed by core data. The black arrow represents the mean vector direction of rose diagrams. During the Middle Cenomanian to Middle Turonian (Une Fm.), rivers transported sediment from the SE toward the sea in the NW, whereas during the Middle Campanian (Lower Guadalupe Fm.), rivers transported sediment toward the sea in a WNW direction. This subtle difference among general paleocurrent trends may have been related to a basin reconfiguration, in which the depocenter

shifted from the NW (Middle Cenomanian- Middle Turonian) towards the West (Middle Campanian), with respect to the study area. Paleocurrent data from Valderrama and Catuneanu, (2024). Topographic base map from NASA, (2000).

3.2. Data and Methods

The ideal sequence stratigraphic workflow is defined by three major steps: 1) understanding the tectonic setting, 2) determining the paleodepositional environment, and 3) constructing the sequence stratigraphic framework (Catuneanu, 2006, p. 63). In applying these steps, both time-framework and paleoecology play crucial roles, as they contribute invaluable insights to the sequence stratigraphic interpretation. In this study, palynology was used as a proxy to build and constrain the relative chronostratigraphic framework of the Upper Cretaceous sequence of the southwestern Llanos Basin, Colombia. Beyond providing information on relative age, palynology also offers additional insights into paleoecology (e.g., de Vernal and Giroux, 1991; de Vernal, 2009).

The chronostratigraphic framework of this study was established based on reported palynological dates/ages from cored well intervals (W-1, W-2, W-3, W-5, and W-6; ICP, 2012, 2013, 2014a, 2014b, 2015, 2021). In parallel, the 'three-broad' palynomorph-group classification of Valderrama and Catuneanu (2024) was implemented for the initial paleoecological definition. This approach uses the palynological yield and the marine index ratio (defined as the ratio of marine to continental elements) to define the following three broad depositional settings:

1. **Continental settings**: Consisting exclusively of continental palynomorphs (i.e., pollen and spores).
2. **Continental marine-influenced settings**: Characterized by a dominance of continental elements, with some occurrence of marine elements (i.e., foraminiferal linings, dinocysts, copepod eggs, and acritarchs). The marine index ratios for this category varies from low to very low values (less than 2, Fig. 3-6a).

3. **Marine to marginal marine settings**: Comprising a mix of continental and marine elements, but with significantly higher total marine counts (TMC > 200) and marine index ratios (M/C ratio > 2) compared to the previous group (Fig. 3-6a).

To bolster depositional environmental interpretations and contribute to the sequence-stratigraphic framework, a sedimentological analysis performed on seven cored wells within the study area was incorporated (W-2, W-4, W-7, W-8, W-9, W-10, and W-11; Valderrama and Catuneanu, 2024; Fig. 3-4). Similarly, the paleocoastline directions and sediment transport directions derived from microresistivity image interpretations of five cored wells (W-2, W-7, W-8, W-9, W-11) were also integrated (Fig. 3-5; Valderrama and Catuneanu, 2024).

Finally, to establish vertical and lateral continuity, several regional and subregional well correlations were conducted, in some cases incorporating the analysis of formation pressure data points. Ultimately, a sequence-stratigraphic framework was developed.

3.3. Chronostratigraphic framework and preliminary paleoecology

A public palynological zonation for the entire Upper Cretaceous was presented by Jaramillo and Rueda (2004). Years later, ICP (2014a) in an internal report, presented a new version with some minor modifications. This latter zonation was selected as the chronostratigraphic framework for the Cretaceous sequence of this study. Specifically, the ICP (2014a) zonation comprises the following three biozones:

1. Droseridites (91.3-88.5 Ma)
2. Dinogymnium (88.5-77.4 Ma) with two subzones:
   Dinogymnium (88.5-79.6 Ma) and
   Unipontidinium/Nematosphaeropsis (79.6-77.4 Ma)
3. Cerodinium (77.4-71.3 Ma) with three subzones:
   Cerodinium (77.4-75.8 Ma)
   Incertae sedis (75.8-73.2 Ma)
   Palaeocystodinium (73.2-71.3 Ma) (Fig. 3-6b).

The following paragraphs of this subsection summarize the biostratigraphic data sources and assumptions made to estimate the probable dates/ages for the cored sites. These approximations ultimately contributed to the establishment of the temporal framework for the Cretaceous wedge of the southwestern Llanos Basin, Colombia.

For W-1, according to ICP (2012), the two sampled intervals (f241-f262 and f347-f359 ft md, plus core shift; Fig. 3-6a) correspond to the Dinogymnium palynozone. However, subsequent revisions by ICP (2013, 2014b) for equivalent stratigraphic intervals in nearby wells (W-5 and W-6; Fig. 3-1) defined the palynozone Cerodinium subzone Cerodinium for the interval f241-f262 ft md (Fig. 3-6a and b). The Dinogymnium palynozone was identified for the samples in the interval f347-f359 ft md of W-1, but no subzone was defined for this latter interval. Based on stratigraphic relationships with additional biostratigraphic well locations (i.e., W-2 and W-3), it can be inferred that the interval f347-f359 ft md of W-1 likely corresponds to the upper part of the subzone Unipontidinium (Fig. 3-6b).

According to the ICP's (2015) report, the cored interval below the Eocene unconformity in W-2 (b865-c010 ft md approx.; Fig. 3-6a) corresponds to the biozone Dinogymnium subzone Unipontidinium (Middle Campanian). However, the same report did not establish any specific date for the analyzed samples within the Une Formation (c410-c670 ft md). Instead, it reported the presence of two palynomorph markers associated with the Turonian and Late Cenomanian periods (*Droseridites senonicus* and *Triorites africaensis*, respectively). Following this idea, we selected the first occurrence of the Turonian 'possible' marker, and the last occurrence of the Late Cenomanian 'possible' marker reported by ICP (2015) to establish a tentative limit between the Cenomanian and the Turonian in W-2 (c481 and c573 ft md plus core shift; orange arrows in Fig. 3-6a and b). Based on this assumption, it could be inferred that the deepest sections of wells W-3 and W-4 (Fig. 3-6a and b) were likely deposited prior to this boundary, possibly during the Middle? Cenomanian. We infer that the onset of Cretaceous sedimentation in the study area began around the Middle? Cenomanian.

According to ICP's (2014a) report, samples from depths b627.5-b735 ft md in W-3 correspond to the Dinogymnium zone, while samples from depths b738-b818 ft md correspond to the Droseridites zone (Fig. 3-6a and b). Based on this information, the ICP (2014a) report inherently defines the limit between the two biozones (Dinogymnium and Droseridites) in W-3. The significance of this boundary lies in the fact that the higher-rank maximum flooding surface (MFS) defined in this study is placed slightly above this limit. Consequently, it is possible (while considering the potential errors in biostratigraphic temporal calibration) to establish and/or speculate that the main MFS of the Cretaceous sequence in the southwestern Llanos Basin may have occurred around the Middle Coniacian (Fig. 3-6b).

In addition to providing a chronostratigraphic framework, the palynological data contains invaluable paleoecological information. Specifically, three samples rich in pollen and spores with no marine elements were reported from W-4 (c103.25, c107.25, and c174.92 ft md plus core shift, Fig. 3-6a; ICP 2021). Moving up in the Une Formation, the palynological study of W-2 (c474.5-c661.8 ft md; blue horizontal bars within the TMC track in Fig. 3-6a) revealed the presence of marine elements (e.g., foraminifers, dinocysts, copepod eggs, and acritarchs) within thin, muddy layers interbedded within the large-stacked sandstone beds of the Une Formation. Progressing further up the section (i.e., W-3, W-2, and W-1; b626-b818, b870-c015, f345-f360 ft md respectively; Fig. 3-6a) along the Chipaque Formation, which primarily consists of fine-grained lithologies, the presence of marine elements becomes significantly more pronounced, with total marine counts exceeding up to 500 elements (Fig. 3-6a). Finally, the uppermost Cretaceous section (Lower Guadalupe Formation) situated between two unconformities in well W-1 (the Intra-Campanian and Paleocene unconformities; W-1, f240-f265, Fig. 3-6a) exhibits TMC similar to those found in the lower part of core W-2, however, its marine index ratio reaches higher values than the Une Formation and is similar to some intervals within the Chipaque Formation (W-2 and W-3; Fig. 3-6a).

The palynological group classification of Valderrama and Catuneanu (2024) divided the Cretaceous sequence as follows: The lower section of the Une Formation corresponds to a continental setting, although the location of W-4 may represent a sheltered place (cf. Valderrama and Catuneanu, 2024; Fig. 3-6a). The upper section of the Une Formation is classified as a

continental marine-influenced setting (W-2; Fig. 3-6a). The Chipaque Formation represents a marine to marginal-marine setting (W-2 and W-3; Fig. 3-6a); however, it is important to note that in some cases the palynological data indicates intervals with similar characteristics to those classified as continental marine-influenced within the upper Une Formation. Finally, for the Lower Guadalupe Formation, the palynological content suggests a marine to marginal-marine setting (W-1; Fig. 3-6a). However, the sample interval may overrepresent the entire Lower Guadalupe Formation, as in the study area this unit is mainly composed of sandstones without any significant bioturbation. Therefore, the rest of the Lower Guadalupe Formation is interpreted as a continental marine-influenced setting (W-1; Fig. 3-6a), similar to the upper section of the Une Formation.

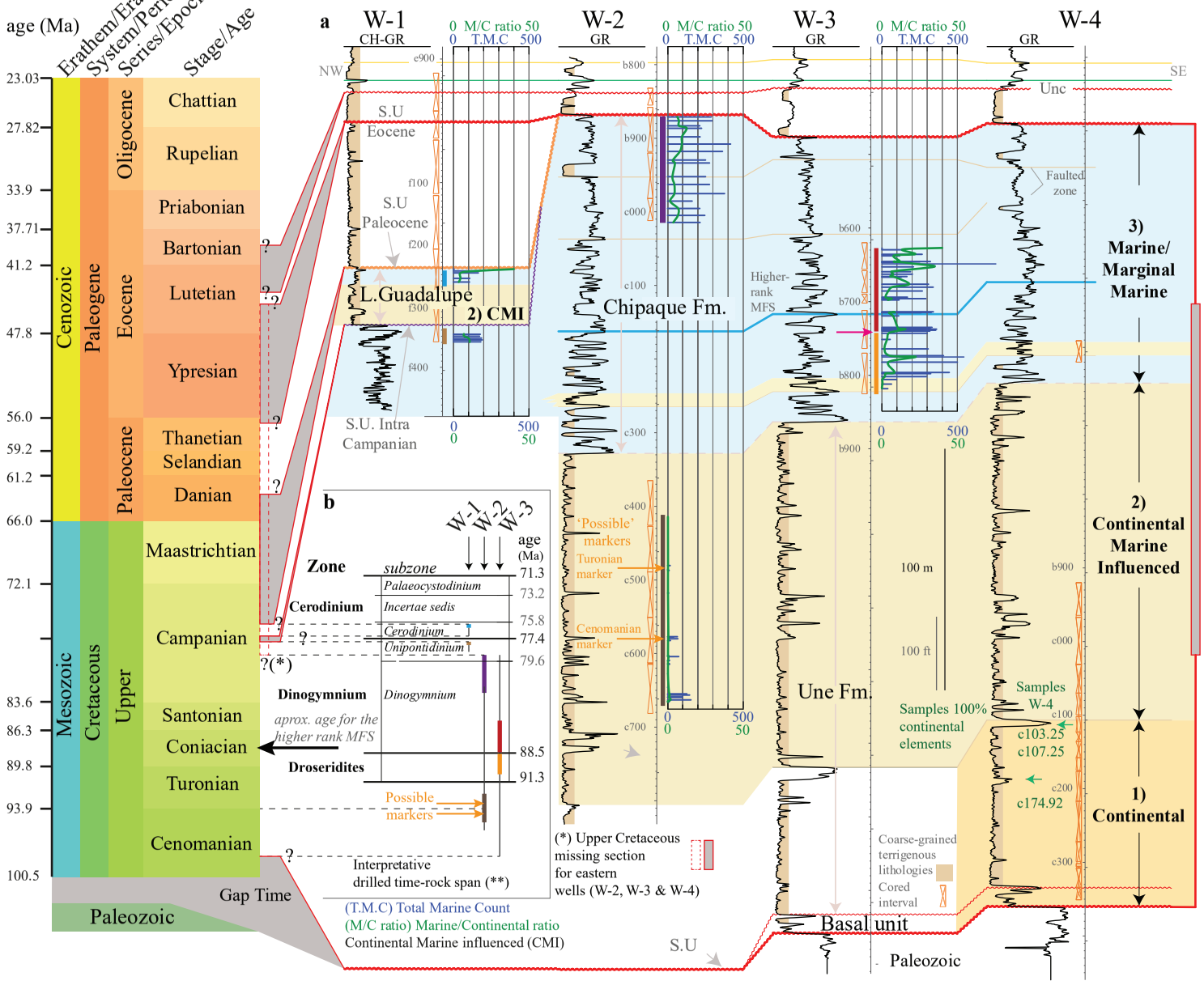
age (Ma)
Erathem/Era
System/Period
Series/Epoch
Stage/Age
Cenozoic
Paleogene
Eocene
Oligocene
Paleocene
Mesozoic
Cretaceous
Upper
Chattian
Rupelian
Priabonian
Bartonian
Lutetian
Ypresian
Thanetian
Selandian
Danian
Maastrichtian
Campanian
Santonian
Coniacian
Turonian
Cenomanian
Gap Time
Paleozoic
23.03
27.82
33.9
37.71
41.2
47.8
56.0
59.2
61.2
66.0
72.1
83.6
86.3
89.8
93.9
100.5
a
W-1
CH-GR
W-2
GR
W-3
GR
W-4
GR
0 M/C ratio 50
0 T.M.C 500
NW
SE
Unc
S.U Eocene
S.U Paleocene
L.Guadalupe
2) CMI
S.U. Intra Campanian
Chipaque Fm.
Higher-rank MFS
Faulted zone
Une Fm.
Basal unit
Paleozoic
3) Marine/ Marginal Marine
2) Continental Marine Influenced
1) Continental
'Possible' markers
Turonian marker
Cenomanian marker
100 m
100 ft
Samples W-4
Samples 100% continental elements
c103.25
c107.25
c174.92
Coarse-grained terrigenous lithologies
Cored interval
b
W-1
W-2
W-3
age (Ma)
Zone
subzone
Palaeocystodinium
Cerodinium
Incertae sedis
Cerodinium
Unipontidinium
Dinogymnium
Dinogymnium
Droseridites
71.3
73.2
75.8
77.4
79.6
88.5
91.3
aprox. age for the higher rank MFS
Possible markers
Interpretative drilled time-rock span (**)
(*) Upper Cretaceous missing section for eastern wells (W-2, W-3 & W-4)
(T.M.C) Total Marine Count
(M/C ratio) Marine/Continental ratio
Continental Marine influenced (CMI)

Figure 3-6. **a**) Relative chronostratigraphic framework and broad palynological paleoecology scheme for the Cretaceous wedge in the southwestern Llanos Basin, Colombia. Modified from Valderrama and Catuneanu, 2024.

Green arrows indicate the sampling depths in W-4, which contains 100% continental palynomorphs. This location could be interpreted as deposited landward of the bayline (*sensu* Bhattacharya, 2010) marked by a complete occurrence of continental palynomorphs whereas the rest, seaward of the bayline, is marked by the incorporation of marine elements. Horizontal blue bars represent the total marine counts reported for each sample (at core depth plus gamma ray shift). Green polylines over the total marine counts, represent the marine index ratio (marine/continental total counts). The purple arrow in W-3 (b743 ft md) indicates the inferred transition among the biozones Dinogymnium and Droseridites. Orange arrows in W-2 indicate the depths of the first Turonian and the last Cenomanian markers. Internal colors on well tracks are placed to enhance visualization of the '3-broad' paleoecological classification: (1) continental, 2) continental marine-influenced, and 3) marine to marginal marine). Question marks (?) represent the uncertainty for the temporal limits.

At western locations (i.e., W-1) the Upper Cretaceous is affected by the Paleocene unconformity and by the Intra-Campanian unconformity; (light gray areas represent gap time or missing section). (*) At eastern locations (i.e., W-2, W-3, and W-4), the Middle Eocene unconformity puts Eocene rocks in direct contact on top of Middle/Lower Campanian rocks (dashed box line next to the chronostratigraphic chart represent the gap time from the Campanian up to the Eocene). Overall, western locations present progressively younger Cretaceous rocks but are still eroded by the Paleocene unconformity at the top, and conversely, at eastern locations, the sequence is continuously eroded by the Eocene unconformity. According to internal biostratigraphic reports, the Cretaceous record for this area may encompass from the Middle? Cenomanian up to the Middle? Campanian.

Fig. 4-6 **b**) The vertical Cretaceous span for wells W-1, W-2 and W-3 is represented by the vertical lines within the zonation diagram. The analyzed and partially dated palynological intervals (colored vertical thicker bars) have been interpretatively stretched and/or squeezed

based on simple stratigraphic and temporal relationships. The chronostratigraphic framework was built based on the following biostratigraphic internal reports: ICP, 2012, 2013, 2014a, 2014b, 2015 and 2021. *Future absolute and/or relative data can modify the presented relative chronos-tratigraphic chart.* Zonation frame in figure b modified from Jaramillo and Rueda (2004) and internal report ICP (2014a). The Chronostratigraphic chart on the left modified from Cohen et al., (2021).

3.4. Observations and Results

3.4.1. Stage 0. Bypass and erosion

Prior to the Upper Cretaceous sedimentation, the study area underwent a prolonged period of erosion and sediment bypass (negative accommodation; Fig 3-7, stage 0). This is evidenced by the significant hiatus between the Upper Cretaceous and the Paleozoic rocks present in the area (Fig. 3-3). Given the notable magnitude of this subaerial unconformity, it can be classified as the basal sequence boundary for the Cretaceous rock record in the southwestern of Llanos Basin.

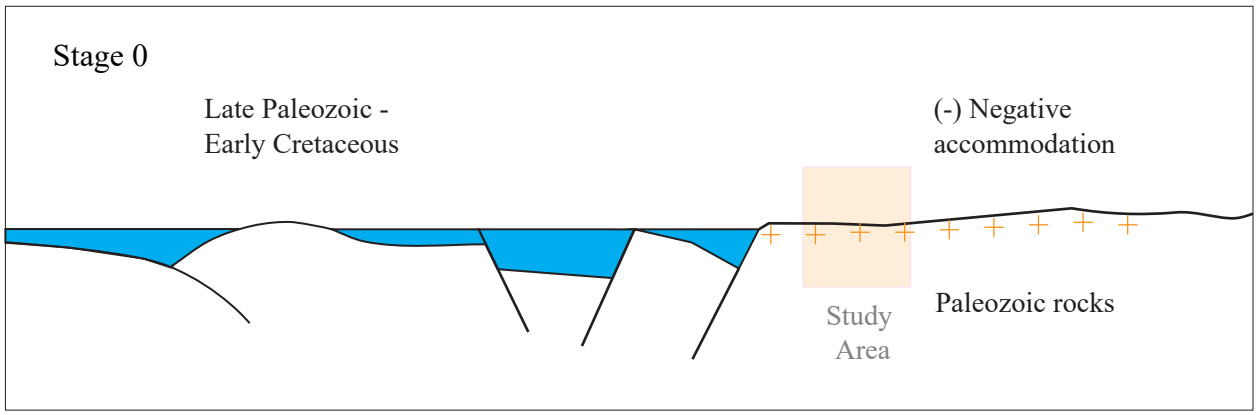

Figure 3-7. Schematic basin interpretation for Stage 0. (Modified from Horton et al., 2010). Prior to the Upper Cretaceous sedimentation onset in the southwestern Llanos Basin, the study area was subaerially exposed, erosion and/or sediment bypass took place. Although, on some occasions there are some sparse remanent deposits separating the proper Upper Cretaceous (Une Formation) from the Paleozoic rocks (Valderrama and Catuneanu 2024).

3.4.2. Stage 1. Cretaceous Lowstand systems tract (Une Fm.)

The first Upper Cretaceous deposits correspond to a lowstand systems tract (LST). A unit characterized by its notorious lowstand-wedge shape (Fig 3-8), wherein onlaps directly Paleozoic rocks landward in an unconformable manner. Although on some occasions, there are some sparse remanent deposits separating the proper Upper Cretaceous (Une Formation) from the Paleozoic rocks (Valderrama and Catuneanu, 2024).

The LST is bounded at the base by the subaerial basal sequence unconformity, which may become a composite surface conformed by more than one erosional period that occurred between the late Paleozoic and the upper Cretaceous (Valderrama and Catuneanu, 2024), and at the top by the maximum regressive surface (MRS), although this surface could have been reworked by the transgressive ravinement surface.

This LST was deposited during the early stage of the base-level rise in which the rates of positive accommodation were outpaced by the rates of sedimentation at the shoreline. In line with that, the reduced accommodation space promoted the sediment reworking and scouring, which is reflected in several rock attributes of Une Formation, such as: 1) predominance of coarse-grained material (high sand/gravel-grained versus low fine-grained ratio sizes), 2) presence of thin and immature paleosols, 3) low to negligible bioturbation, and 4) sparse and discontinuous mudrocks, among others other characteristics (Valderrama and Catuneanu, 2024).

The sedimentation of LST (lithostratigraphically named in the area as Une Formation) occurred in response to the rise of the relative sea-level at the shoreline during the (Middle) Cenomanian (age based on palynology). This action triggered the aggradation of the new upcoming riverborne sediments and shallow marine sediments into the area.

As long as sedimentation outpaced accommodation, sedimentation progressively expanded both upstream and downstream. Upstream (southeastern) sedimentation continuously

built the fluvial onlap geometry seen on Figure 3-8. At the same time (downstream), however, the coastline experienced a net displacement prograding towards the northwest (Fig. 3-5).

Palynological evidence (e.g., dinocysts and foram linings), from the fine-grained interbeds, supports the proximity of the sea and the occurrence of sea invasions, at least during the sedimentation of the middle and upper section of the Une Formation (W-2, Fig 3-6A). These marine invasions can be related to high-frequency events or autogenic processes, as the sparse muddy interbeds lack a regional character that afford to classify them as stratigraphic surfaces.

In terms of reservoir characteristics, this LST (Une Formation) is characterized by its good reservoir properties, including high porosity, permeability, and connectivity. These attributes are directly linked to their depositional systems, as Une Formation is a unit mainly composed of coastal normal regressive deposits, specifically deltaic braided channel fill deposits and shallow marine deposits, in which, the sparse muddy layers do not constitute significant vertical and/or lateral barriers (Valderrama and Catuneanu, 2024). Therefore, significant hydrocarbon accumulations are expected to be mainly related to structural barriers instead of stratigraphic barriers.

3.4.1. Stage 2 Cretaceous Transgressive systems tract (Lower Chipaque)

The following unit in the rock record is a transgressive systems tract (TST), which based on palynology, is estimated to have been deposited from Middle Turonian up to the Early/Middle? Coniacian. The hallmark of this unit is the overall fining-upward trend that can be observed in the Gamma ray log (Figs. 3-4, 3-8, 3-9, 3-10) and in core data. Unlike the previous unit (LST), where the rates of sedimentation outpaced the accommodation space, during this unit's deposition (TST), the rates of accommodation space exceeded the rates of sedimentation at the shoreline causing a backstepping of the coastline towards the SE and E (opposite directions of main sediment transport of the Une, Chipaque and Lower Guadalupe Formations; Fig. 3-5). This change started at the maximum regressive surface and ended up at the main (high order) maximum flooding surface. The observed contact in core W-9 between the underlying LST and

the overlying estuarine facies of the TST was apparently not reworked by tidal- or wave-ravinement surfaces, however, cannot be discarded the reworking process.

Facies analysis reveals that this TST is predominantly composed of estuarine facies deposited within a brackish water tidally influenced setting (Valderrama and Catuneanu, 2024), in which the coarser deposits are mostly encased in a matrix of fine-grained lithologies. Since the estuarine facies change rapidly vertically and laterally, hydrocarbon trapping can be expected to occur in structural traps of a few tens of feet of throw onwards, however, consistently governed by strong stratigraphic control both vertically and laterally.

Within the TST, multiple thin beds of coals and/or coaly mudrocks can be identified. Above the main maximum flooding surface (MFS) or within the HST these facies are absent, departing slightly from the standard sequence model (c.f. Catuneanu, 2006, p. 178).

A detailed well-correlation analysis coupled with the integration of static formation pressure points, revealed and corroborated the occurrence of lower-rank events nested within the higher-rank TST (Fig. 3-10). Close to the contact between the Une and Chipaque Formations (Fig. 3-10) there is a lower-order MFS which can be traced across field B (Fig. 3-1b). This MFS works as a vertical barrier among reservoirs.

In well-correlation Figure 3-10, several noteworthy points can be extracted: 1) in general, each well that contains formation pressure data within the ‘massive’ LST unit, exhibits a continuous upward decreasing trend. However, this tendency is pulled apart below and above the lower-rank maximum flooding surface. The offset (whether positive or negative) from the underlying trend correlates directly with the volume of total liquids extracted in the surrounding area of the drilled well. Specifically, exploited areas typically display pressure values below the underlying trend as a consequence of the depletion in the area/interval. Conversely, virgin areas commonly exhibit pressure values above the underlying trend.

Through the integration of electric-logs and formation pressure data, it can be illustrated that the lower-order TST functions as a baffle, and the lower-order MFS at the top of this

systems tract, marks the upper limit of pressure connectivity. Above this lower-order MFS, the rock succession is not hydraulically connected with the underlying ‘massive’ rocks of the LST (Fig. 3-10).

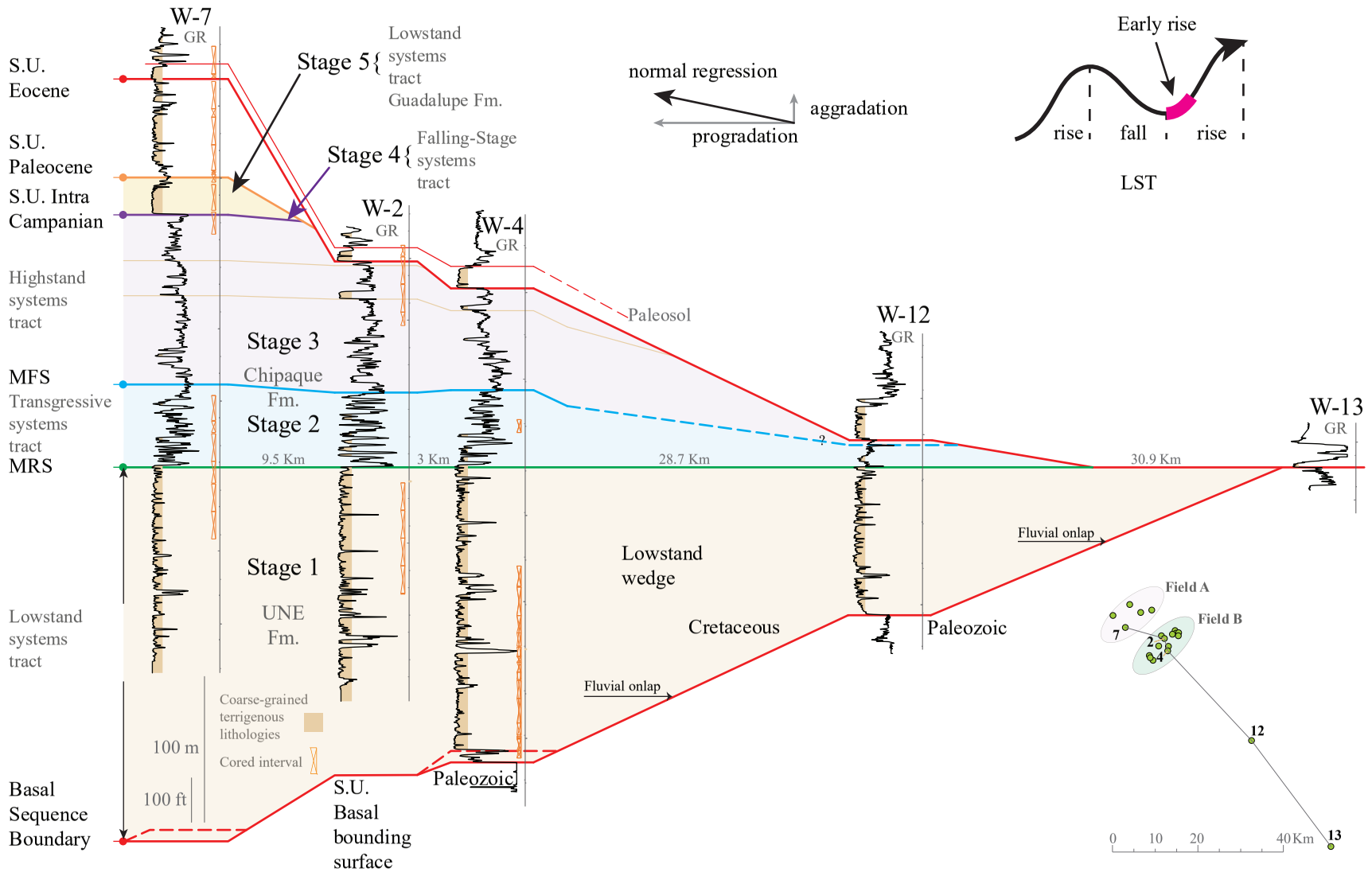
W-7
GR
W-2
GR
W-4
GR
W-12
GR
W-13
GR
S.U.
Eocene
S.U.
Paleocene
S.U. Intra
Campanian
Highstand
systems
tract
MFS
Transgressive
systems
tract
MRS
Lowstand
systems
tract
Basal
Sequence
Boundary
Stage 5
Lowstand
systems
tract
Guadalupe Fm.
Stage 4
Falling-Stage
systems
tract
Stage 3
Chipaque
Fm.
Stage 2
Stage 1
UNE
Fm.
Paleosol
9.5 Km
3 Km
28.7 Km
30.9 Km
Lowstand
wedge
Cretaceous
Paleozoic
Fluvial onlap
Fluvial onlap
Paleozoic
S.U.
Basal
bounding
surface
Coarse-grained
terrigenous
lithologies
Cored interval
100 m
100 ft
normal regression
aggradation
progradation
Early rise
rise
fall
rise
LST
Field A
Field B
7
2
4
12
13
0
10
20
40 Km

Figure 3-8. Southeastern Cretaceous wedge-shaped well-cross section. Cross-section is flattened at the maximum regressive surface (top of the LST). The condition sedimentation > accommodation space, promotes the normal regressive stacking patter reflected, in part, by the wedge-shaped geometry of the Une Formation, which onlaps the sequence boundary unconformity (base of the LST). The Une Formation represents the early rise in the base-level fluctuation curve. (MFS) Maximum flooding surface. (MRS) Maximum regressive surface. (S.U.) Subaerial unconformities. S.U.0 and S.U.1., form a composite surface in some areas. Base-level curve and shoreline trajectories modified from Catuneanu, 2002.

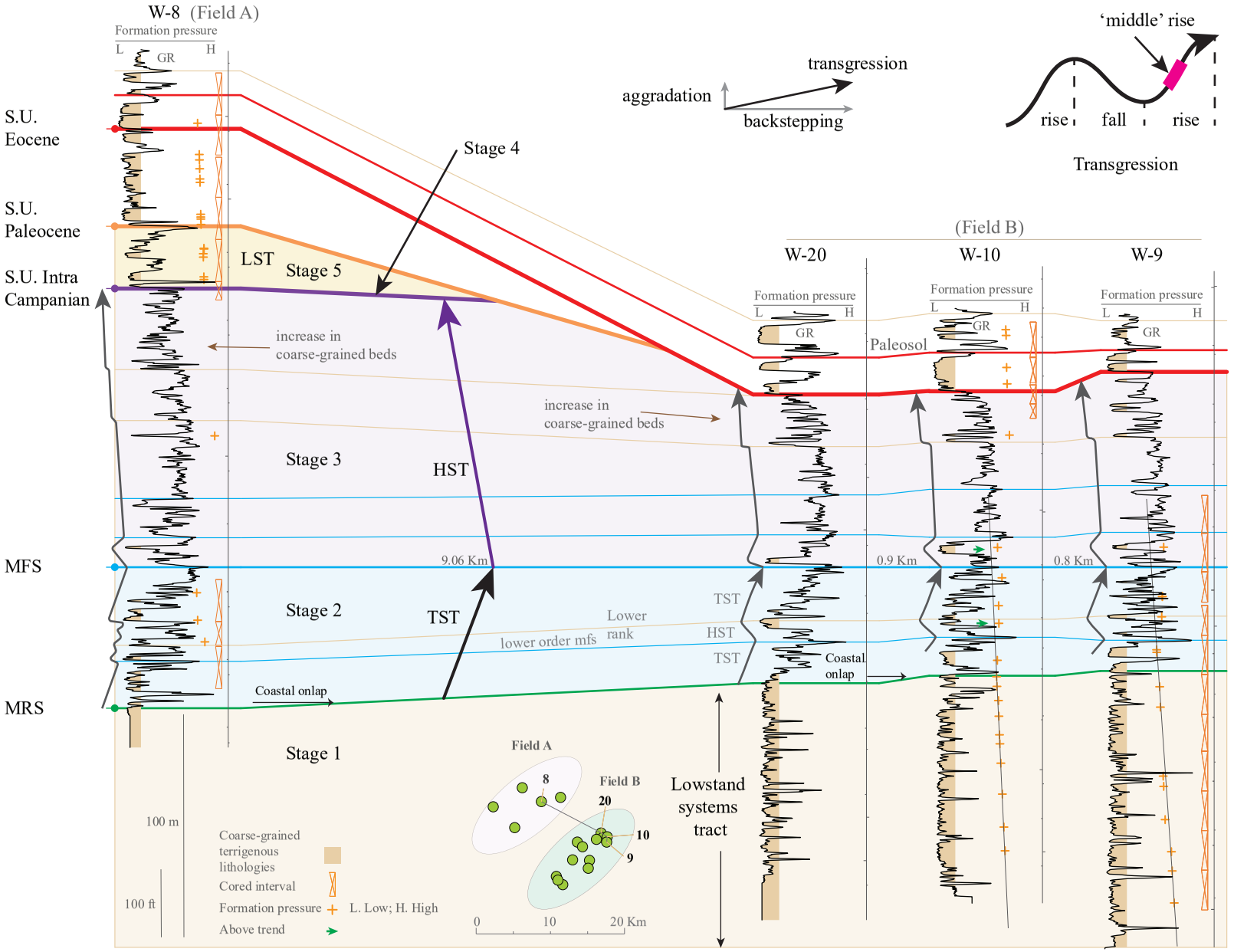
W-8 (Field A)
Formation pressure
L
H
GR
S.U. Eocene
S.U. Paleocene
S.U. Intra Campanian
MFS
MRS
LST
Stage 5
Stage 4
Stage 3
Stage 2
Stage 1
HST
TST
increase in coarse-grained beds
increase in coarse-grained beds
9.06 Km
Coastal onlap
lower order mfs
Lower rank
TST
HST
TST
Coastal onlap
aggradation
transgression
backstepping
'middle' rise
rise
fall
rise
Transgression
(Field B)
W-20
W-10
W-9
Paleosol
0.9 Km
0.8 Km
Field A
Field B
8
20
10
9
0
10
20 Km
Lowstand systems tract
100 m
100 ft
Coarse-grained terrigenous lithologies
Cored interval
Formation pressure
L. Low; H. High
Above trend

Figure 3-9. Lowstand, Transgressive and Highstand systems tracts well correlation (fields A and B) in dip direction. This figure illustrates the correlation among northeastern wells of field A and B, oriented in a near-parallel direction with respect to the sediment transport directions. The correlation focuses on the Transgressive and Highstand systems tracts. Both the main TST and the HST are punctuated by minor lower-rank events within them. Initial formation pressure values within the TST and HST show a positive offset compared to the underlying trend from LST (W-10 and W-9 were perforated prior to the onset of large-scale production from the TST unit in field B). Base-level curve and shoreline trajectories modified from Catuneanu, 2002.

3.4.1. Stage 3 Cretaceous Highstand systems tract (Upper Chipaque)

The succeeding unit in the sequence is a highstand systems tract (HST). This package is characterized by its coarsening-upward profile, however, similarly to the underlying TST, this unit is punctuated by several lower-rank events (Figs. 3-8, 3-9, and 3-10). According to Catuneanu (2002), the HST is bounded at the base by the MFS and at the top by a composed surface of up to three surfaces:1) the subaerial unconformity (SU), 2) the basal surface of force regression (BSFR) and 3) the regressive surface of marine erosion (RSME), however, the study area is affected by several major unconformities in uneven manner, specifically, toward the east, the Eocene subaerial unconformity erased the uppermost part of this HST putting in direct contact Eocene rocks on top of HST-Campanian rocks (Fig. 3-6a); nevertheless, westward, the HST appears completer and progressively affected by older unconformities such as the Paleocene S.U. and particularly the Intra-Campanian subaerial unconformity (Figs. 3-8 and 3-9), which is interpreted as part of the upper limit for the HST at the study area (Fig. 3-12).

In terms of lithostratigraphy, both the underlying TST and this HST comprise Chipaque Formation, separated them by the main maximum flooding surface, which works as an inflexion point among the two stacking patterns (transgression and normal regression; Figs. 3-4, 3-8, 3-9, and 3-10)

The upper section of the HST is marked by a significant increase of coarser material (Figs. 3-4, 3-8, 3-9, and 3-10). This feature is part of the hallmark characteristic of the highstand

normal regression type (e.g., Catuneanu et al., 2011), and it is explained as a result of decelerating rates of creation space versus the rates of sedimentation (Catuneanu, 2006) or, in other words, by the increase of the progradation rates versus a decrease of the aggradation rates with time (Catuneanu, 2022).

In terms of reservoir and source rock, the lower section of the HST (immediately above the MFS) is expected to concentrate the largest amount of organic material for this systems tract, however, as can be observed in Figure 3-10 (brown arrows), the base of the HST in wells W-20, W-21, W-9 and W-10, is punctuated by some coarser-grain packages. This 'minor' prograding body remains as a local event with no major effect in the rest sites as can be observed on the well correlation. These facies changes or variations commonly occur along strike, as the conditions (accommodation vs sedimentation) rates change from one location to another. This event also exemplifies how the sequence is constantly punctuated by higher-frequency events or autogenic processes that do not change the overall depositional trend.

Core facies analysis from the area indicates that most of the mudrocks present in the HST lack any bioturbation signal and when it does, it is associated to the arrival of 'event' beds (Valderrama and Catuneanu, 2024). This lack of bioturbation is commonly associated with stressful depositional setting, specifically anoxic bottoms, wherein prevent the life of benthic communities (Gingras et al., 2007, MacEachern et al., 2007). That situation (anoxic bottoms), therefore, can be directly associated to the organic matter preservation, this in turn, explains, at least in part, why Chipaque Formation, and is equivalent basinward La Luna Formation, are considered by several authors as a prime petroleum source rock (e.g., Rangel et al., 2000; Villamil, 2003).

The upper section of this HST shows the larger amount of coarser material (relatively to the entire unit), making of this interval a probable target to pursue in this and other areas (Figs. 3-9 and 3-10). However, as can be deducted from the logs, the degree of amalgamation which finally impacts the connectivity is still low, therefore small tanks/pools are expected to be found in this interval. Although, in a hypothetical scenario, the degree of amalgamation is expected to

improve landward, in reality the Eocene unconformity progressively removed this interval eastward (Fig. 3-8).

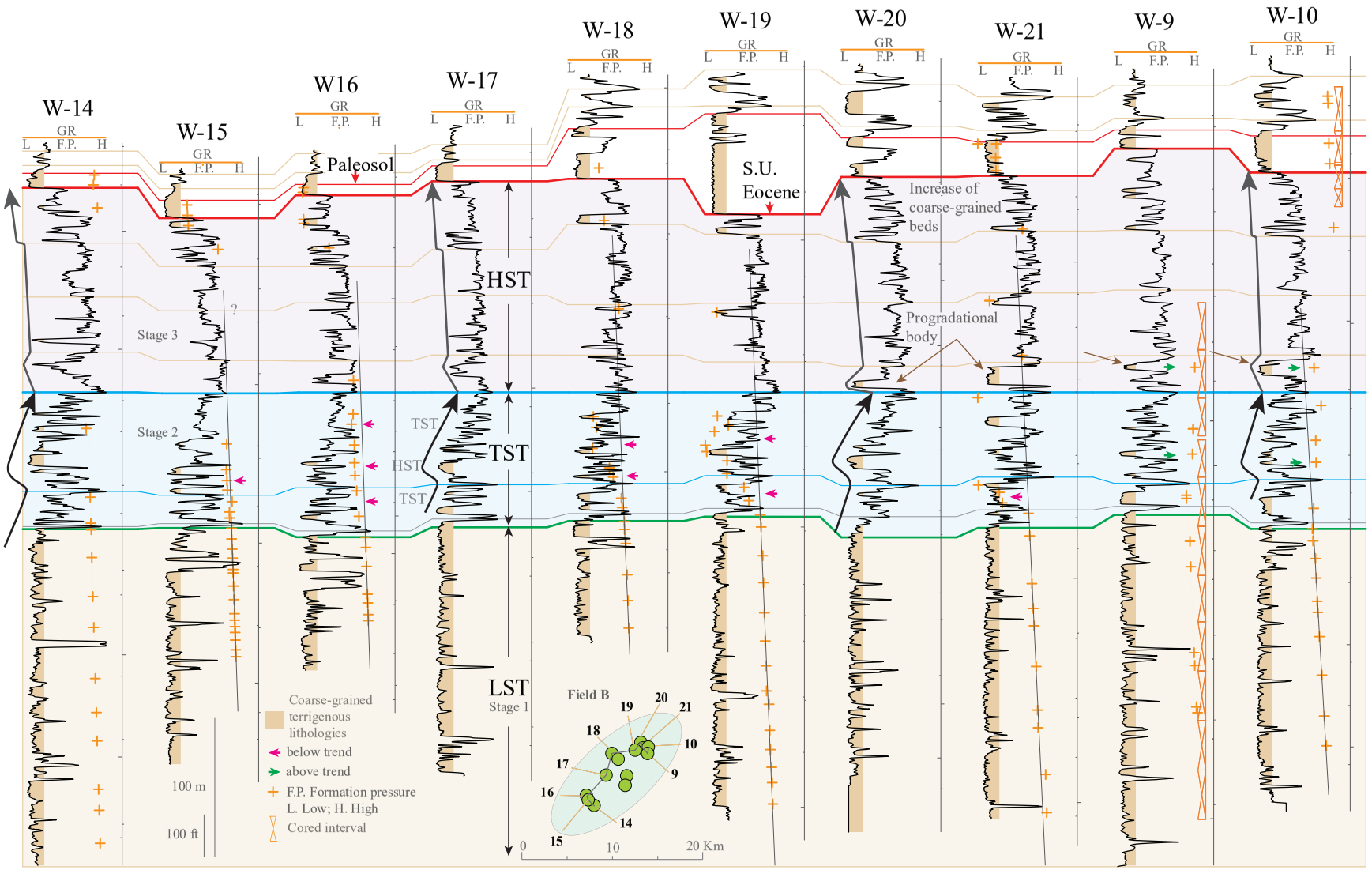
W-14
W-15
W16
W-17
W-18
W-19
W-20
W-21
W-9
W-10
GR
L F.P. H
Paleosol
S.U.
Eocene
Increase of
coarse-grained
beds
Progradational
body
HST
TST
HST
TST
LST
Stage 1
Stage 2
Stage 3
?
Coarse-grained
terrigenous
lithologies
below trend
above trend
F.P. Formation pressure
L. Low; H. High
Cored interval
100 m
100 ft
Field B
19
20
21
18
10
17
9
16
14
15
0
10
20 Km

Figure 3-10. Upper Cretaceous strike-detailed-well-correlation across field B. In most wells, the stratigraphic signal within the higher-rank TST is identifiable, however, frequent departures commonly occur; these departures may arise from autogenic process, higher-frequency events, or both. Formation pressure measurements are denoted by orange cross symbols (+). Pressure trends within the higher-rank TST diverge from the underlying lowstand systems tract (LST). This variance depends on the interval, degree, and timing of reservoir exploitation, that is, wells in pristine areas (unexploited areas) exhibit a positive (right) pressure offset (i.e., W-9), while those near previously exploited areas, show a negative (left) offset; this latter results from reservoir production, leading to a drop in reservoir pressure. Above the maximum regressive surface (MRS), denoted by the green line, the hydraulic vertical communication is altered due to the presence of multiples surfaces, such us flooding surfaces and maximum flooding surfaces; these surfaces compartmentalize the reservoir vertically.

3.4.2. Stages 4 and 5 Cretaceous Falling-stage systems tract and Lowstand systems tract (Lower Guadalupe Formation)

The Lower Guadalupe Formation at western locations (e.g., W-1, W-7, and W-8; Figs. 3-6a, 3-8, 3-9, and 3-11) is bounded by two subaerial unconformities, one at the top, the Paleocene SU, (which removed a significant portion of time/rock, probably >10 My), and one at the base, the Intra-Campanian unconformity, (which may had removed a few million years).

The Intra-Campanian unconformity represents a keystone for the sequence stratigraphic framework, as it gives us clues about the preceding process that took place before the sedimentation of the Lower Guadalupe Formation. In other words, the occurrence of a subaerial unconformity on top of the HST (Upper Chipaque), however, within the temporal span of rocks at western locations without any apparent gap (conformable contact between Chipaque and Lower Guadalupe Formations), points out the existence of a falling-stage systems tract (FSST) in the study area, in which the force regressive deposits should had been deposited westward of the ancient normal fault system that controlled the creation of accommodation space into the depocenter, whereas at eastern locations erosion materialized (Fig. 3-12).

Solid evidence for the Intra-Campanian unconformity occurrence, at the eastern location of the ancient normal fault system, is present in the analyzed core data. The rock alteration together with ferric oxide mineralization (Fig. 3-11), supports the interpretation of a period of subaerial exposure around Middle Campanian (Valderrama and Catuneanu, 2024) for the study area.

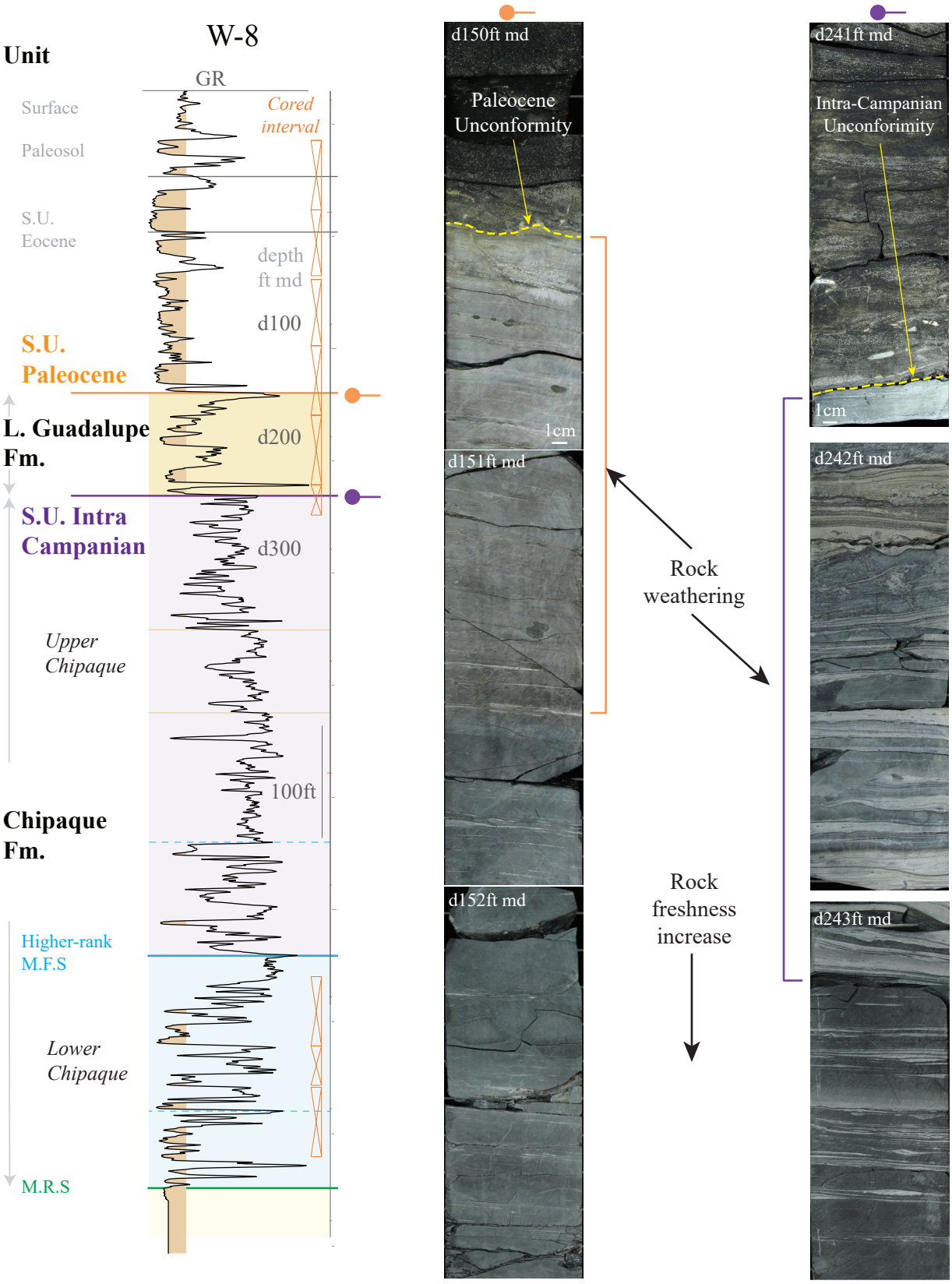
W-8
Unit
GR
Surface
Paleosol
S.U.
Eocene
Cored
interval
depth
ft md
d100
S.U.
Paleocene
L. Guadalupe
Fm.
d200
S.U. Intra
Campanian
d300
Upper
Chipaque
100ft
Chipaque
Fm.
Higher-rank
M.F.S
Lower
Chipaque
M.R.S
d150ft md
Paleocene
Unconformity
1cm
d151ft md
d152ft md
Rock
weathering
Rock
freshness
increase
d241ft md
Intra-Campanian
Unconforimity
1cm
d242ft md
d243ft md

Figure 3-11. Rock weathering evidence of subaerial exposure. The core photographs illustrate evidence of rock weathering resulting from two distinct subaerial exposures periods. The left set corresponds to the Paleocene unconformity, while the right set corresponds to the Intra-Campanian unconformity. In both sets, the uppermost layers below the unconformities, exhibit a dull color, indicative of weathering, whereas deeper layers regain the 'freshness' of the rock. Both unconformities display sharp contacts and the sandstones overlying each unconformity contain rip-up clasts from the underlying units. The photographs' parameters remain unaltered.

After a period of erosion and non-deposition (which corresponds to the span of the Intra-Campanian unconformity) in the study area, however, with the continuation of the sedimentation to the west/northwest as afore mentioned, a resume of normal regression conditions took place (Fig. 3-12), and with that, the deposition on top of the Intra-Campanian unconformity of Lower Guadalupe Formation in the study area.

Sedimentological and palynological analysis of this unit indicates it was deposited in a coastal prograding setting under normal regression conditions (Valderrama and Catuneanu, 2024). Some similarities to the bottom LST are good porosity and permeability, and fair to good vertical and lateral continuity. At western locations, this unit is present with a larger thickness, followed by younger and conformable units (e.g., Guerrero and Sarmiento, 1996).

In terms of base-level cycle, this unit represents the return to the early-rise leg, a lowstand systems tract. This LST was, however, in the area highly affected by the Paleocene and Eocene unconformities, and with that, leaving behind just a fraction of the total uppermost Cretaceous sequence (Figs. 3-8 and 3-9). Stratigraphic traps are not expected, as the overlying units (Paleocene and Eocene rocks) are mainly composed by sandstones and conglomerates with similar petrophysical properties (high porosities and permeabilities), that will behave as carrier beds for any migrated hydrocarbons.

3.4.3. The Upper Cretaceous Sequence Stratigraphic framework for the Southwestern Llanos Basin: A summary

The Upper Cretaceous sequence in the southwestern Llanos Basin can be envisaged through five units that explain the interaction between accommodation and sedimentation. The first deposits correspond to a (1) lowstand system tract as a product of a relative sea-level rise; this was followed by a (2) transgressive event, that pushed back the coastline further to the southeast/east; after that, a normal regressive cycle represented by a (3) highstand systems tract, flipped back the shoreline trajectory; this trend continued, however, through a cycle of negative accommodation represented by a (4) forced regression, in which, part of the previous highstand systems tract was eroded (by the Intra-Campanian SU) and sedimentation solely took place at locations further to the west regarding to the study location. Finally, the relative sea-level rose again, bringing newly the sedimentation into the area with a (5) lowstand systems tract represented by the Lower Guadalupe Formation. After that, the entire Cretaceous sequence was differentially affected by several major erosive events represented by the Paleocene and Eocene unconformities (Fig. 3-12).

3.5. Hierarchy

The first order sequence boundaries of the Upper Cretaceous stratigraphic framework are as follows: at the base, the basal subaerial unconformity that separates the Upper Cretaceous sediments from the Paleozoic rocks; at the top, the boundary is defined by the Paleocene subaerial unconformity, although this surface is reworked and eroded by the Eocene subaerial unconformity in more eastern locations. These bounding surfaces —the basal and the Paleocene subaerial unconformities— are associated to the onset and termination of the back-arc basin period (Figs. 3-3 & 3-12).

This large-scale cycle, representing the Upper Cretaceous sequence in the southwestern Llanos Basin, is further subdivided by the intra-Campanian subaerial unconformity. Hence, the maximum regressive surface and the maximum flooding surface (Fig. 3-12), correspond to second-order internal subdivisions. Finally, some smaller-scale cycles, however, can be observed

within the second-order transgressive systems tract of Figure 3-10. They correspond to third-order internal subdivisions.

3.6. Discussions

One of the main points of discussion in this article should be around the interpretation of the falling-stage systems tract.

Associated with the falling-stage systems tract will be a break in the sequence succession and a detachment of depositional systems represented by the sedimentation of the forced regressive deposits seaward with an offset from the previous coastal line (Fig. 3-12).

In our case, the break in succession is evidenced by the subaerial unconformity that removes part of the underlying highstand systems tract or upper Chipaque (Fig. 3-11). However, the immediate question that arises regarding the forced regressive deposits is: where are they located?

In theory, the forced regressive deposits should be overlaid by the following unit, a lowstand systems tract represented here by the Lower Guadalupe (Figs. 3-12). Since both units may exhibit relatively similar coarse-grained lithologies, they could be erroneously seeing it as one, in such case, they could have been grouped under the Lower Guadalupe Formation (also named in the Eastern Cordillera as Dura Formation).

Although there are methods to differentiate these deposits, such as the grain size, the data from the nearby areas of Bogota (e.g., Julivert, 1962; Renzoni, 1962; Perez and Salazar, 1978; Figs. 3-1) and San Luis de Gaceno (e.g., Guerrero and Sarmiento, 1996; Figs. 3-1) apparently do not display such grain size differences.

The isochore map of Fajardo et al., (2000) for the entire Guadalupe unit presents a series of thicker sections, which are related to the filling of incision valleys on top of the Chipaque highstand systems tract resulting from the fluvial downcutting action during the exposure time.

This fact reinforces our interpretation of a falling-stage systems tract occurrence during the middle Campanian. Moreover, it sheds light on the potential location of at least a portion of the forced regressive deposits. In that sense, these deposits should be situated in front of the end of these incision valleys along the axis of the Eastern Cordillera. Further work to corroborate this hypothesis arises as an opportunity to continue understanding past events that took place during the Upper Cretaceous.

The second point for discussion in this article should focus on the placement of the internal and bounding stratigraphic surfaces of the transgressive systems tract. It is clear that the Llanos Basin experienced a transgressive event during the sedimentation of the Lower Chipaque Formation. In the central and northern areas of the Llanos Basin, this transgression is recorded near the base of the Chipaque Formation, leaving the majority of the formation associated with a normal regression.

However, in the southwestern region of the Llanos Basin, the stratigraphic signal within the Lower Chipaque Formation appears relatively noisier, introducing additional uncertainties in the interpretation of the stratigraphic surfaces. This noise in the signal can be attributed to the inherent nature of marginal marine settings, such as the study area, which are prone to recording not only lower-frequency events but also autogenic processes and higher-frequency events.

We acknowledge that this combination of variables results in a patterns' nesting that may affect the final pinpoint of the interpreted surfaces, however, the overall depositional trend prevailed.

A third point of discussion should be around the timing of the events; The proposed time framework here was constructed based on palynological data, which is often referred to as 'relative' dating. It's important to note that the error or uncertainty associated with relative data, as opposed to absolute data, can be significant. Hence, the temporality of the time framework presented here remains open for future refinements and adjustments. In addition, it is known that the sedimentation rates are not constant and are commonly influenced by fluctuations, including periods of high and low sedimentation rates, as well as by bed reworking (Miall, 2016).

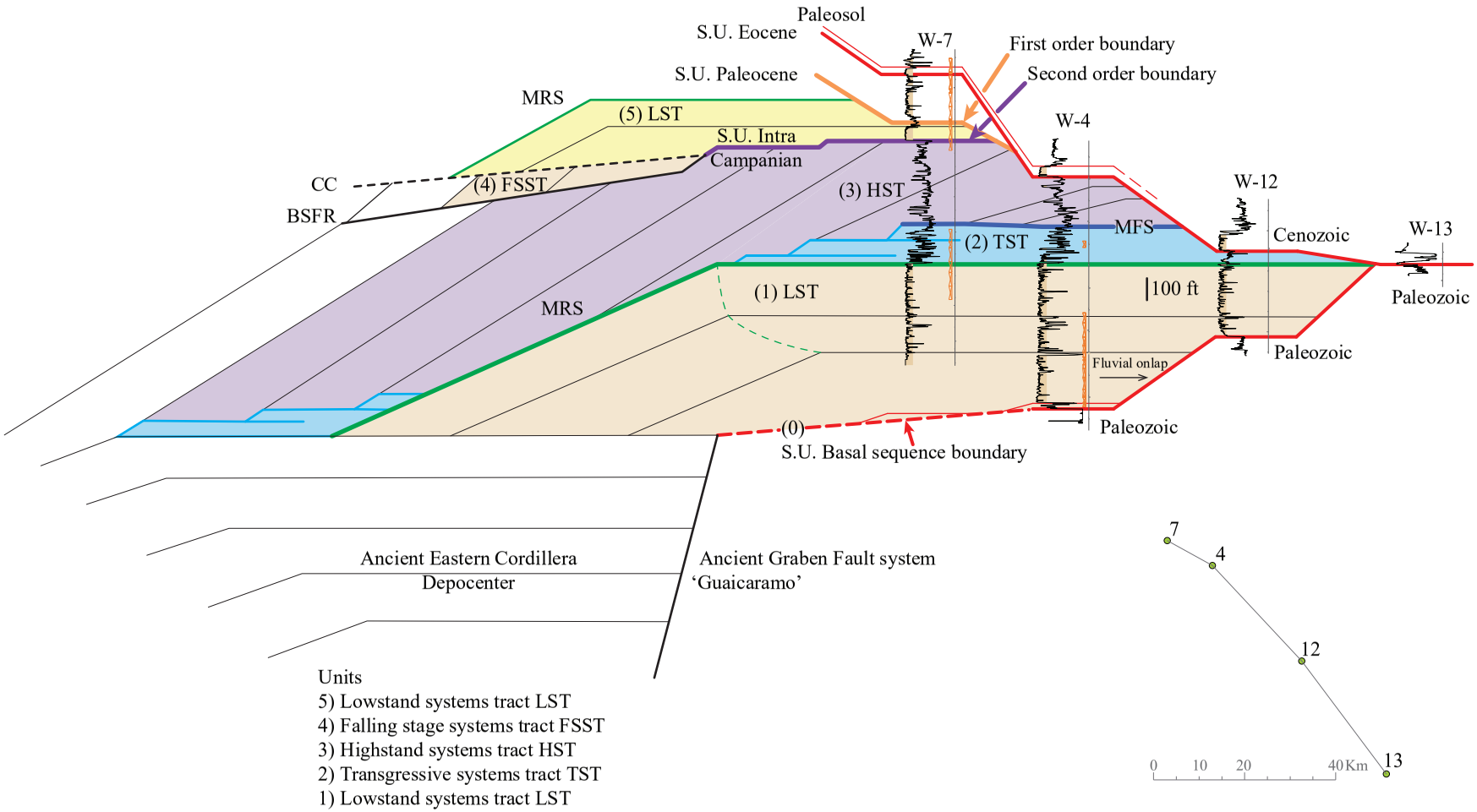
Paleosol
S.U. Eocene
S.U. Paleocene
W-7
First order boundary
Second order boundary
MRS
(5) LST
S.U. Intra
Campanian
W-4
CC
(4) FSST
BSFR
(3) HST
W-12
MFS
(2) TST
Cenozoic
W-13
(1) LST
100 ft
MRS
Paleozoic
Paleozoic
Fluvial onlap
(0)
Paleozoic
S.U. Basal sequence boundary
Ancient Eastern Cordillera
Depocenter
Ancient Graben Fault system
'Guaicaramo'
Units
5) Lowstand systems tract LST
4) Falling stage systems tract FSST
3) Highstand systems tract HST
2) Transgressive systems tract TST
1) Lowstand systems tract LST
7
4
12
13
0
10
20
40 Km

Figure 3-12. Sequence stratigraphic framework for the southwestern Llanos Basin, Colombia. Basal surface of forced regression (BSFR); Correlative conformity (CC); Falling-stage systems tract (FSST); Highstand systems tract (HST); Lowstand systems tract (LST); Maximum flooding surface (MFS); Maximum regressive surface (MRS); Subaerial unconformity (SU); Transgressive systems tract (TST).

Therefore, the estimation of probable boundaries or interval rock span is subject to a certain magnitude of uncertainty, however, based on the available data, the estimation presented here is one of many probable scenarios.

3.7. Conclusions

A new sequence stratigraphic model is proposed for the entire Cretaceous wedge of the southwestern area of Llanos Basin, Colombia. This model predicts the occurrence of forced regressive deposits further to the west of the study area, probably to the west of the ancient Guaicaramo fault system. The interpretation of the Falling-stage Systems Tract unit is backed by the occurrence of an Intra-Campanian subaerial unconformity and by the stratigraphic relationships with the underlying and overlying units.

In terms of sequence stratigraphy, the Chipaque Formation is composed of two units, a Lowstand Systems Tract at the base and a Highstand Systems Tract at the top. These units are genetically separated by a higher-rank maximum flooding surface. The occurrence of this maximum flooding event pushed the coastline landward to the southeast or east, and with that, moving back the estuarine tidally modulated facies.

The Une Formation was constantly punctuated by marine invasions as palynological data points out, however, the lack of continuity of these fine-grained intervals impedes its classification as high-frequency transgressions, relegated them as the product of autogenic processes.

3.8. References

Aspden, J.A., McCourt, W.J., and Brook, M. (1987). Geometrical control of subduction-related magmatism: the Mesozoic and Cenozoic plutonic history of western Colombia. Journal of the Geological Society. Vol. 144. p. 893-905.

Barron, E.J. and Washington, W.M. (1985). Warm Cretaceous climates: high atmospheric CO2 as a plausible mechanism, in: Sundquist, E.T. and Broeker, W.S., eds. The carbon cycle and atmospheric CO2: Natural variation Archean to present. Geophysical Monograph Series 1985. American Geophysical Union. Washington DC. p. 546-553.

Bhattacharya, J.P. (2010). Deltas. in James, N.P., and Dalrymple, R.W., eds, Facies Models 4: GEOtext 6, Geological Association of Canada, St. John's, Newfoundland, 233-264.

Blakey, R.C. (2008). Gondwana paleogeography from assembly to breakup—A 500 m.y. odyssey *in:* Fielding, C.R., Frank T.D., and Isabell, J.L., eds., Resolving the Late Paleozoic Ice Age in Time and Space. Geological Society of America Special Paper 441. p. 1-28 doi:10.1130/2008.2441(01)

Blakey, R.C., and Ranney, W.D. (2018). The Continental Arc, Sevier Orogeny, Western Interior Seaway and Flat-Slab Subduction: Cretaceous Period: Ca. 145–65 Ma. In: Ancient Landscapes of Western North America. Springer, Cham. https://doi.org/10.1007/978-3-319-59636-5_8

Catuneanu, O. (2002). Sequence stratigraphy of Clastic Systems: concepts, merits, and pitfalls. Journal of African Earth Sciences. Vol 35/1, p. 1-43.

Catuneanu, O. (2006). Principles of Sequence Stratigraphy. 1st Ed. Elsevier, Amsterdam, 375p.

Catuneanu, O., Galloway, W., Kendall, C., Miall, A., Posamentier, H., Strasser, A. and Tucker, M. (2011). Sequence stratigraphy: Methodology and nomenclature. Newsletters on Stratigraphy. Vol. 44 No. 3. p. 173-245. DOI: 10.1127/0078-0421/2011/0011

Catuneanu, O. (2020). Chapter 23 - Sequence stratigraphy *in*: editors Scarselli N., Adam J., Chiarella D., Roberts D. and Bally A. Regional Geology and Tectonics 2nd ed. Elsevier. p. 605-686. https://doi.org/10.1016/B978-0-444-64134-2.00021-3.

Catuneanu, O. (2022). Principles of Sequence Stratigraphy. 2nd Ed. Elsevier, Amsterdam, 494p. https://doi.org/10.1016/C2009-0-19362-5

Cohen, K.M., Finney, S.C., Gibbard, P.L. and Fan, J.X. (2013; updated) The ICS International Chronostratigraphic Chart Episodes 36, p. 199-204. URL: http://www.stratigraphy.org/ICSchart/ChronostratChart2021-10.pdf

Cooper, M., Addison, F., Alvarez, R., Coral, M. Graham, R. et al., (1995). Basin development and tectonic history of the Llanos basin, Eastern Cordillera, and Middle Magdalena Valley, Colombia. AAPG Bulletin. Vol. 79. No 10. p. 1421-1143.

De Vernal, A., and Giroux, L. (1991). Distribution of organic walled microfossils in recent sediments from the Estuary and Gulf of St. Lawrence: some aspects of the organic matter fluxes. Canadian Journal of Fisheries and Aquatic Sciences. Vol. 113. p. 189-199

De Vernal, A. (2009). Marine palynology and its use for studying nearshore environments, IOP C. Ser. Earth and Environmental Science. Vol. 5. p. 1–13. https://doi.org/10.1088/1755-1307/5/1/012002

Etayo, F., Renzoni, G. and Barrero, D., (1976). Contornos sucesivos del mar Cretácico en Colombia. Primer Congreso Colombiano de Geología, Mem., Bogotá, p. 217-252.

Fajardo, A., Rojas, L.E., and Cristancho, J. (2000). Definición del modelo estratigráfico en el intervalo Cretáceo Superior a mioceno Medio en la cuenca de Llanos Orientales y Piedemonte llanero. Informe final ICP-ECOPETROL Piedecuesta, Santander, Colombia. 144 p. CIT: CR, 212.411.2, E156df. (Internal Report).

Gingras, M.K., Bann, K.L., MacEachern, J.A., Waldron, J., and Pemberton, S.G. (2007). A conceptual framework for the application of trace fossils, *in*: MacEachern, J.A., Bann, K.L., Gingras, M.K., and Pemberton, S.G., eds., 2007. Applied Ichnology, SEPM Short Course Notes #52, 380p.

Guerrero, J. and Sarmiento, G. (1996). Estratigrafía Física, Palinología, Sedimentológica y Secuencial del Cretácico Superior y Paleoceno del Piedemonte Llanero. Implicaciones en Exploración Petrolera. Geología Colombiana No. 20 p 3-66 Bogotá.

Haywood, A.M., Valdes, P.J., Aze, T., Barlow, N., Burke, A. Dolan, A.M. von der Heydt A. S., Hill, D. J., Jamieson S.S.R., Otto-Bliesner, B.L., Salzmann, U., Saupe, E. and Voss J. (2019). What can paleoclimate modelling do for you?. Earth Systems and Environment. Vol 3. 1-18. https://doi.org/10.1007/s41748-019-00093-1

Hoorn, C., Wesselingh, F.P., ter Steege, H., Bermudez, M.A., Mora, A., Sevink, J., Sanmartín, I., Sanchez-Meseguer, A., Anderson, C.L., Figueiredo, J.P., Jaramillo, C., Riff, D.,

Negri, F.R., Hooghiemstra, H., Lundberg, J., Stadler, T., Särkinen, T., and Antonelli, A. (2010). Through Time: Andean Uplift, Climate Change, Landscape Evolution, and Biodiversity. Science. Vol. 330.

Horton, B.K., Saylor, J.E., Nie, J., Mora, A., Parra, M., Reyes-Harker, A., and Stockli, D.F. (2010). Linking sedimentation in the northern Andes to basement configuration, Mesozoic extension, and Cenozoic shortening: Evidence from detrital zircon U-Pb ages, Eastern Cordillera, Colombia. Bulletin of Geological Society of America. Vol. 122. No 9-10. p. 1423-1442. https://doi.org/10.1130/B30118.1

ICP, (2012). W-1. Internal report 08-12. Ecopetrol-ICP. Piedecuesta, Colombia.

ICP, (2013). W-6. Internal report 11-13. Ecopetrol-ICP. Piedecuesta, Colombia.

ICP, (2014a). Sagu Creek, las Blancas Creek and wells W-3 and Ctal-1. Internal report 20-14. Ecopetrol-ICP. Piedecuesta, Colombia.

ICP, (2014b). W-5. Internal report 08-14. Ecopetrol-ICP. Piedecuesta, Colombia.

ICP, (2015). W-2. Internal report 13-15. Piedecuesta, Colombia.

ICP, (2021). W-4. Internal report 01-21. Ecopetrol-ICP. Piedecuesta, Colombia.

Jaramillo, C., and Rueda, M. (2004). Impact of biostratigraphy on oil exploration. 3ra Convencion tecnica. ACGGP.

Julivert, M. (1962). La Estratigrafia de la formación Guadalupe y las estructuras por gravedad en la serrania de Chia (Sabana de Bogota). Boletin de Geología UIS. No. 11. p. 5-21 Bucaramanga. Colombia.

Kerr, A.C. (1998). Oceanic Plateau formation: A cause of mass extinction and black shale deposition around the Cenomanian-Turonian boundary? Journal of the Geological Society. Vol. 155. p. 619-626.

Kerr, A.C. (2005). Oceanic LIPs: The kiss of Death. Elements. Vol. 1. p. 289-292.

MacEachern, J.A., Pemberton, S.G., Bann, K.L. and Gingras, M.K. (2007). Departures from the archetypal ichnofacies: effective recognition of physico-chemical stresses in the rock record, *in*: MacEachern, J.A., Bann, K.L., Gingras, M.K., and Pemberton, S.G., eds., 2007. Applied Ichnology, SEPM Short Course Notes #52, 380p.

Miall, A. (2016). Stratigraphy: A modern synthesis. Springer. 454p. https://doi:10.1007/978-3-319-24304-7

Montes, C., Rodriguez-Corcho A.F., Bayona, G., Hoyos N., Zapata, S. and Cardona, A. (2019). Continental margin response to multiple arc-continent collisions: The northern Andes-Caribbean margin. Earth-Science Reviews. Vol. 198. p. 1-19. https://doi.org/10.1016/j.earscirev.2019.102903

Mora, A., Gaona, T., Kley, J., Montoya, D., Parra, M., Quiroz, L. I., Reyes, G. and Strecker, M. R. (2009). The Role of inherited extensional fault segmentation and linkage in contractional orogenesis: a reconstruction of Lower Cretaceous inverted rift basin in the Eastern Cordillera of Colombia. Basin Research. Vol. 21. p. 111-137. doi: 10.1111/j.1365-2117.2008.00367.x

Moreno, C.J., Horton, B.K., Caballero, V., Mora, A., Parra, M. and Sierra J. (2011). Depositional and provenance record of the Paleogene transition from foreland to hinterland basin evolution during Andean orogenesis, northern Middle Magdalena Valley Basin, Colombia. Journal of South American Earth Sciences. Vol 32. p. 246-263. doi:10.1016/j.jsames.2011.03.018

NASA. 2000. Suttle radar topography mission. https://www.earthdata.nasa.gov/sensors/srtm

Perez, G., and Salazar, A. (1978). Estratigrafía y facies del Grupo Guadalupe. Geología Colombiana No. 10. p. 1-116 Bogotá. Colombia.

Poulsen, C.J., Gendaszek, A.S., and Jacob, R.L. (2003). Did the rifting of the Atlantic Ocean cause the Cretaceous thermal maximum? Geological Society of America. Vol. 31. No. 2. p. 115-118.

Rangel, A., Parra, P. and Niño C. (2000). The La Luna formation: chemostratigraphy and organic facies in the Middle Magdalena Basin. Organic Geochemistry. Vol. 31. p. 1267-1284.

Renzoni, G. (1962). Apuntes acerca de la litología y tectónica de la zona al este y sureste de Bogotá. Boletín Geológico 10 59-79 Servicio Geológico Nacional. Bogotá.

Reyes-Harker, A., Ruiz Valdivieso, C.F., Mora, A., Ramirez-Arias, J.C., Rodriguez, G., De la Parra, F., Caballero, V., Parra, M., Moreno, N., Horton, B.K., Saylor, J.E., Silva, A., Valencia V., Stockli, D., and Blanco, V. (2015). Cenozoic paleogeography of the Andean foreland and retroarc hinterland of Colombia. AAPG Bulletin. Vol. 99. No. 8. p. 1407-1453.

Sarmiento-Rojas, L.F. (2001). Mesozoic rifting and Cenozoic basin inversion history of the Eastern Cordillera Colombian Andes inferences from tectonic models. PhD. Thesis Univ. of Amsterdam. 295 p.

Sarmiento-Rojas, L.F. (2011) Llanos Basin. Geology and hydrocarbon potential. In: Cediel F. and Ojeda G. Y. (eds). Petroleum geology of Colombia, Vol 9. Universidad Eafit for ANH, Medellín, p 192.

Sarmiento-Rojas, L.F. (2019). Cretaceous stratigraphy and paleo-facies maps of northwestern South America. In: Cediel F and Shaw R. P eds. Geology and Tectonics of Northwestern South America: The Pacific-Caribbean-Andean Junction. Frontiers in Earth Sciences. p. 673-747. https://doi.org/10.1007/978-3-319-76132-9_10

Valderrama, Y., and Catuneanu, O. (2024). The Upper Cretaceous rock record in the Southwest of Llanos Basin, Colombia: An integrated Facies Analysis. *In preparation (Previous Chapter)*.

Villagomez, D., Spikings, R., Magna, T., Kammer, A. Winkler, W. and Beltran, A. (2011). Geochronology, geochemistry and tectonic evolution of the Western and Central cordilleras of Colombia. Lithos Vol. 125. p. 875-896.

Villamil, T. (1996). Depositional and geochemical cyclicity in the Cretaceous fine-grained strata of Colombia. A model for organic matter content. CTF. Vol 1. No. 2. p. 5-23.

Villamil, T. (1998). Chronology, Relative Sea-Level History and a New Sequence Stratigraphic Model for Basinal Cretaceous Facies of Colombia. *in*: J.I. Pindel and C. Drake, eds., Paleogeographic Evolution and Non-Glacial Eustasy Northern South America. Society for Sedimentary Geology (SEPM). Special Publication No. 58. p. 161-216. https://doi.org/10.2110/pec.98.58.0161

Villamil, T. (1999). Campanian-Miocene tectonostratigraphy, depocenter evolution and basin development of Colombia and western Venezuela. Palaeogeography, Palaeoclimatology, Palaeoecology Vol. 153. Iss. 1-4. p. 239-275. https://doi.org/10.1016/S0031-0182(99)00075-9

Villamil, T. (2003). Regional hydrocarbon systems of Colombia and western Venezuela: Their origin, potential, and exploration, in Bartolini C, Buffler, R. T. and Blickwede, J. eds., The Circum-Gulf of Mexico and the Caribbean: Hydrocarbon habitats, basin formation, and plate tectonics: AAPG Memoir. vol. 79, p. 697-734.

Chapter 4. Discussion and Conclusions.

Traditionally, only three formations are recognized in the area: the Une, Chipaque, and Guadalupe formations. However, we present evidence of a laterally discontinuous basal unit that separates the Une Formation from underlying fine-grained Paleozoic rocks. Based on core and log data we interpret that this basal unit consists of sparse alluvial deposits trapped during erosional periods, specifically between the base of the Une Formation and the Paleozoic rocks. To corroborate this interpretation, these deposits need to be accurately dated to determine if they afford a significant distinction from the Une Formation and/or the Paleozoic sequence; otherwise, they will be considered part of one of these two units.

Radiometric dating of the entire Cretaceous sequence of the study area would contribute to refining the available relative palynological data. Similarly, additional palynological sampling sites would bolster palynological interpretations of the Cretaceous sequence, as some units have been penetrated or sampled in a limited number of wells. For example, the lower section of the multistory channel deposits of the Une Formation has only been sampled in one location (i.e., W-4) and its palynological yield indicates a continental setting; however, this may correspond to a sheltered location.

The addition of new palynological control points could potentially modify the proposed sequence stratigraphic framework presented here. For example, if the basal part of Une Formation continues to show continental affinity, the proposed transgressive cycle must be adjusted and placed at a greater depth within the Une Formation. Conversely, if the new sites corroborate marine influence within the lower part of the Une Formation, the lower section in well W-4 will remain classified as a sheltered location, and the sequence stratigraphic framework will not require modification within its lower lowstand systems tract.

The depositional environments interpreted in this study are the result of integrating various disciplines, including sedimentology, palynology, electrical log analysis, and bioturbation indices. This comprehensive approach strengthens and validates the proposed interpretations on a

regional scale. However, detailed studies of ichnogenera are still needed. Incorporating new information on ichnogenera identification could aid in recognizing sub-environments and/or architectural elements, which are crucial for the reservoir characterization of oil and gas fields.

Bioturbation observed within the Chipaque Formation primarily occurred in coarser-grained intervals, while the black mudrocks remain largely unbioturbated. This contrast is attributed to varying oxygen levels; specifically, the lack of bioturbation in the black mudrocks suggests deposition under unfavorable anoxic or dysoxic conditions for benthic communities. The study of trace elements within these fine-grained intervals may offer further insights into the specific paleoceanographic conditions of the Upper Cretaceous Colombian Basin, as well as possible relationships with global anoxic events and submarine volcanism in the ancient Pacific.

Based on sedimentological and sequence stratigraphic analysis, our interpretation subdivides the Chipaque Formation into two sections: Lower and Upper. The Lower section is interpreted to have been deposited in a transgressive brackish water tidally influenced setting, while the Upper section is interpreted as having been deposited in a regressive proximal offshore or embayed area. The Upper section is interpreted to cover a broader range of depositional environments (proximal offshore to embayed area). The application of trace element analysis may provide new insights into the degree of connectivity between the study area and the basin, potentially leading to a more refined interpretation of the black, unbioturbated mudrocks within the Chipaque Formation.

The upper limit of the Chipaque Formation is characterized by three subaerial unconformities: the intra-Campanian, Paleocene, and Eocene. In all three cases, the analyzed core data provide clear evidence of these subaerial unconformities. However, outcrop data have not yet confirmed the occurrence of the intra-Campanian unconformity. Additionally, our sequence stratigraphic interpretation suggests the presence of forced regressive deposits associated with the intra-Campanian unconformity westward of the ancient Guaicaramo fault system, which have also not yet been reported.

Detailed mineralogical studies on the reported outcrops may reveal hidden characteristics that are a result of weathering or the structural complexity of the outcrops. A focused investigation should be conducted in areas corresponding to the inferred incision valleys, as indicated by isochore thickness maps of the Upper Chipaque and Lower Guadalupe formations.

Core data also has limitations, such as low spatial coverage and/or a limited number of cored sites. These limitations can be mitigated by the combined use of core data and image logs. Oil fields within the studied area offer a greater number of sites with image logs than cores, providing an opportunity to implement facies characterization based on image logs.

Bibliography

Allen, J.R.L. (1982). Sedimentary structures: their character and physical basis. V2 Elsevier. New York 663p.

Aspden, J.A., McCourt, W.J., and Brook, M. (1987). Geometrical control of subduction-related magmatism: the Mesozoic and Cenozoic plutonic history of western Colombia. Journal of the Geological Society. Vol. 144. p. 893-905.

Bann, K.L., Tye, S.C., MacEachern, J.A., Fielding, C.R., and Jones, B.G. (2008). Ichnological and sedimentologic signatures of mixed wave-and storm-dominated deltaic deposits: Examples from the Early Permian Sydney Basin, Australia. *In*: G.J. Hampson, R.J. Steel, P.B. Burgess, R.W. Dalrymple (Eds.), Recent Advances in Models of Siliciclastic Shallow-Marine Stratigraphy, SEPM Spec. Publ., vol. 90 (2008), p. 293-332.

Barron, E.J. and Washington, W.M. (1985). Warm Cretaceous climates: high atmospheric CO2 as a plausible mechanism, in: Sundquist, E.T. and Broeker, W.S., eds. The carbon cycle and atmospheric CO2: Natural variation Archean to present. Geophysical Monograph Series 1985. American Geophysical Union. Washington DC. p. 546-553.

Bhattacharya, J.P. (2010). Deltas. in James, N.P., and Dalrymple, R.W., eds, Facies Models 4: GEOtext 6, Geological Association of Canada, St. John's, Newfoundland, 233-264.

Bayona, G., Cortes, M., Jaramillo, C., Ojeda, G., Aristizabal, J.J., and Reyes-Harker, A. (2008). An integrated analysis of an orogen-sedimentary basin pair: Latest Cretaceous-Cenozoic evolution of the linked Eastern Cordillera orogen and the Llanos foreland basin of Colombia. GSA Bulletin. Vol. 120. No. 9/10. p. 1171-1197. doi: 10.1130/B26187.1

Bayona, G., Bustamante, C., Nova, G., and Salazar-Franco, A.M. (2020). Jurassic evolution of the northwestern corner of Gondwana: Present knowledge and future challenges in studying Colombian Jurassic rocks. In: Gomez J., and Pinilla-Pachon A. O. (editors). The Geology of Colombia, Vol. 2 Mesozoic. Servicio Geológico Colombiano. Publicaciones Geológicas Especiales N. 36. p. 171-207. Bogotá. https://doi.org/10.32685/pub.esp.36.2019.05

Blakey, R.C. (2008). Gondwana paleogeography from assembly to breakup—A 500 m.y. odyssey *in:* Fielding, C.R., Frank T.D., and Isabell, J.L., eds., Resolving the Late Paleozoic

Ice Age in Time and Space. Geological Society of America Special Paper 441. p. 1-28 doi:10.1130/2008.2441(01)

Blakey, R.C., and Ranney, W.D. (2018). The Continental Arc, Sevier Orogeny, Western Interior Seaway and Flat-Slab Subduction: Cretaceous Period: Ca. 145–65 Ma. In: Ancient Landscapes of Western North America. Springer, Cham. https://doi.org/10.1007/978-3-319-59636-5_8

Caballero, V., Naranjo, J., De La Parra, F., Mora, A., and Reyes-Harker, A. (2015). Estratigrafía de secuencias de los principales reservorios de la cuenca Llanos. XV Congreso Colombiano de Geología. Bucaramanga. Colombia.

Caballero, V.M., Rodríguez, G., Naranjo, J.F., Mora, A. and De La Parra, F. (2020). From facies analysis, stratigraphic surfaces, and depositional sequences to stratigraphic traps in the Eocene – Oligocene record of the southern Llanos and northern Magdalena Basin. In: Gómez J. and Mateus–Zabala, D. (eds). The Geology of Colombia. Vol. 3 Paleogene – Neogene. Servicio Geológico Colombiano. Publicaciones Geológicas Especiales 37. 48 p. Bogotá. https://doi.org/10.32685/pub.esp.37.2019.10

Carvajal Torres, J.S. (2021). The role of tectonism in the development of stratigraphic surfaces in the Colombian Llanos Foreland Basin. MSc Thesis 221 p.

Catuneanu, O. (2002). Sequence stratigraphy of Clastic Systems: concepts, merits, and pitfalls. Journal of African Earth Sciences. Vol 35/1, p. 1-43.

Catuneanu, O. (2006). Principles of Sequence Stratigraphy. 1st Ed. Elsevier, Amsterdam, 375p.

Catuneanu, O. (2020). Chapter 23 - Sequence stratigraphy *in*: editors Scarselli N., Adam J., Chiarella D., Roberts D. and Bally A. Regional Geology and Tectonics 2nd ed. Elsevier. p. 605-686. https://doi.org/10.1016/B978-0-444-64134-2.00021-3.

Catuneanu, O. (2022). Principles of Sequence Stratigraphy. 2nd Ed. Elsevier, Amsterdam, 494p. https://doi.org/10.1016/C2009-0-19362-5

Catuneanu, O., Galloway, W., Kendall, C., Miall, A., Posamentier, H., Strasser, A. and Tucker, M. (2011). Sequence stratigraphy: Methodology and nomenclature. Newsletters on Stratigraphy. Vol. 44 No. 3. p. 173-245. DOI: 10.1127/0078-0421/2011/0011Cohen, K.M., Finney, S.C., Gibbard, P.L. and Fan, J.X. (2013; updated) The ICS International Chronostratigraphic Chart Episodes 36, p. 199-204. URL: http://www.stratigraphy.org/ICSchart/ChronostratChart2021-10.pdf

Collinson, J.D. (1969). The sedimentology of the Grindslow shales and the Kinderscout grit: A deltaic complex in the Namurian of northern England. *Journal of Sedimentary Petrology*, Vol. 39, p. 194-221.

Cooper, M., Addison, F., Alvarez, R., Coral, M. Graham, R. et al., (1995). Basin development and tectonic history of the Llanos basin, Eastern Cordillera, and Middle Magdalena Valley, Colombia. AAPG Bulletin. Vol. 79. No 10. p. 1421-1143.

Cortes, M., Colleta, B. and Angelier, J. (2006). Structure and tectonics of the central segment of the Eastern Cordillera of Colombia. Journal of South American Sciences. Vol. 21. p. 437-465. doi:10.1016/j.jsames.2006.07.004

Dalrymple, R.W. (2010a). Interpreting sedimentary successions: facies analysis and facies models, in James, N.P., and Dalrymple, R.W., eds, Facies Models 4: GEOtext 6, Geological Association of Canada, St. John's, Newfoundland, 3-18.

Dalrymple, R.W. (2010b). Tidal depositional systems, *in*: James, N.P., and Dalrymple, R.W., eds, Facies Models 4: GEOtext 6, Geological Association of Canada, St. John's, Newfoundland, 201-231.

Davis, R.A. (2012). Tidal signatures and their preservation potential in stratigraphic sequences. *in*: Davis R.A. and Dalrymple R.W. (eds.), Principles of Tidal Sedimentology. https://DOI10.1007/978-94-007-0123-6_3

De Vernal, A., and Giroux, L. (1991). Distribution of organic walled microfossils in recent sediments from the Estuary and Gulf of St. Lawrence: some aspects of the organic matter fluxes. Canadian Journal of Fisheries and Aquatic Sciences. Vol. 113. p. 189-199

De Vernal, A. (2009). Marine palynology and its use for studying nearshore environments, IOP C. Ser. Earth and Environmental Science. Vol. 5. p. 1–13. https://doi.org/10.1088/1755-1307/5/1/012002

Diessel Claus, F.A. (2007). Utility of coal for sequence-stratigraphy analysis. International Journal of Coal Geology, 70, 3-34. https://doi:10.1016/j.coal.2006.01.008

Etayo, F., Renzoni, G. and Barrero, D., (1976). Contornos sucesivos del mar Cretácico en Colombia. Primer Congreso Colombiano de Geología, Mem., Bogotá, p. 217-252.

Fajardo, A., Rojas, L.E., and Cristancho, J. (2000). Definición del modelo estratigráfico en el intervalo Cretáceo Superior a mioceno Medio en la cuenca de Llanos Orientales y Piedemonte

llanero. Informe final ICP-ECOPETROL Piedecuesta, Santander, Colombia. 144 p. CIT: CR, 212.411.2, E156df. (Internal Report).

Flores, R.M. (2014). Coal and coalbed gas: fueling the future. 1st Ed. Elsevier, Waltham, MA. 697p.

Fox, A. and Vickerman, K., (2015). The value of borehole image logs. Reservoir, Canadian Society of Petroleum Geologist. January, p. 30-34.

Gelvez, J., Villamizar, C., Velasquez, A., Mora, A., Caballero V., De La Parra F., Ortiz J., and Cardozo, E. (2016). Re-thinking reservoirs: The case of the T2 sands in the southern Llanos basin of Colombia. AAPG ICE Conference paper. Search and discovery article No. 80559.

Gingras, M.K., Bann, K.L., MacEachern, J.A., Waldron, J., and Pemberton, S.G. (2007). A conceptual framework for the application of trace fossils, *in*: MacEachern, J.A., Bann, K.L., Gingras, M.K., and Pemberton, S.G., eds., 2007. Applied Ichnology, SEPM Short Course Notes #52, 380p.

Gingras, M.K., MacEachern, J.A., and Dashtgard, S.E. (2011). Process ichnology and the elucidation of physico-chemical stress. Sedimentary Geology, 237, 115-134. https://doi:10.1016/j.sedgeo.2011.02.006

Greb, S.F., and Archer, A.W. (2007). Soft-sediment deformation produced by tides in meizoseismic area, Turnagain Arm, Alaska. The Geological Society of America. 35, 5, 435-438. https://doi:10.1130/G23209A.1

Guerrero, J. and Sarmiento, G. (1996). Estratigrafía Física, Palinología, Sedimentológica y Secuencial del Cretácico Superior y Paleoceno del Piedemonte Llanero. Implicaciones en Exploración Petrolera. Geología Colombiana No. 20 p 3-66 Bogotá.

Guerrero, J., Sarmiento, G. and Navarrete, R. (2000). The stratigraphy of the W side of the Cretaceous Colombian basin in the Upper Magdalena Valley. Reevaluation of selected areas and type localities including Aipe, Guaduas, Ortega, and Piedras. Geología Colombiana. Vol. 25. Bogotá. p. 45-110.

Haywood, A.M., Valdes, P.J., Aze, T., Barlow, N., Burke, A. Dolan, A.M. von der Heydt A. S., Hill, D. J., Jamieson S.S.R., Otto-Bliesner, B.L., Salzmann, U., Saupe, E. and Voss J. (2019). What can paleoclimate modelling do for you?. Earth Systems and Environment. Vol 3. 1-18. https://doi.org/10.1007/s41748-019-00093-1

Hoorn, C., Wesselingh, F.P., ter Steege, H., Bermudez, M.A., Mora, A., Sevink, J.,

Sanmartín, I., Sanchez-Meseguer, A., Anderson, C.L., Figueiredo, J.P., Jaramillo, C., Riff, D., Negri, F.R., Hooghiemstra, H., Lundberg, J., Stadler, T., Särkinen, T., and Antonelli, A. (2010). Through Time: Andean Uplift, Climate Change, Landscape Evolution, and Biodiversity. Science. Vol. 330.

Horton, B.K., Saylor, J.E., Nie, J., Mora, A., Parra, M., Reyes-Harker, A., and Stockli, D.F. (2010). Linking sedimentation in the northern Andes to basement configuration, Mesozoic extension, and Cenozoic shortening: Evidence from detrital zircon U-Pb ages, Eastern Cordillera, Colombia. Bulletin of Geological Society of America. Vol. 122. No 9-10. p. 1423-1442. https://doi.org/10.1130/B30118.1

Hubach, E. (1957). Contribución a las unidades estratigráficas de Colomba. Informe No. 1212 Instituto Geológico Nacional. Bogotá 166 p.

ICP, (2012). W-1. Internal report 08-12. Ecopetrol-ICP. Piedecuesta, Colombia.

ICP, (2013). W-6. Internal report 11-13. Ecopetrol-ICP. Piedecuesta, Colombia.

ICP, (2014a). Sagu Creek, las Blancas Creek and wells W-3 and Ctal-1. Internal report 20-14. Ecopetrol-ICP. Piedecuesta, Colombia.

ICP, (2014b). W-5. Internal report 08-14. Ecopetrol-ICP. Piedecuesta, Colombia.

ICP, (2015). W-2. Internal report 13-15. Piedecuesta, Colombia.

ICP, (2021). W-4. Internal report 01-21. Ecopetrol-ICP. Piedecuesta, Colombia.

Jaramillo, C., and Rueda, M. (2004). Impact of biostratigraphy on oil exploration. 3ra Convencion tecnica. ACGGP.

Jelby, M.E., Grundvåg, S.-A., Helland-Hansen, W., Olaussen, S., and Stemmerik, L., (2020). Tempestite facies variability and storm-depositional processes across a wide ramp: Towards a polygenetic model for hummocky cross-stratification. Sedimentology 67, 742-781. https://doi.org/10.1111/sed.12671

Julivert, M. (1962). La Estratigrafia de la formación Guadalupe y las estructuras por gravedad en la serrania de Chia (Sabana de Bogota). Boletin de Geología UIS. No. 11. p. 5-21 Bucaramanga. Colombia.

Kerr, A.C. (1998). Oceanic Plateau formation: A cause of mass extinction and black shale deposition around the Cenomanian-Turonian boundary? Journal of the Geological Society. Vol. 155. p. 619-626.

Kerr, A.C. (2005). Oceanic LIPs: The kiss of Death. Elements. Vol. 1. p. 289-292.

Lai, j., Wang, G., Wang, S., Cao, J., Li, M., Pang, X., Han, C., Fan, X., Yang, L., He, Z., and Qin, Z. (2018). A review on the applications of image logs in structural analysis and sedimentary characterization. Marine and petroleum geology. Vol 95. p. 139-166.

Leckie, R.M., Bralower, T.J., and Cashman, R. (2002). Oceanic anoxic events and plankton evolution: Biotic response to tectonic forcing during the mid-Cretaceous. Paleoceanography. Vol. 17. No. 3. https://doi.org/10.1029/2001PA000623

MacEachern, J.A., Pemberton, S.G., Bann, K.L. and Gingras, M.K. (2007). Departures from the archetypal ichnofacies: effective recognition of physico-chemical stresses in the rock record, *in*: MacEachern, J.A., Bann, K.L., Gingras, M.K., and Pemberton, S.G., eds., 2007. Applied Ichnology, SEPM Short Course Notes #52, 380p.

MacEachern, J.A., Pemberton, S.G., Gingras, M.K. and Bann, K.L. (2010). Ichnology and facies models, *in*: James, N.P., and Dalrymple, R.W., eds, Facies Models 4: GEOtext 6, Geological Association of Canada, St. John's, Newfoundland, 201-231.

Martin, C.A.L. and Turner, B.R. (1998). Origins of massive-type sandstones in braided rivers systems. Earth-Science Reviews, 44, 15-38

Miall, A. (2016). Stratigraphy: A modern synthesis. Springer. 454p. https://doi:10.1007/978-3-319-24304-7

Montes, C., Rodriguez-Corcho A.F., Bayona, G., Hoyos N., Zapata, S. and Cardona, A. (2019). Continental margin response to multiple arc-continent collisions: The northern Andes-Caribbean margin. Earth-Science Reviews. Vol. 198. p. 1-19. https://doi.org/10.1016/j.earscirev.2019.102903

Montoya, D. and Reyes, G. (2005). Geología de la Sabana de Bogotá. Ingeominas. Bogota. Colombia. 104 p.

Mora, A., Gaona, T., Kley, J., Montoya, D., Parra, M., Quiroz, L. I., Reyes, G. and Strecker, M. R. (2009). The Role of inherited extensional fault segmentation and linkage in contractional orogenesis: a reconstruction of Lower Cretaceous inverted rift basin in the Eastern Cordillera of Colombia. Basin Research. Vol. 21. p. 111-137. doi: 10.1111/j.1365-2117.2008.00367.x

Moreno, C.J., Horton, B.K., Caballero, V., Mora, A., Parra, M. and Sierra J. (2011). Depositional and provenance record of the Paleogene transition from foreland to hinterland basin evolution during Andean orogenesis, northern Middle Magdalena Valley Basin, Colombia. Journal of South American Earth Sciences. Vol 32. p. 246-263. doi:10.1016/j.jsames.2011.03.018

NASA. 2000. Suttle radar topography mission. https://www.earthdata.nasa.gov/sensors/srtm

Nichols, G. (2009). Sedimentology and stratigraphy 2nd ed. Wiley-Blackwell. 419 p.

Novak, A., and Egenhoff, S. (2019). Soft-sediment deformation structures as a tool to recognize synsedimentary tectonic activity in the middle member of the Bakken Formation, Williston Basin, North Dakota. Marine and Petroleum Geology, 105, 124-140. https://doi.org/10.1016/j.marpetgeo.2019.04.012

Parravano, V., Teixell, A., and Mora, A. (2015). Influence of salt in the tectonic development of the frontal thrust belt of the Eastern Cordillera, Guatiquía area, Colombian Andes. Interpretation 3, p. SAA17-SAA27. https://doi.org/10.1190/INTe2015e0011.1.

Perez, G., and Salazar, A. (1978). Estratigrafía y facies del Grupo Guadalupe. Geología Colombiana No. 10. p. 1-116 Bogotá. Colombia.

Poulsen, C.J., Gendaszek, A.S., and Jacob, R.L. (2003). Did the rifting of the Atlantic Ocean cause the Cretaceous thermal maximum? Geological Society of America. Vol. 31. No. 2. p. 115-118.

Rangel, A., Parra, P. and Niño C. (2000). The La Luna formation: chemostratigraphy and organic facies in the Middle Magdalena Basin. Organic Geochemistry. Vol. 31. p. 1267-1284.

Renzoni, G. (1962). Apuntes acerca de la litología y tectónica de la zona al este y sureste de Bogotá. Boletín Geológico 10 59-79 Servicio Geológico Nacional. Bogotá.

Reyes-Harker, A., Ruiz Valdivieso, C.F., Mora, A., Ramirez-Arias, J.C., Rodriguez, G., De la Parra, F., Caballero, V., Parra, M., Moreno, N., Horton, B.K., Saylor, J.E., Silva, A., Valencia V., Stockli, D., and Blanco, V. (2015). Cenozoic paleogeography of the Andean foreland and retroarc hinterland of Colombia. AAPG Bulletin. Vol. 99. No. 8. p. 1407-1453.

Sarmiento-Rojas, L.F. (2001). Mesozoic rifting and Cenozoic basin inversion history of the Eastern Cordillera Colombian Andes inferences from tectonic models. PhD. Thesis Univ. of Amsterdam. 295 p.

Sarmiento-Rojas, L.F. (2011) Llanos Basin. Geology and hydrocarbon potential. In: Cediel F. and Ojeda G. Y. (eds). Petroleum geology of Colombia, Vol 9. Universidad Eafit for ANH, Medellín, p 192.

Sarmiento-Rojas, L.F. (2019). Cretaceous stratigraphy and paleo-facies maps of northwestern South America. In: Cediel F and Shaw R. P eds. Geology and Tectonics of Northwestern

South America: The Pacific-Caribbean-Andean Junction. Frontiers in Earth Sciences. p. 673-747. https://doi.org/10.1007/978-3-319-76132-9_10

Snyder, M.E. and Waldron, J.W.F. (2021). Deformation of soft sediments and evaporites in a tectonically active basin: Bay St. George sub-basin, Newfoundland, Canada. Atlantic Geology, 57, 275-304. https://doi:10.4138/atlgeol.2021.013

Villagomez, D., Spikings, R., Magna, T., Kammer, A. Winkler, W. and Beltran, A. (2011). Geochronology, geochemistry and tectonic evolution of the Western and Central cordilleras of Colombia. Lithos Vol. 125. p. 875-896.

Villamil, T. (1996). Depositional and geochemical cyclicity in the Cretaceous fine-grained strata of Colombia. A model for organic matter content. CTF. Vol 1. No. 2. p. 5-23.

Villamil, T. (1998). Chronology, Relative Sea-Level History and a New Sequence Stratigraphic Model for Basinal Cretaceous Facies of Colombia. *in*: J.I. Pindel and C. Drake, eds., Paleogeographic Evolution and Non-Glacial Eustasy Northern South America. Society for Sedimentary Geology (SEPM). Special Publication No. 58. p. 161-216. https://doi.org/10.2110/pec.98.58.0161

Villamil, T. (1999). Campanian-Miocene tectonostratigraphy, depocenter evolution and basin development of Colombia and western Venezuela. Palaeogeography, Palaeoclimatology, Palaeoecology Vol. 153. Iss. 1-4. p. 239-275. https://doi.org/10.1016/S0031-0182(99)00075-9

Villamil, T. (2003). Regional hydrocarbon systems of Colombia and western Venezuela: Their origin, potential, and exploration, in Bartolini C, Buffler, R. T. and Blickwede, J. eds., The Circum-Gulf of Mexico and the Caribbean: Hydrocarbon habitats, basin formation, and plate tectonics: AAPG Memoir. vol. 79, p. 697-734.

Appendix 1.

Supplementary material: marine and continental counts

Well	Unit	Total continental	Total marine	Total counting	Ratio Marine/Continental
W-1	Guadalupe	0	5	5	
W-1	Guadalupe	12	171	183	14.3
W-1	Guadalupe	34	165	199	4.9
W-1	Guadalupe	23	108	131	4.7
W-1	Guadalupe	30	106	136	3.5
W-1	Chipaque	26	178	204	6.8
W-1	Chipaque	25	173	198	6.9
W-1	Chipaque	19	186	205	9.8
W-1	Chipaque	18	191	209	10.6
W-1	Chipaque	17	181	198	10.6
W-2	Chipaque	46	288	334	6.3
W-2	Chipaque	40	294	334	7.4
W-2	Chipaque	29	213	242	7.3
W-2	Chipaque	18	224	242	12.4
W-2	Chipaque	23	215	238	9.3
W-2	Chipaque	45	417	462	9.3
W-2	Chipaque	45	363	408	8.1
W-2	Chipaque	77	251	328	3.3
W-2	Chipaque	59	277	336	4.7
W-2	Chipaque	83	251	334	3.0
W-2	Chipaque	64	277	341	4.3
W-2	Chipaque	88	377	465	4.3
W-2	Chipaque	102	162	264	1.6
W-2	Chipaque	31	213	244	6.9
W-2	Chipaque	37	246	283	6.6
W-2	Chipaque	60	215	275	3.6

Well	Unit	Total continental	Total marine	Total counting	Ratio Marine/Continental
W-2	Une	36	0	36	0.0
W-2	Une	14	0	14	0.0
W-2	Une	227	17	244	0.1
W-2	Une	204	4	208	0.0
W-2	Une	225	10	235	0.0
W-2	Une	215	7	222	0.0
W-2	Une	207	64	271	0.3

W-2	Une	145	40	185	0.3
W-2	Une	197	67	264	0.3
W-2	Une	223	19	242	0.1
W-2	Une	191	9	200	0.0
W-2	Une	223	6	229	0.0
W-2	Une	168	73	241	0.4
W-2	Une	207	13	220	0.1
W-2	Une	152	8	160	0.1
W-2	Une	228	11	239	0.0
W-2	Une	213	13	226	0.1
W-2	Une	133	3	136	0.0
W-2	Une	12	5	17	0.4
W-2	Une	143	127	270	0.9
W-2	Une	115	145	260	1.3
W-2	Une	156	99	255	0.6
W-2	Une	135	97	232	0.7
W-2	Une	86	154	240	1.8
W-2	Une	229	14	243	0.1
W-2	Une	213	8	221	0.0
W-2	Une	78	6	84	0.1

Well	Unit	Total continental	Total marine	Total counting	Ratio Marine/Continental
W-3	Chipaque	0	2	2	
W-3	Chipaque	10	137	147	13.7
W-3	Chipaque	12	266	278	22.2
W-3	Chipaque	15	118	133	7.9
W-3	Chipaque	27	321	348	11.9
W-3	Chipaque	32	251	283	7.8
W-3	Chipaque	12	171	183	14.3
W-3	Chipaque	36	757	793	21.0
W-3	Chipaque	6	209	215	34.8
W-3	Chipaque	29	189	218	6.5
W-3	Chipaque	27	202	229	7.5
W-3	Chipaque	30	166	196	5.5
W-3	Chipaque	15	128	143	8.5
W-3	Chipaque	17	308	325	18.1
W-3	Chipaque	49	340	389	6.9
W-3	Chipaque	62	267	329	4.3
W-3	Chipaque	69	169	238	2.4
W-3	Chipaque	44	291	335	6.6
W-3	Chipaque	28	113	141	4.0
W-3	Chipaque	46	341	387	7.4

W-3	Chipaque	38	327	365	8.6
W-3	Chipaque	56	261	317	4.7
W-3	Chipaque	15	111	126	7.4
W-3	Chipaque	32	332	364	10.4
W-3	Chipaque	30	321	351	10.7
W-3	Chipaque	23	362	385	15.7
W-3	Chipaque	28	356	384	12.7
W-3	Chipaque	32	317	349	9.9
W-3	Chipaque	67	300	367	4.5
W-3	Chipaque	16	55	71	3.4
W-3	Chipaque	175	306	481	1.7
W-3	Chipaque	84	408	492	4.9
W-3	Chipaque	24	540	564	22.5
W-3	Chipaque	114	502	616	4.4
W-3	Chipaque	53	446	499	8.4
W-3	Chipaque	128	323	451	2.5
W-3	Chipaque	147	295	442	2.0
W-3	Chipaque	252	97	349	0.4
W-3	Chipaque	147	64	211	0.4
W-3	Chipaque	343	2	345	0.0
W-3	Chipaque	283	39	322	0.1

Appendix 2.

Supplementary material: Petrophysical values of porosity and permeability for the coarse-grained Cretaceous rocks in the study area:

Unit	Porosity %	Permeability
Lower Guadalupe	18-20	2-3 D
Upper Chipaque	12-16	600-700 mD
Lower Chipaque	15-18	700-800 mD
Une	18-20	2-3 D

D Darcy

mD milli Darcy